Theses and Dissertations

December 2017

# Design and Implementation of a True Decentralized Autonomous Control Architecture for Microgrids

Abedalsalam Ahmed Bani-Ahmed
*University of Wisconsin-Milwaukee*

# DESIGN AND IMPLEMENTATION OF A TRUE DECENTRALIZED

# AUTONOMOUS CONTROL ARCHITECTURE FOR MICROGRIDS

by

Abedalsalam A. Bani-Ahmed

A Dissertation Submitted in

Partial Fulfillment of the

Requirements for the Degree of

Doctor of Philosophy

in Engineering

at

The University of Wisconsin-Milwaukee

December 2017

# ABSTRACT

DESIGN AND IMPLEMENTATION OF A TRUE DECENTRALIZED
AUTONOMOUS CONTROL ARCHITECTURE FOR MICROGRIDS

by

Abedalsalam Bani-Ahmed

The University of Wisconsin-Milwaukee, 2017
Under the Supervision of Professor Adel Nasiri

Microgrids can serve as an integral part of the future power distribution systems. Most microgrids are currently managed by centralized controllers. There are two major concerns associated with the centralized controllers. One is that the single controller can become performance and reliability bottleneck for the entire system and its failure can bring the entire system down. The second concern is the communication delays that can degrade the system performance. As a solution, a true decentralized control architecture for microgrids is developed and presented. Distributing the control functions to local agents decreases the possibility of network congestion, and leads to the mitigation of long distance transmission of critical commands. Decentralization will also enhance the reliability of the system since the single point of failure is eliminated. In the proposed architecture, primary and secondary microgrid controls layers are combined into one physical layer. Tertiary control is performed by the controller located at the grid point of connection. Each decentralized controller is responsible of multicasting its status and local measurements, creating a general awareness of the microgrid status among all decentralized controllers. The proof-of concept implementation provides a practical evidence of the successful mitigation of the drawback of control command transmission over the network. A Failure Management Unit comprises failure detection mechanisms and a recovery algorithm is

proposed and applied to a microgrid case study. Coordination between controllers during the recovery period requires low-bandwidth communications, which has no significant overhead on the communication infrastructure. The proof-of-concept of the true decentralization of microgrid control architecture is implemented using Hardware-in-the-Loop platform. The test results show a robust detection and recovery outcome during a system failure. System test results show the robustness of the proposed architecture for microgrid energy management and control scenarios.

iv

*Dedicated to Utopia, whatever that is.*

# ACKNOWLEDGMENTS

# TABLE OF CONTENTS

ix

# LIST OF FIGURES

# LIST OF TABLES

# LIST OF ACRONYMS

| | |
|---|---|
| **AC** | ALTERNATING CURRENT |
| **AGC** | AUTOMATIC GENERATION CONTROL |
| **BP** | BARLOW-PORSCHAN |
| **CAN** | CONTROL ACCESS NETWORK |
| **CPS** | CYBER-PHYSICAL SYSTEM |
| **DC** | DIRECT CURRENT |
| **DER** | DISTRIBUTED ENERGY RESOURCE |
| **DERMS** | DISTRIBUTED ENERGY RESOURCES MANAGEMENT SYSTEM |
| **DG** | DISTRIBUTED GENERATION |
| **DMGC** | DECENTRALIZED MICROGRID CONTROLLER |
| **DNP** | DISTRIBUTED NETWORK PROTOCOL |
| **EMS** | ENERGY MANAGEMENT SYSTEMS |
| **EPA** | ENHANCED PERFORMANCE ARCHITECTURE |
| **ES** | ENERGY STORAGE |
| **FPGA** | FIELD PROGRAMMABLE GATE ARRAY |
| **GOOSE** | GENERIC OBJECT-ORIENTED SUBSTATION EVENTS |
| **GUI** | GRAPHICAL USER INTERFACE |
| **HIL** | HARDWARE IN THE LOOP |
| **HMI** | HUMAN MACHINE INTERFACE |
| **IED** | INTELLIGENT ELECTRONIC DEVICE |
| **IIOT** | INDUSTRIAL INTERNET OF THINGS |
| **IOT** | INTERNET OF THINGS |
| **IP** | INTERNET ADDRESS |
| **LAN** | LOCAL AREA NETWORK |
| **LFC** | LOAD FREQUENCY CONTROL. |
| **MAS** | MULTI-AGENT SYSTEMS |
| **MCM** | MARKOV CHAIN MODEL |
| **MG** | MICROGRID |
| **MGC** | MICROGRID CONTROLLER |
| **MMS** | MANUFACTURER MESSAGE SPECIFICATION |
| **MRM** | MARKOV RELIABILITY MODEL |
| **MTBF** | MEAN TIME BETWEEN FAILURES |
| **MTTF** | MEAN TIME TO FAIL |
| **MTTR** | MEAN TIME TO REPAIR |
| **NIST** | NATIONAL INSTITUTE OF STANDARDS AND TECHNOLOGY |
| **NTP** | NETWORK TIMING PROTOCOL |
| **OPENFMB** | OPEN FIELD MESSAGE BUS |
| **OSI** | OPEN SYSTEMS INTERCONNECTION |
| **PSP** | PUBLISH/SUBSCRIBE PROTOCOL |

**RBD**         RELIABILITY BLOCK DIAGRAM
**SCADA**     SUPERVISORY CONTROL AND DATA ACQUISITION
**SG**           SMART GRID
**SMV**       SAMPLES MEASURED VALUE
**SSH**        SECURE SHELL
**TCP**        TRANSFER CONTROL PROTOCOL
**WAN**      WIDE AREA NETWORK

# Chapter 1 Introduction

## 1.1    Background

The usage of the term "grid" is growing immensely feeding from the multi-disciplinary pool of research and future visions of the electrical grid forming what is now referred to as "Smart Grid". The basic concept of Smart Grid is to add monitoring communication to current partially traditional grid. It also adds control in a manner that moves this traditional grid into a two-way power and information flow era. This will allow consumers to take the role of a producer of power, which will now have multiple economic and environmental projections on the future of power industry.

A perspective view to the Smart Grid shows one entity consisting of multiple domains [1] [2]. These domains can be viewed as a chain of domains for power service. Starting from the generation and ending with the customer. However, these domains are coupled with the help functional support systems that involve many aspects of data management and communications, insuring system resiliency and efficiency and subsequently economic and environmental projections. National Institute of Standards and Technology (NIST) defines the smart grid domains.

National Institute of Standards and Technology defines the SG domains as shown in Figure 1-1 [1]. Electricity generation is the process of creating electricity from other forms of energy, which may include a wide variety of sources, using chemical combustion, nuclear fission, flowing water, wind, solar radiation, and geothermal heat. These resources may be directly integrated into the distribution system, or share a local bus forming a microgrid. Transmission systems connect the Bulk Generation systems to the Distribution system carrying electricity over long distances.

These systems are normally designed to operate at very high voltage levels to minimize the electricity losses.



**Figure 1-1 Smart Grid Domains**

The Distribution system consists of the electrical network carrying the flow of electricity from bulk transmission system to the customers. The Distribution system can also provide the network connection for Distributed Generation, Distributed Energy Resources and storage systems to supply electricity to customers.

Smart grid customers have been broken into three different types of residential, commercial, and industrial. Customers may also generate, store, and manage the use of energy. A Service Provider is the organizations providing services to electrical customers and to utilities. Service Providers perform services to support the business processes of power system producers, distributors, and customers. These business processes range from traditional utility services, such as billing and customer account management, to enhanced customer services, such as management of energy use and home energy generation

In the deregulated energy industry, there are two markets; Energy market and Transmission market. The Energy market provides a competitive marketplace for energy and other energy products (e.g. ancillary services), whereas the Transmission market provides a competitive marketplace for transmission rights to carry electricity from one place to another. Power system operations involve the management of electricity flow ensuring that the electricity is delivered in a reliable, safe and economic manner. Power system operations can be divided into bulk Transmission Operation, Distribution Operation and Field Devices Operations.

Foundational Support Systems include the non-energy industry process which supports energy industry processes. Examples of these processes include information technology (IT), cyber and physical security, architecture solutions for IT support systems, cost benefits analysis and other supporting processes which need to be executed to support energy industry processes. Each of the aforementioned domains feature its own subdomains.

## 1.2 Microgrid Definition

A microgrid is a localized grouping of electricity sources and loads that normally operates connected to and synchronous with the traditional centralized grid (macrogrid), but can disconnect and function autonomously as physical and/or economic conditions dictate. [1]. United States Department of Energy Microgrid Exchange Group defines a microgrid as a group of interconnected loads and distributed energy resources within clearly defined electrical boundaries that acts as a single controllable entity with respect to the grid. A microgrid can connect and disconnect from the grid to enable it to operate in both grid-connected or island-mode [1].

As the electricity grid continues to modernize, Distributed Energy Resources (DERs) such as storage and advanced renewable technologies can help facilitate the transition to smarter grid

3

islanding capabilities [2]. Microgrids also support management of critical and non-critical loads to available generation. Other microgrid requirements involve secure operations, deploying secure communications network that guarantee distributed and resilient supervisory control architecture. Typical microgrid requirements involves grid connection capabilities, and optimization for economic operation. Support integration of renewables with high penetration and energy harvesting. Microgrid also supports market participation of smaller power sources that can be aggregated to provide power necessary to meet regular demand called Distributed Energy Resources (DER) [3].
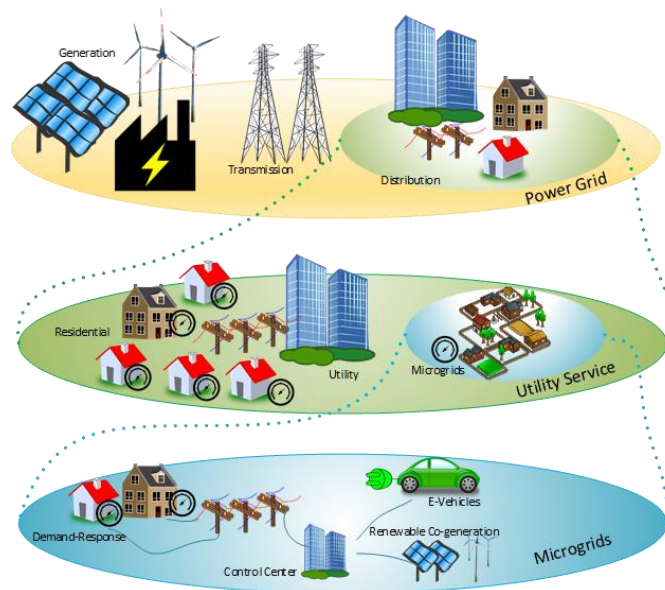


**Figure 1-2 Layered view of the power grid map showing a microgrid.**

Figure 1-2 shows one possible type of microgrids on the power grid map. The distribution network in power grids supports residential and industrial areas providing utility services where microgrids are deployed in order to support local power demand and respond to ancillary services requests. A detailed look at a microgrid structure is shown in Figure 1-3 Microgrid Cyber-Physical System, power components and controls., DERs in microgrids may involve backup generators (NG), Energy Storage (ES), renewable (i.e. Photovoltaic, Wind), and any other type of DERs

4

where the integration into a microgrid is possible. A layer of communication infrastructure is essential to ensure a continuous monitoring and control to the microgrid operation, and achieve higher avaiablility of the microgrid system.
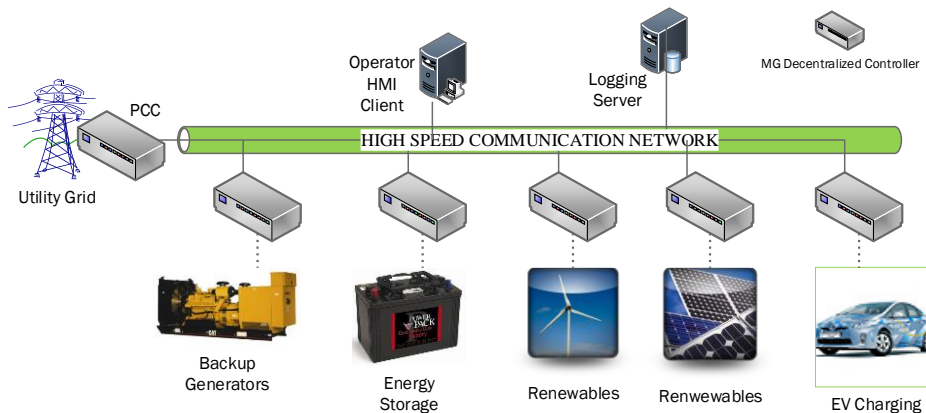


**Figure 1-3 Microgrid Cyber-Physical System, power components and controls.**

## 1.3    Microgrid Control overview

Microgrid control methods can be classified into many categories, depending on the availability of master controllers, slave controllers, communications, load sharing strategy. Centralized and distributed (decentralized) control methods differ in many aspects. Generally, if the DGs can generate its own commands locally, is considered distributed control [9].

The distributed control is a variant on the master/slave control. A central control block controls the reference voltage and influences the output current of the units. The voltage magnitude, frequency and power sharing are centrally controlled. In distributed control, only low bandwidth communication is required, opposed to in the master/slave control scheme. voltage regulation and fundamental power sharing are controlled centrally and requires high bandwidth due to the high amount of traffic required. The distributed control method is distributed in the sense that the critical

5

control components are dealt with by local controllers. Figure 1-3 shows an example of a microgrid decentralized control system.

Centralized methods of operation are more susceptible to single point failures. Reliability is essential since microgrid concept is defined as solution for distribution system reliability improvement, therefore, Emerging smart grid concept compels microgrids to adopt decentralized methods due to the highly dynamic behavior of the microgrids. Two research areas are pursued in decentralized control architecture for microgrids: 1) The distributed control algorithm, including the control hierarchy. 2) Data exchange for decentralized control systems [9] [10]. Some efforts targeted the primary control layer, as it relates to the autonomous operation at the device level [8]. Local frequency control [16] and voltage regulation [17] at the primary control level are the major drives for decentralized controls of microgrids. Other controlled variables include active and reactive power are managed by the Energy Management System (EMS) at the secondary and tertiary control levels [18]. The variation of decentralized primary control techniques for different microgrid components as grid-forming and grid-feeding sources relies on the behavior of the component and the controllability of microgrid variable at the source terminal. As microgrid topologies vary, the control methods consider inverter-based power sources only [20], or a combination of AC and DC sources [13] [21]. Methods have been proposed enabling real-time management of microgrids involving energy storage units over a decentralized secondary control.

## 1.4   Problem Statement

The concept of microgrid is experiencing a significant growth to provide reliable and efficient power and integrate renewable and distributed energy resources. Emerging smart grid concept compels microgrids to adopt decentralized control methods. Centralized methods of operation are

more susceptible to failure due to single point of failure held by the central controller. Despite the vast literature on distributed microgrid control that handles specific issues in microgrid operation; many assumptions are made which makes the practical side accuracy less probable to achieve due to the unforeseen system integration issues [24]. In any control system, delays in communications are unpredictable, uncertainty of data exchange delays, which leads to inaccurate modeling. This makes the communication delays a challenge against system stability, even if the theoretical side resulted with an acceptable system behavior. In microgrids, specifically, the challenge of a control layer is more significant, since the main objective of a microgrid is to maintain the stability of a local bus system, and in case of a grid-tied microgrid, support the grid system through ancillary services

As a solution, true decentralized control architecture for microgrids is proposed in this dissertation. Decentralizing the control operation to local agents decreases the possibility of network congestion to occur, and avoiding long distance transmission for control commands. Decentralization enhances the reliability of the system since the single point of failure is being replaced with a distributed architecture. The proof-of-concept of true decentralization of microgrid control architecture is implemented using Hardware-in-The-Loop platform, developed using real physical communication links and network components, and applying the concept of decentralization dynamically over a network of real-time controllers. The proposed system ensures reliable data exchange between controllers and microgrid components. The control concept is truly distributed and does not require a master or central controller. Load and generation forecasting can be integrated as well as energy storage operation, improving unit commitment and performance.

# Chapter 2 Review of Microgrid Controls

## 2.1 Microgrid Control Hierarchy

Microgrid control hierarchy [9] identifies three levels of controls; where each level satisfies certain requirements and roles in maintaining power reliability, quality, and economical constraints. Details of each layer are as follows:

### 2.1.1 Primary Control

Device level control entails interacting with the local DER itself to perform certain functions including: physical isolation, on/off, fault clearing (device switching), fault sensing, fault controls, re-synchronization (device protection). For inverter: power conversion, power control, voltage and frequency regulation, primary frequency control (inverter droops, governor droops), island detection, re-synchronization). Most device level controls are performed through tightly-coupled communication media, guaranteeing command delivery and signal delay mitigation.

At this control layer (Figure 2-1), each inverter will have an external power loop based on droop control or any predesigned control mechanism [40]. The purpose is to improve the system performance and stability through sharing active and reactive power among DG units and regulating both the frequency and the magnitude of the output voltage. In droop control, voltage and frequency stability are achieved by drooping the voltage and frequency according to active and reactive power requirement for this control level. For resistive microgrid P/V droop is generally preferred [5], [16].
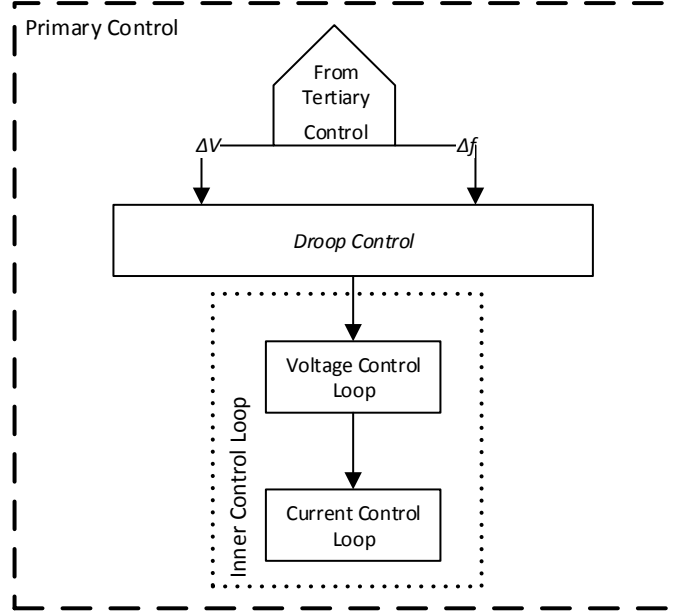
**Figure 2-1 Microgrid primary control**

The various types of droop controllers depending upon the nature of microgrid system, the following are droop equations:

$$f = f_0 - m(P - P_0) \tag{2-1}$$

$$V = V_0 - n(Q - Q_0) \tag{2-2}$$

where $m$ is the frequency droop coefficient; $n$ is the voltage droop coefficient; $f_0$ is the nominal frequency; $V_0$ is the nominal phase voltage amplitude.

Needless to communicate, conventional droop control makes a satisfactory choice for wide area microgrids. The droop control method changes $P$ as a function of the grid frequency, and is based on the inertia of the synchronous machines. As the inverter-based microgrids generally lack this inertia, the *P/f* droop method in microgrids is based on the line characteristics. Power flow equations in this case are:

$$P \approx \frac{V_1}{R^2 + X^2}[R(V_1 - V_2 \cos \delta) + X V_2 \sin \delta] \qquad (2\text{-}3)$$

$$Q \approx \frac{V_1}{R^2 + X^2}[-RV_2 \sin \delta + X(V_1 - V_2 \cos \delta)] \qquad (2\text{-}4)$$

Where *P, Q* are the output active and reactive power, respectively. $V_1$ and $\delta$ are the source voltage and phase angle, to a voltage $V_2$ with zero reference phase angle. Through line impedance *Z=R+jX.*

With the resistive nature of low-voltage microgrids, line resistance cannot be ignored, which leads to a concern when implementing droop control. In this case, the power flow equations are

$$P \approx \frac{V_1[V_1 - V_2]}{R} \qquad (2\text{-}5)$$

$$Q \approx \frac{V_1[-V_2 \delta]}{R} \qquad (2\text{-}6)$$

Measuring active power is relatively easier than measuring instantaneous frequency. Therefore, a droop with frequency as a function of active power is used. Droop control method is not suitable when the microgrid has nonlinear loads due to the harmonic current [20]. Moreover, all the resources in the microgrid contribute power to the load and operate autonomously.

With a wide variation of droop control schemes [82]. Voltage droop control is a variation of *P/f* droop control. As shown if Figure 2-2, the droop controller consists of a combination of terminal voltage $V_g$ and the DC-link voltage $V_{dc}$ ($V_g$ /$V_{dc}$ inverter-based DER), and $P/V_g$ droop controller. Changes in the dc-link voltages indicate a difference between the ac-side power injected into the microgrid and the input power from the dc-side of the inverter.

10
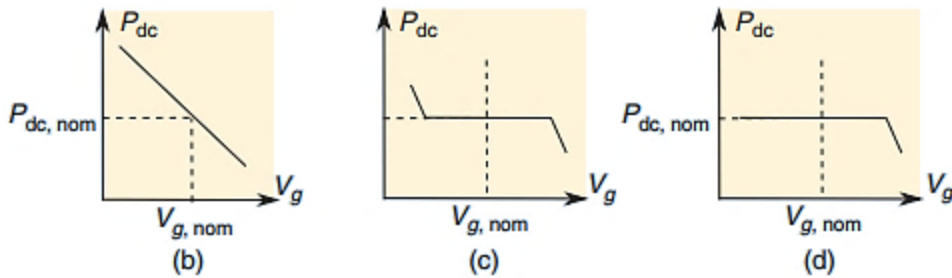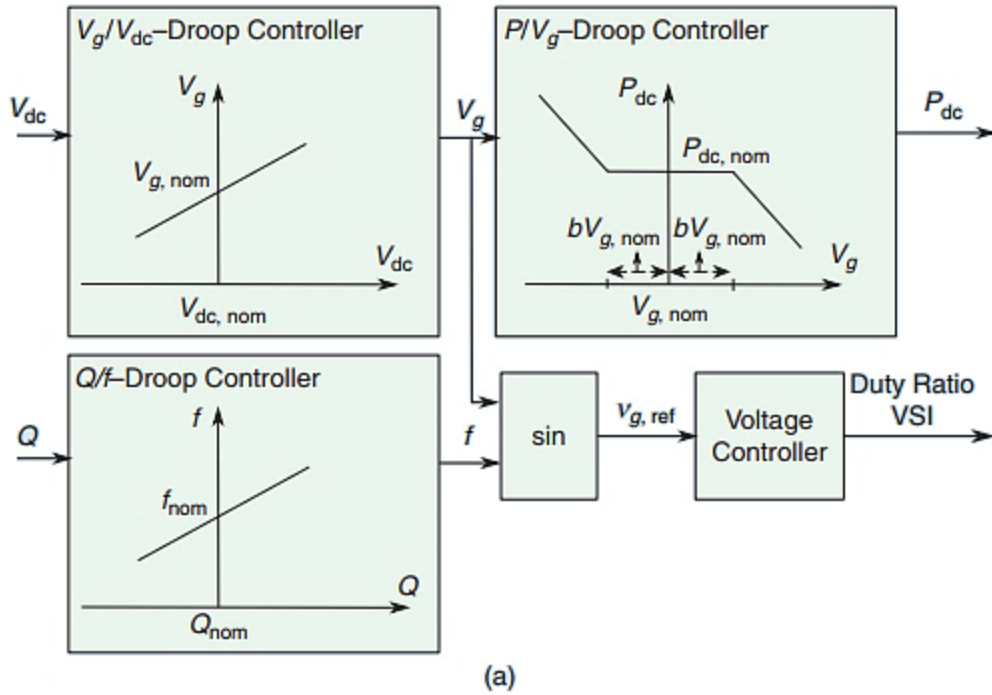
**Figure 2-2 VBD control. (a) Control strategy. (b)–(d) Constant power bands of dispatchable versus less dispatchable DG units: (b) a fully controllable unit, (c) a less controllable unit, (d) a renewable energy source (without storage or controllable consumption) [82]**

In virtual Droop Control (VDC) [23], a virtual frequency and voltage are created to regulate the active and reactive power output of the sources. The active power output of the energy storage inverter determines the virtual frequency from virtual droop curve. The droop curve is defined between energy storage active power output and virtual frequency. The virtual frequency will determine the active power commands for natural gas generators from a droop relationship, defined between the virtual frequency and active power command of each source. The same

11

concept applies to system voltage. A virtual voltage is determined according to reactive power output of the energy storage inverter. The virtual voltage will determine the reactive power command for natural gas generators from a droop relationship, defined between the virtual voltage of the system and reactive power command of each source. It should be noted that since energy storage inverter is placed in a voltage mode, it supplies the difference between load active and reactive power and other sources in the microgrid. It behaves as a slack bus in a power system concept. Power commands of backup generators are updated only when load variation is greater than defined value. Load variation less than defined value is taken care of by the energy storage inverter [5].

### 2.1.2   Secondary Control

To achieve the main goal of controllability of the microgrid, A secondary layer of control is used to solve the shortcomings of the primary control. The conventional approach for secondary controllers is to use a microgrid central controller (MGC), which includes slow control loops and low-bandwidth communication systems, and sends the control output information to each DG unit. This centralized control concept was used in large utility power systems for years to control the frequency of a large-area electrical network and has been applied to microgrids in the last years for voltage and frequency restoration. Primary control level is responsible of frequency regulation. During transient operation, deviation of voltage and frequency may occur due to the load power demand fluctuations or intermittency of renewable DGs. In microgrid systems, an advantage of energy storage is enabling the microgrid to compensate for frequency and voltage deviations in a fast manner. The role of secondary control comes at a slower response to frequency fluctuations in comparison the primary control.

Other objectives regarding voltage control and power quality, such as voltage unbalance and harmonic compensation using the secondary controller, have been proposed recently [79]. The active power sharing has been improved by computing and setting the phase angle of the DGs instead of its frequency in the conventional frequency droop control and by using communication [80]. A method for increasing the accuracy of the reactive power-sharing scheme has been presented in [81], which introduces an integral control of the measured load bus voltage, combined with a reference that is drooped against the local reactive power output.
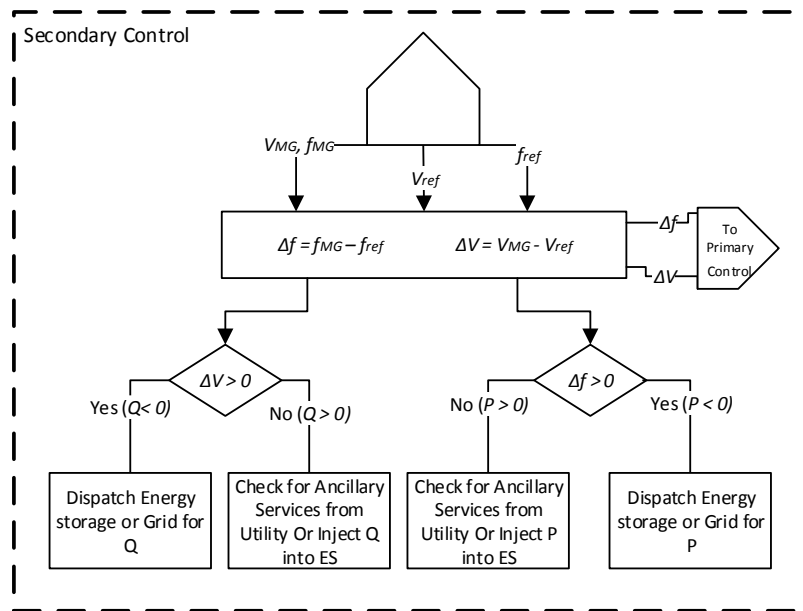


**Figure 2-3 Microgrid Secondary Control.**

Figure 2-3 shows the function of the secondary control that works collaboratively to achieve optimization, protection, power calculations (with predefined system constraints), and failure management (see Chapter 5). Recently, efforts referred to the secondary control as the Energy Management System (EMS), where it continuously monitors the microgrid parameters, going into through data verification, and interacting with the Failure Management Unit. EMS dispatches

microgrid components such as energy storage or backup generators for active and reactive power and commands the primary level.

The secondary layer represents the Distributed Energy Resource Management Systems (DERMS) [1]. From the utility perspective, DERs can be in a form of a microgrid (sharing the same bus), or distributed over multiple different feeders in the Distribution System. The following sections explains the operations of this layer, and how they relate the concept of DERMS as a part of microgrid controllers.

2.1.3   Tertiary Control

Generally, the tertiary control level manages the bidirectional power flow between the microgrid and the grid at the point of common coupling (PCC). As in Figure 2-4, this control level also ensures optimal economical dispatch of the Microgrid through data analytics, machine learning, optimization, and forecasting techniques [41]. This layer can coordinate the power flow within the microgrid, by using an optimal power flow solver. The optimization process includes power flow optimization, where active and reactive power are determined as an optimal power flow; and energy optimization, where a day ahead of energy supply can be optimized according to generation/load forecast, as well as weather forecast which affect the output power of the renewable resources.
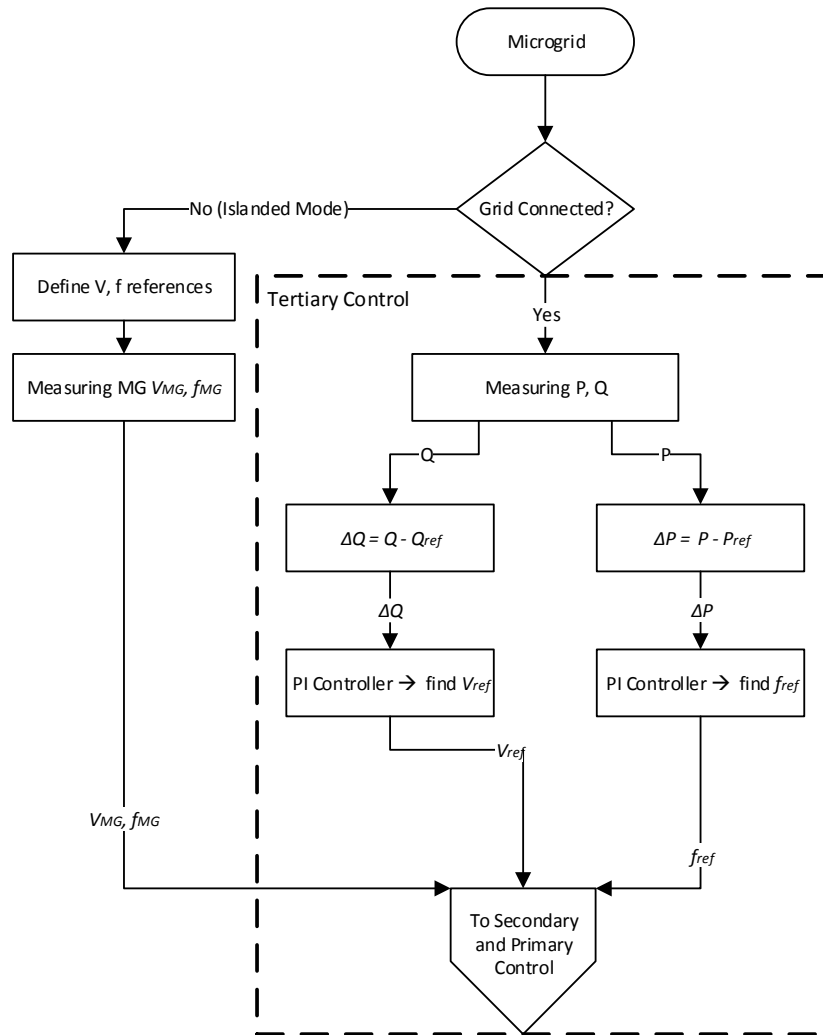
**Figure 2-4 Microgrid Tertiary Control.**

## 2.2 Microgrid Distributed Control

The vision of next generation smart grid suggests a decentralized manner of control and management of system components. In microgrid, the number of Distributed generation (DG) units pose a significant problem to a central control architecture as it increases the computational burden due to the multitude of the controllable resources, communication a tremendous needs due to the geographical span, frequent reengineering of the central controller that has a negative effect on the scalability and plug-and-play capability. Other drives of the decentralization of microgrid controls is the reliability and security vulnerability of the central controller as a common point of failure.

Many efforts have investigated the decentralized architecture for microgrid controls. Although the main concept among all previous efforts is the same, the difference in the terminology is present due to the lack of standardization of the concept, and the variation in control techniques for the three levels of controls in microgrids. Terminologies include decentralized control, distributed control [30], Multi-Agent Systems [27]. This section provides an overview on recent efforts that propose a decentralized control system, or target one or more features of decentralization.

As the computer sciences and electrical engineering converges at the control level. The concept of decentralized controls has been introduced as Multi-Agents Systems (MAS). MASs have been widely studied in the field of computer science [33]. Recently, MAS based system caught the attention of energy researchers, specifically for energy systems and microgrids as a solution for distributed control and energy management [37,33]. A multi-agent system for optimizing the hybrid renewable energy system was presented in [37]. Meanwhile in [18], a distributed management solution based on MAS was proposed to provide an improved system reliability than conventional centralized energy management systems. In [33], a MAS based hierarchical decentralized coordinated control was presented to solve the energy management issue of a distributed generation system (DG) by ensuring energy supply with high security. A MAS and fuzzy cognitive map were used in [32] for a decentralized energy management system of an autonomous generation microgrid. In [34], a decentralized MAS was used for demand side integration that could reduce the energy cost, and improve energy efficiency while increase security and quality of supply. Furthermore, MAS has also been used for reactive power management in distribution networks with renewable energy sources to enhance the dynamic voltage stability

Due to a higher complexity in management under a decentralized architecture, and the requirement of certain level of intelligence, efforts have introduced artificial intelligence methods to ensure a virtually centralized control for microgrids [31] [32]. Other efforts defined the basic requirement of agents such as control agents, management agents, and ancillary agents for optimal energy exchange between the production units of the microgrid and the local loads, as well as the main grid [26]. In [25], a decentralized architecture of multi-agent system for the microgrid with power electronic interfaces. Three step communication algorithms enable the system work with least communication data, only real and reactive power mismatch data for neighbor to neighbor communication.

In [27], optimal dispatch of DGs and distributed feeder within a distribution system were investigated based on a distributed MAS [27], DC microgrids and a decentralized control algorithm for inverter-based microgrid were proposed in [29]. Most efforts validate the decentralized control operation and its claimed optimality using simulations, while other efforts have a higher accuracy requirements, and used a Hardware-In-the Loop testbed [30]. In [30] a comprehensive study of distributed cooperative control framework for synchronized Reconnection of a multi-bus microgrid have been conducted. In this framework, DGs work collaboratively in a distributed manner using minimum and sparse communication. Plug and play Multi agents systems. In [26], the proposed method relies only on local measurements and actions without the use of additional communication channels. The proposed strategy considers proper dynamic behavior and reliable operation modes for the islanded power system.

This section reviewed the main efforts in decentralization of microgrid controls. More efforts are mentioned across this dissertation according to the architecture feature being discussed.

17

# Chapter 3 Communications in Microgrids

In a Microgrid, there are no specific configurations or certain protocols that can be used; this decision is based on the availability of the communications options and the cost of implementing them. However, other considerations are involved in the decision, such as the harshness of the environment where the Microgrid is located and the communication method characteristics, data traffic, cost, degree of availability, and number of DERs in the network. Communication configurations can be divided into three categories: Tightly coupled, loosely coupled, and broadcast/multicast communications.

Tightly coupled communications require the highest possible availability for the network, since the distributed resources in loosely-coupled and broadcast are able to manage their operation independently, which may imply that the Microgrid control system is fully or semi-autonomous, thus, reasonable availability is acceptable in these two cases. On the other hand, Local Area Network (LAN) configuration works for either case [5], but can be expanded to Wide Area Network (WAN) in the case of broadcast/Multicast, which brings up the quality of service requirement to ensure communications to all DERs.

Integration of communications is required for implementing reliable, safe, secure, sustainable, and cost-effective microgrid control architecture. This can be achieved by utilization of the Internet communications protocol suit. The most widely used and most widely available protocol suite is TCP/IP protocol suit. A protocol suit consists of a layered architecture where each layer depicts some functionality which can be carried out by one or more protocols. Each layer usually has more than one protocol options to carry out the responsibility to which the layer adheres. TCP/IP is normally considered to be a four-layer system: Application, Transport, Internet,

and Link Layer (Figure 3-1). Enhanced Performance Architecture (EPA) is used occasionally since

it does not require all seven layers of OSI model for interfacing the architecture of a control system

and message exchange between Microgrid components [18].
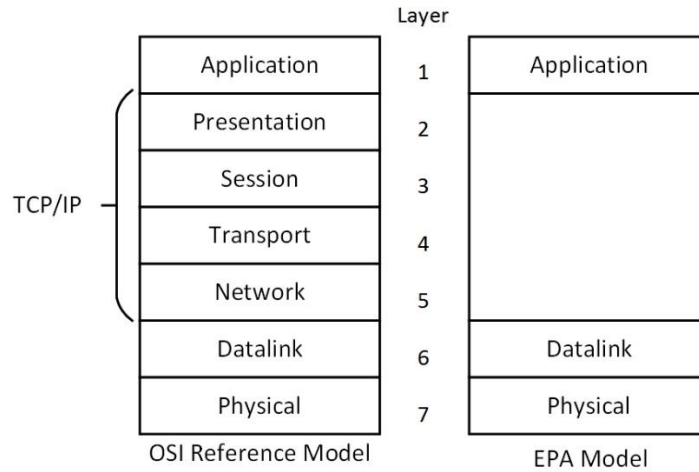


**Figure 3-1 The open system interconnection (OSI) model showing the TCP/IP layers, and the enhanced performance architecture (EPA) model.**

Microgrid control systems employ several protocols to enable communication between the

different types of power and cyber actors. Figure 3-2 shows a generic schematic of a Microgrid

communications system. Intelligent Electronic Devices (IEDs) receive data from sensors and issue

control commands to power components such as DERs, Energy Storage, and loads. As an example,

Microgrid controller communicates with IEDs and other components using the standard IEC

61850 [42] over Ethernet (TCP/IP), the interconnection network basically ensures reliable and

secure communication between components by employing the internet communication protocol

suit, and may contain routing and switching at certain points. The architecture also suggests the

presence of Human Machine Interface Client (HMI) for monitoring and controlling purposes, in

addition to data Logging Server in order to record system profiles and certain events during any

mode of operation. Moreover, Intelligent Electronic Devices (IEDs) has the capability to receive

20

power data from the DERs and send them to the Microgrid controller as a feedback loop for the control system. Based on the data, control signals and reference values of voltage, frequency, active and reactive power are issued by the Microgrid controller to the IEDs where they issue the appropriate control signals to their allocated DERs or controllable loads.
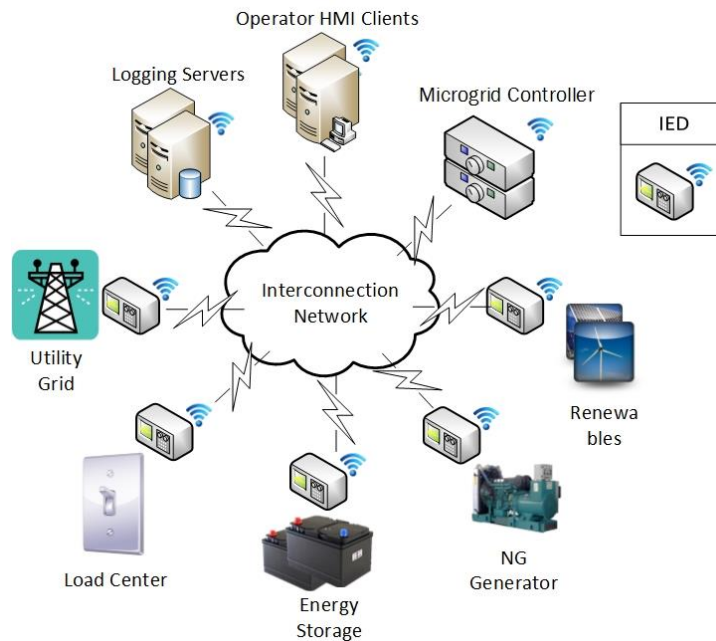


**Figure 3-2 Generic microgrid components with communication requirements.**

## 3.1   Communication Protocols and Standards

### 3.1.1   Internet Protocol Suit

The purpose of each layer as follows: The application layer has different protocols that govern process-to-process communication, enabling applications on the same or different hosts for data sharing. Such protocols can be Network Timing Protocol (NTP) [43], Secure Shell (SSH), XML-RPC, Hypertext Transfer Protocol HTTP, Modbus, Control Access Network (CANbus), and DNP3 (Distributed Network Protocol) [44] which are usually used between component in process automation systems. The Transport layer serves the purpose of host-to-host communications on either the same network or on networks separated by routers. Protocols that lie into this layer are Transmission Control Protocol (TCP) and User Datagram Protocol (UDP). The sole purpose of

21

these protocols is to create a basic data channel that can be used by an application for data exchange related to a specific task. Employment of either TCP or UDP within a microgrid control system network will be based primarily on the importance of speed versus reliability and the necessity for error detection.

A closer look to the interconnection network, all components communicate with each other independently using unicast or multicast techniques through wired or wireless physical links. This capability is provided by the Internet Layer using the Internet Protocol (IPv4, IPv6). This Layer also provides authentication and encryption in a communication session through Internet Protocol Security (IPsec). The Link Layer is a combination of Datalink Layer and Physical Layer (as in OSI model); protocols of these two layers support local network communication without intervening routers (i.e. through Switches), and taking advantage of Ethernet networks primarily, but may include some serial communications.

3.1.2   Modbus

Modbus is considered one of the legacy protocols in power systems; it was developed for process control systems. As mentioned before, it lies on the application layer of OSI model. Basically, it is used for client/server communications, which is the case of a Microgrid communication system where the main controller or the HMI can act as a server and other DERs as clients. Message types in Modbus are generally queries and responses, sometimes are broadcasting some control signals to all DERs at once. For Modbus over TCP/IP, Excerptions are reported to the server by clients. All microgrid components communicate with each other independently using unicast or multicast techniques through wired or wireless physical links. This capability is provided Modbus can be transmitted over different physical links such as RS-232,

22

RS485, and Ethernet (TCP/IP) using intermediate converters. Figure 3-3 shows haw a Modbus frame can be encapsulated in a TCP packet.
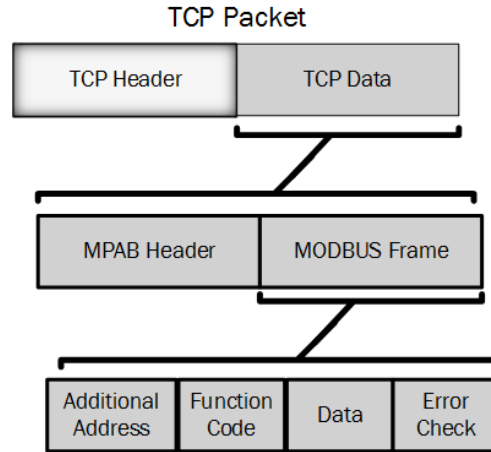


**Figure 3-3 Modbus Frame encapsulation in TCP/IP Packet.**

### 3.1.3    Distributed Network Protocol (DNP3)

DNP3 now the dominant Master/Slave protocol in electrical utility Supervisory Control and Data Acquisition (SCADA) systems [15], and is gaining popularity in other industries, including Oil & Gas, Water, and Waste Water. Its specification supports multiple methods of reading inputs individually or as a group, multiple types of data can be encapsulated in a single message to improve efficiency. Time stamps and data quality information can also be included. Unlike Modbus, DNP3 user slave devices can send updates as values change, without having to wait for a poll from the Master.

Table 1 shows a brief comparison between Modbus and DNP3 protocols. Both protocols are open domain and available to public, they also has active user groups that drives the adoption of these technologies in distributed automation systems. They also support multiple data types with the dominancy of DNP3 in the variety of data types and supporting other services such as timing and file transfer.

23

**Table 3-1 Comparison between Modbus and DNP3 Protocols.**

| Feature | Modbus | DNP3 |
|---|---|---|
| Open Domain | Y | Y |
| Active User Grouup | Y | Y |
| Multiple Data Types | Y | Y |
| Standarized data formats | N | Y |
| Time-Stamping | N | Y |
| Data quality indication | N | Y |
| Reporting by exception | Y (TCP) | Y |

### 3.1.4   IEC 61850

IEC 61850 [12] is a standard defines data models and exchange of data and events between power systems substations; it can be mapped to number of protocols such as Manufacturer Message Specification (MMS), Generic Object-Oriented Substation Events (GOOSE), and Sampled Measured Values (SMV). However, IEC 61850 was not designed for former serial communication protocols, its functionality is introduced to run over Ethernet networks, reflecting a positive impact on the cost of design and operation of power systems laying over the application layer and above. Leveraging the services of this standard is proposed to achieve reliability and security. Some of the services in this standard are: Retrieving the self-description of a device, fast and reliable host-to-host exchange of status information, reporting any set of data or sequence of events, data logging, retrieving samples values from sensors, time synchronization, and file transfer for online configuration of components. Table 3-2 shows the structure of the IEC 61850 standard.

**Table 3-2 Structure of IEC 61850 Standard**

| Part # | Title |
|---|---|
| 1 | Introduction and Overview |
| 2 | Glossary of terms |
| 3 | General Requirements |
| 4 | System and Project Management |
| 5 | Device Models |
| 6 | Configuration Description Language for Communication in Electrical Substations Related to IEDs |

| 7 | Basic Communication Structure for Substation and Feeder Equipment |
|---|---|
| 7.1 | Principles and Models |
| 7.2 | Abstract Communication Service Interface (ACSI) |
| 7.3 | Common Data Classes (CDC) |
| 7.4 | Compatible logical node classes and data classes |
| 8 | Specific Communication Service Mapping (SCSM) |
| 8.1 | Mappings to MMS(ISO/IEC 9506 – Part 1 and Part 2) and to ISO/IEC 8802-3 |
| 9 | Specific Communication Service Mapping (SCSM) |
| 9.1 | Sampled Values over Serial Unidirectional Multidrop Point-to-Point Link |
| 9.2 | Sampled Values over ISO/IEC 8802-3 |
| 10 | Conformance Testing |

Communication protocols define how data bits are transmitted on the wires or the transmission media. However, they do not define the data organization in an IED or any device with communication capability. As for Microgrid components, each DER has unique functionality. Some data attributes may not be present in certain DERs but are available in others, even different manufacturers of IEDs has different naming criteria to the data. Therefore, IEC 61850 data naming are based on power systems context, which guarantees interoperability between multi-vendor devices in the same communication system. Moreover, the abstraction of the data objects is presented in part 7.4 (Table 2), these data objects are referred to as Logical Nodes (LN). One or multiple logical nodes form a logical device. A logical node consists group of data elements that are related to certain functionality of the device, each data element has a unique name that is defined by the standard.

The services of the IEC 61850 form a functional Microgrid communications system. The capability of transmission over Ethernet and the mapping of other protocols into the standard simplifies the design of the communication system, and minimizes the cost of integrating multi-vendor devices. In addition to that, leveraging the Object-Oriented representation of the data from

multiple devices eliminates the dependency of the communication protocols that is used in different DERs in a Microgrid, not to mention the circuit breakers, transformers, voltage sensors and current sensors.

## 3.2 Communication Architectures

A generic power system control architecture consists of three major layers. As shown in Figure 3-4, the first layer (bottom) is the power equipment layer, which contains the distributed energy sources, relays and breakers. The second layer is the communication layer, which contains the cyber-physical network backbone and the communication protocols and standards. The third layer is the control layer.
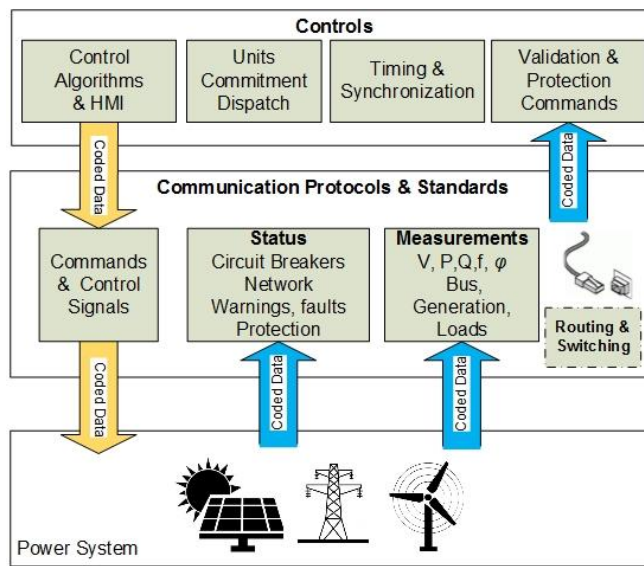


**Figure 3-4 Generic Power System Control Process.**

Data traffic starts from the power system layer, where the components transmit their status data and measurements through the communication layer. Status data can be breaker status, device warnings and flags, measurements of voltage, active and reactive power, and frequency of each power component. The control layer receives data from the communication layer, validates the received information and synchronizes clocks. Ensuring that the data received is the most recent

26

measurements, considering possible delays or dropped data packets within the communication layer. Unit commitment and control algorithm process the inputs and sends back commands through the communication layer, which is responsible of routing the commands to the designated power component.

## 3.3 Impact of Communication latencies and failures

3.3.1 Communication Delays

Communications play an essential role power system, through which control, monitoring and operation are performed at high reliability. One can find communication gear in virtually all stages of electric power systems, starting with power generation, up to transmission, down to distribution. In the conventional power system, the communication system was mostly seen in the transmission network, where it served as the backbone for real-time monitoring, centralized control and protection. Recently, with the introduction of smart grid technology, communication systems are being deployed in distribution networks, where they are needed by the distributed intelligence platforms [45].

Latency can be defined as the total time it takes a signal to travel from one point to another, generally from a transmitter through a network to a receiver. In a distributed control system, latency is seen as the amount of time it takes a message to be passed from the sending source and received at the receiving sink.
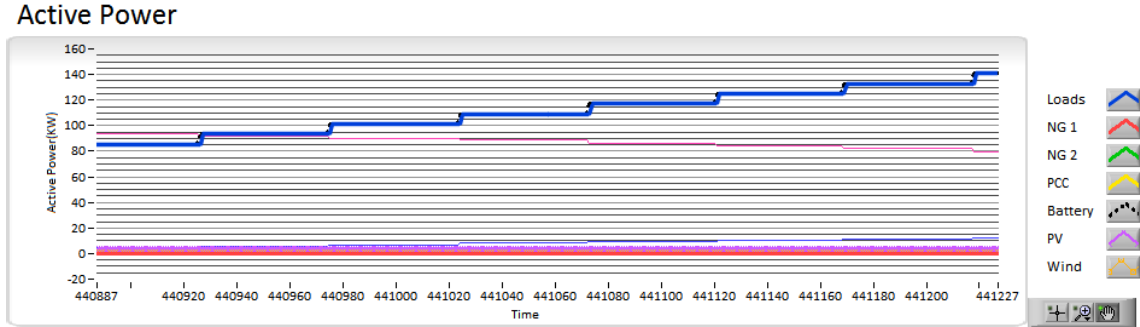
**Figure 3-5 Buffering impact on sampling time.**

### 3.3.2 Sources of Communication delays

When investigating trade-offs in communication architectures, it is important to recognize that the time per communication operation breaks down into portions that involve different machine resources: the processor, the network interface, and the actual network. A worst case of communication delay of switched ethernet with one switch in the network can be calculated using the timing diagram in Figure 3-6. Assuming no buffering for the data transmitted the minimum communication delay ($D_{Cmin}$) can be defined as follows

$$D_{Cmin} = D_S + 2(D_F + D_P) + D_D \tag{3-1}$$

Where $D_S$ is the processing delay for transmission at the source; $D_D$ is the processing delay for reception at the destination; $D_F$ is the frame transmission delay, which is defined as the number of bits in the frame divided by the data rate; and $D_P$ is the propagation delay as the electrical signal is propagated from the source to the switching hub, which is proportional to the length of the cable connecting the station and switching hub. Taking an example of a 20-m cable, the propagation delay is about 0.1 μs at the propagation speed of $2.0 \times 10^8$ m/s. In (3-1), we simply use twice the propagation delay from a station to the hub assuming that the cable lengths are identical for all the stations [47].

28
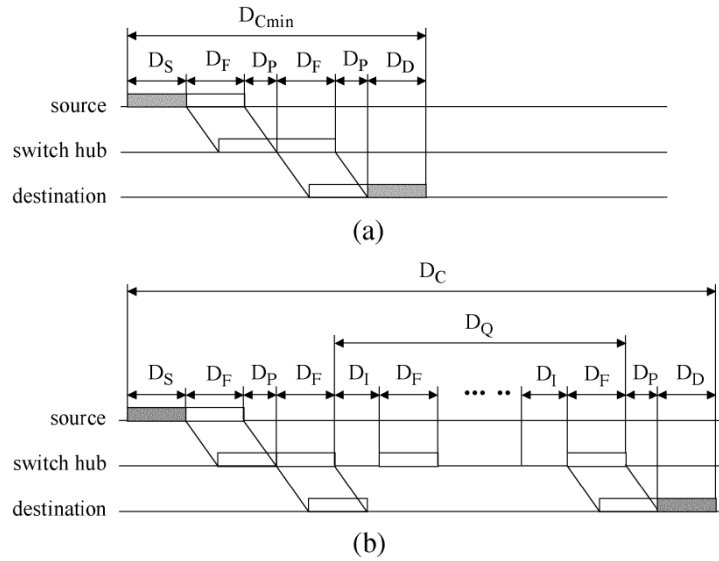
**Figure 3-6 Communication delay of switched Ethernet with one switching hub [47].**

The complexity of the backbone network plays a significant role on the communication delays. The transmission rate, however, takes the complexity of determining the delays of a communication system to a higher level, due to other concerns such as network congestion, and frame dropping. Other issues may emerge involve data consistency and coherency.

### 3.3.3   Communication delay impact on Microgrid operations.

#### *3.3.3.1   Cyber physical model for microgrids*

The frequency should remain nearly constant for a satisfactory microgrid operation. The frequency control and power generation is commonly referred to load frequency control (LFC), which is a major function of automatic generation control (AGC) systems [46]. In a microgrid system, a control area (group of generators and loads) should to be used, where all the generators respond to load variations settings. This section proposes a study demonstration to illustrate the delay within a microgrid system, and its impact on the frequency deviation.

29
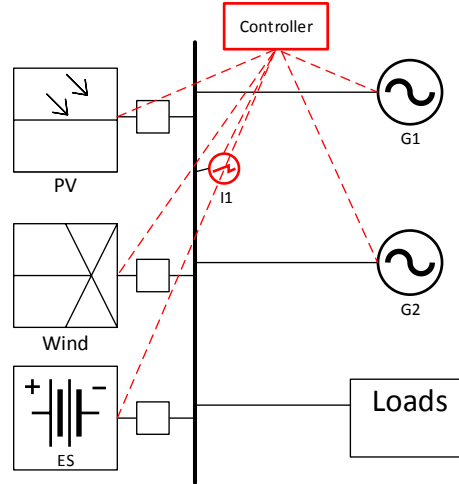
**Figure 3-7 Sample cyber-physical model for a microgrid.**

Figure 3-7 shows basic components of the cyber-physical model for a microgrid. The basic elements are two distributed synchronous generators, PV and wind generators based on inverters, and energy storage. The central controller provides a monitoring and control mechanism to the architecture. A simplified dynamic model is shown in Figure 3-7, two distributed generators (diesel generator), and one distributed PV generator, and one wind generator, in addition to the energy storage unit. The small power generation network supplies the local demand. Assume that the small power generation network is not connected to the wide power grid, and it always operates independently as an islanded power system. Another assumption is that each DER has its own local controller. coordinating with a central controller.

Based on [46] The generator cyber-physical module is shown in Figure 3-8. In this module, we identify one cyber output ($\Delta f$) corresponding to the frequency deviation of the system, one cyber input ($Ug$), and a physical output ($Ps$). $Ug$ input corresponds to the microgrid controller signal control, defined as a cyber input and the sensing frequency deviation $\Delta f$ is as a cyber output. Also, we identify a physical output ($Pg$), that corresponds to output power of diesel generator. Following the methodology proposed in [48], each cyber and physical module must have a

30

dynamic model associated. This model only considers the low-frequency domain to control. The dynamics for the diesel generator and energy storage are represented by a transfer function as follows:

For Natural Gas Generator 1:

$$G_{g1}(s) = \frac{P_{G1}(s)}{U_{g1}(s)} = \frac{1}{sT_{g1} + 1} \tag{3-2}$$

$$U_g(s) = U_I + U_P = -\left(\frac{K_I}{s} + K_P\right)$$

$$\dot{P}_{G1} = \frac{U_I}{T_{g1}} + \frac{K_P \Delta f}{T_{g1}} - \frac{P_{G1}}{T_{g1}} \tag{3-3}$$

Similarly, for Natural Gas Generator 2

$$G_{g2}(s) = \frac{P_{G2}(s)}{U_{g2}(s)} = \frac{1}{sT_{g2} + 1} \tag{3-4}$$

$$\dot{P}_{G2} = \frac{U_{I2}}{T_{g2}} + \frac{K_{P2} \Delta f}{T_{g2}} - \frac{P_{G2}}{T_{g2}} \tag{3-5}$$

For Energy storage:

$$ES(s)\frac{P_{ES}(s)}{U_{g\_ES}(s)} = \frac{1}{sT_{ES} + 1} \tag{3-6}$$

$$\dot{P}_{ES} = \frac{U_{I\_ES}}{T_{ES}} + \frac{K_{P\_ES} \Delta f}{T_{ES}} - \frac{P_{ES}}{T_{ES}} \tag{3-7}$$

Where $T_{g1}$, $T_{g2}$ is the time constants of the corresponding diesel generators. $T_{ES}$ is the time constant for energy storage.

We assume that variation in load demand and power supplied by the PV and wind generators are compensated by the generator power. Load demand varies between 0 p.u and 1 p.u. The load demand model includes the load demand, PV generation, and wind generation, as negative loads.

$$\Delta P_S = P_{G1} + P_{G2} + P_{ES} - P_{Demand} \tag{3-8}$$

$$P_{Demand} = P_L - P_{wind} - P_{Solar} \tag{3-9}$$

A simple PI control strategy [49] is used to control the frequency error, where the control output is defined as

$$U_g(s) = -(U_I(s) + U_P(s)) \tag{3-10}$$

$$U_I(s) = \frac{K_I}{s} \Delta f \tag{3-11}$$

$$\dot{U}_I = K_I \Delta f$$
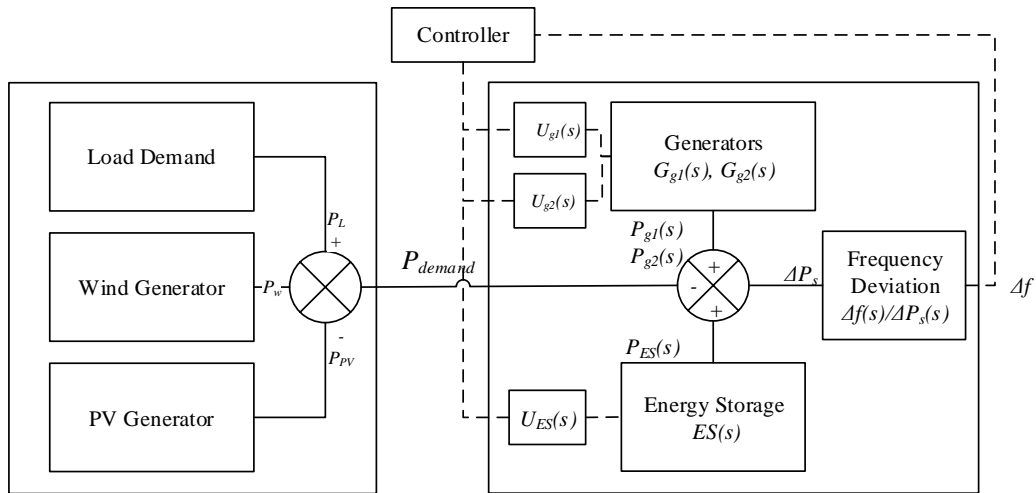


**Figure 3-8 Cyber-physical module for a Microgrid. The dotted line corresponds to a cyber signal, while the solid line corresponds to a physical signal**
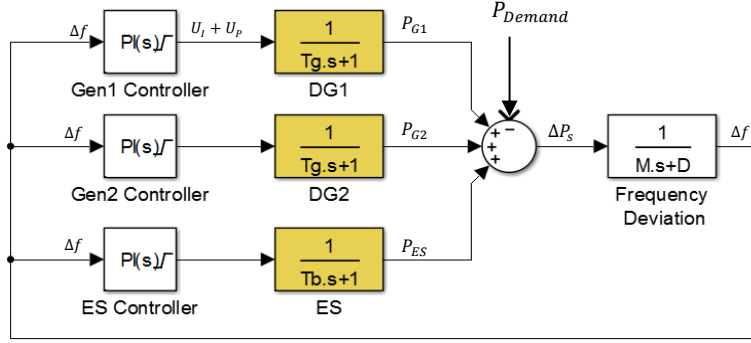
**Figure 3-9 Simulink Model of the cyber-physical microgrid system.**

In low voltage microgrids, it is possible to assume that there exists a relation between active power generated and bus frequency variation [49]. For this reason, dynamic behavior in frequency in a low voltage MG is represented as

$$\frac{\Delta f(s)}{\Delta P_S(s)} = \frac{1}{sM + D}$$

(3-12)

where $\Delta P_S$ corresponds to power imbalance between power demanded $P_S$ and power generated $P_g$, $D$ is the load damping constant and $M$ is the inertia constant.

### 3.3.3.2 Microgrid cyber-physical State-Space model

In order to analyze the general system performance, a state space representation model of closed-loop DG based on the CPS for the Microgrid system in Figure 3-8 is following. For simplicity, assume that $\Delta P_S = 0$

$$\dot{x}(t) = Ax(t) + Bu(t)$$

(3-13)

$$y(t) = Cx(t)$$

Where:

$$x(t) = [\Delta f \quad P_{G1} \quad P_{G2} \quad P_{ES} \quad U_{I1} \quad U_{I2} \quad U_{I\_ES}]$$

$$\dot{x}(t) = \begin{bmatrix} \dot{\Delta f} & \dot{P}_{G1} & \dot{P}_{G2} & \dot{P}_{ES} & \dot{U}_{I1} & \dot{U}_{I2} & \dot{U}_{I\_ES} \end{bmatrix}$$

A state representation of the form $\dot{x} = Ax$ is performed, without time delay and where the state vector is defined

$$A = \begin{bmatrix}
-\dfrac{D}{M} & \dfrac{1}{M} & \dfrac{1}{M} & \dfrac{1}{M} & 0 & 0 & 0 \\[2mm]
\dfrac{K_{P1}}{T_{G1}} & -\dfrac{1}{T_{G1}} & 0 & 0 & \dfrac{1}{T_{G1}} & 0 & 0 \\[2mm]
\dfrac{K_{P2}}{T_{G2}} & 0 & -\dfrac{1}{T_{G2}} & 0 & 0 & \dfrac{1}{T_{G2}} & 0 \\[2mm]
\dfrac{K_{P\_ES}}{T_{ES}} & 0 & 0 & -\dfrac{1}{T_{ES}} & 0 & 0 & \dfrac{1}{T_{ES}} \\[2mm]
K_I & 0 & 0 & 0 & 0 & 0 & 0 \\[1mm]
K_I & 0 & 0 & 0 & 0 & 0 & 0 \\[1mm]
K_{I\_ES} & 0 & 0 & 0 & 0 & 0 & 0
\end{bmatrix}$$  (3-14)

$$B = \begin{bmatrix} 1 & 0 & 0 & 0 & 0 & 0 & 0 \end{bmatrix}^T$$

$$C = \begin{bmatrix} 1 & 0 & 0 & 0 & 0 & 0 & 0 \end{bmatrix}$$

We obtain a microgrid state-spate model with delay using the parameters in Table 3-3.

**Table 3-3 Simulation parameters of a microgrid system.**

| Parameter | Value |
|---|---|
| Inertia Constant M | 0.008 puMWs/Hz |
| Damping Constant D | 0.15 puMWs/Hz |
| Generator Time Constant $T_{G1,2}$ | 5 s |
| Battery time constant $T_{ES}$ | 0.1 s |
| $K_i$, $K_p$ | 3.4, 5 |
| $K_{i\_ES}$, $K_{p\_ES}$ | 0.5, 1.3 |

The eigenvalues of this matrix A based on the given parameters are $\Lambda_{1,2} = -13.9864 \pm 63.0068i$, $\Lambda_{3,4} = -0.4886 \pm 0.4466i$, $\Lambda_5 = -0.2$. Which implies that the system without time-delay in the microgrid control output is stable, as illustrated in Figure 3-10 .

34
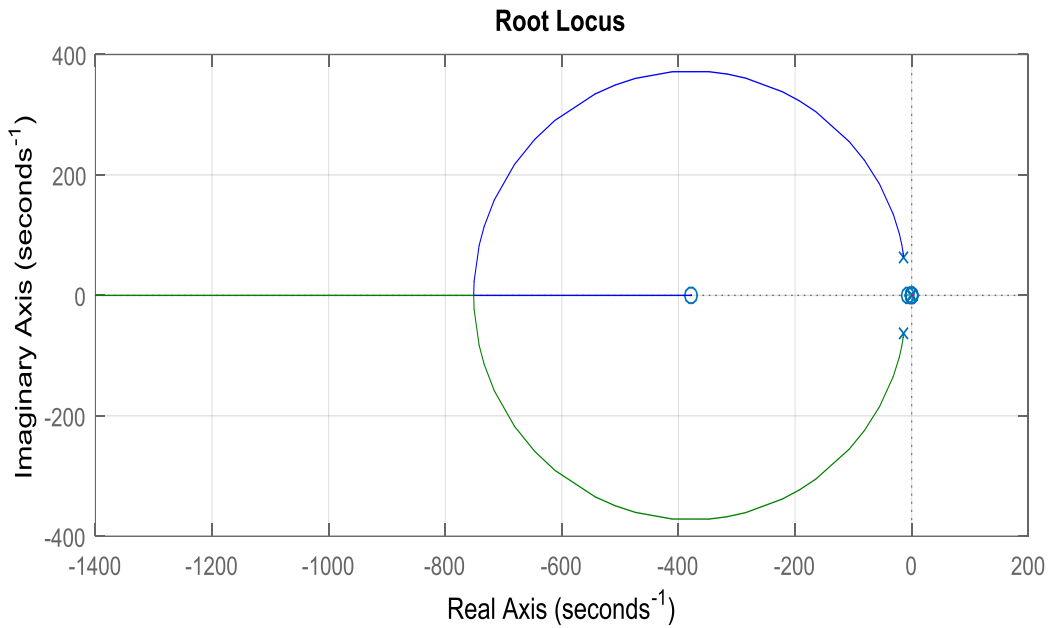
**Figure 3-10 Root locus diagram of the microgrid transfer function.**

*3.3.3.3   Delay injection Simulation results*

In order to illustrate the impact of communication delays on the microgrid operation in Figure 3-7, an equivalent Simulink model of the microgrid were implemented. The delay free operation of the microgrid is shown in Figure 3-11, The response of the power generation is fast enough where the frequency deviation of the bus remains within ± 0.1. In Figures (3-12 to 3-17), the frequency deviation with an injection of 50 ms and 10 ms respectively. We can see that the response of the energy storage is affected the most since the time constant of the ES is relatively smaller than the rest of the system.
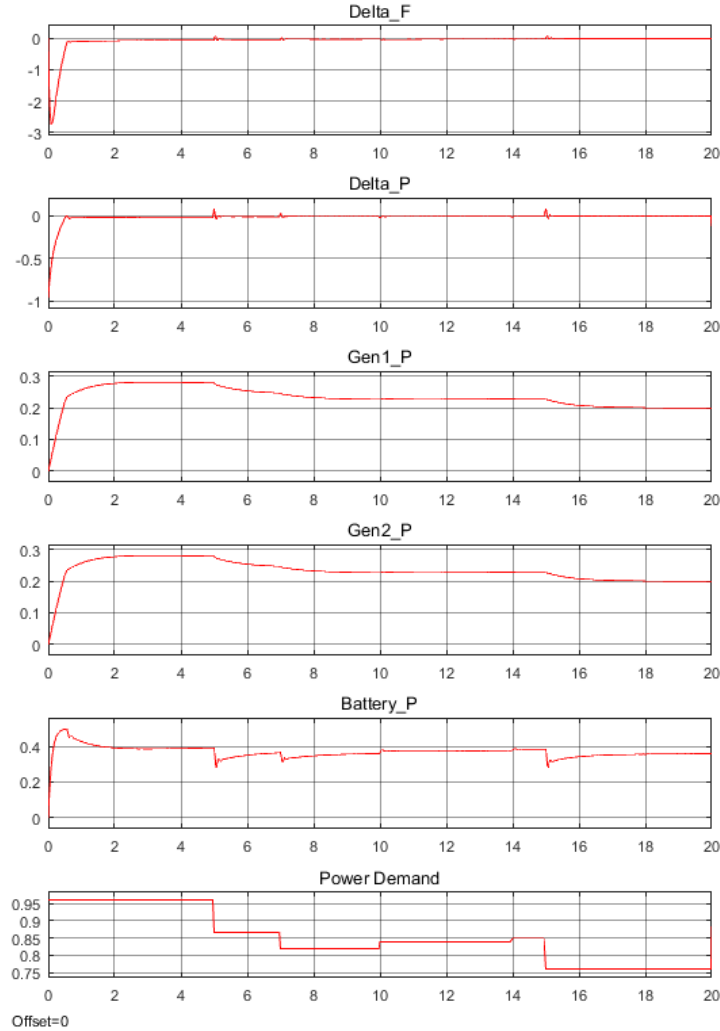
**Figure 3-11 Simulation results without delay injection.**

From Figure 3-11, we can see that the frequency deviation $\Delta f$ close to zero when no delays have been injected into the cyber layer. While Figure 3-12 and Figure 3-13 show a comparison of the frequency deviation when a 50 ms and 10 ms, respectively, are injected into three different locations: i) at the energy storage controller output. ii) at the generators controller output. iii) at the feedback loop. It can be easily determined that the frequency response of the system becomes unstable when the energy storage control signal is impacted by the delay. While the generators signals does not have the same impact due to the inertia of the source and the slower nature of response from the generators.

36
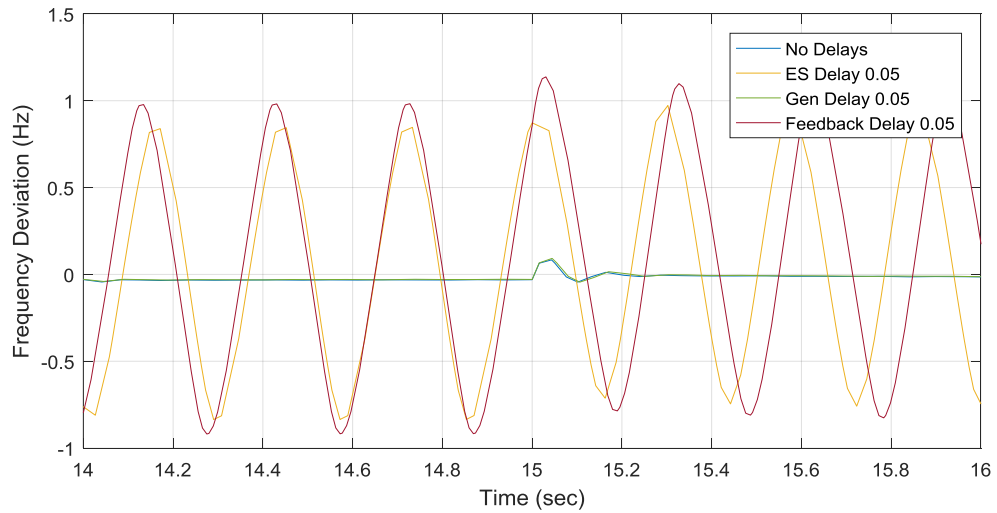
**Figure 3-12 System response when 50 ms delay is injected at Feedback, Generators, and ES separately.**
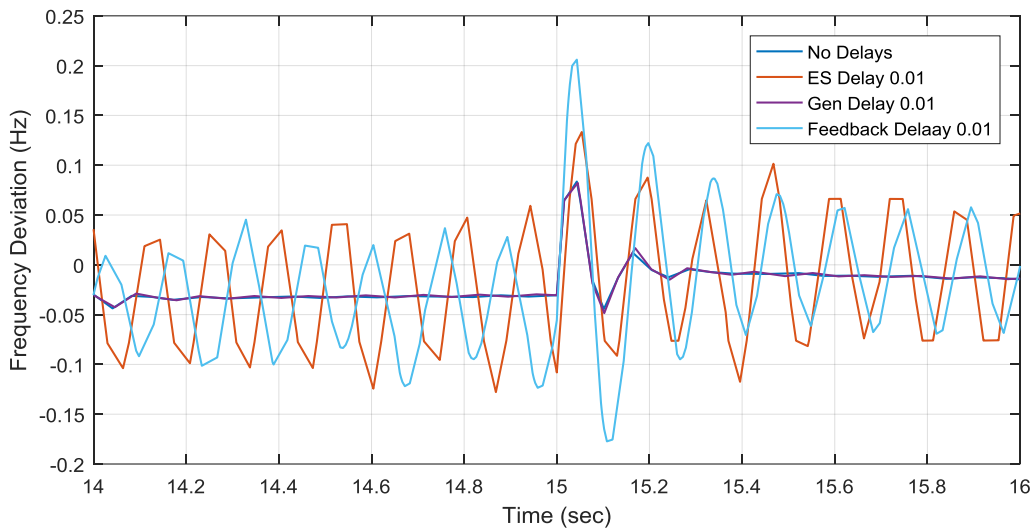


**Figure 3-13 System response when 10 ms delay is injected at Feedback, Generators, and ES separately**

Figure 3-14 to Figure 3-15 show the impact of the previously injected delays on the system response. We can observe the same impact on the active power which leads the to frequency deviation instability, according to the Equation 3-12.
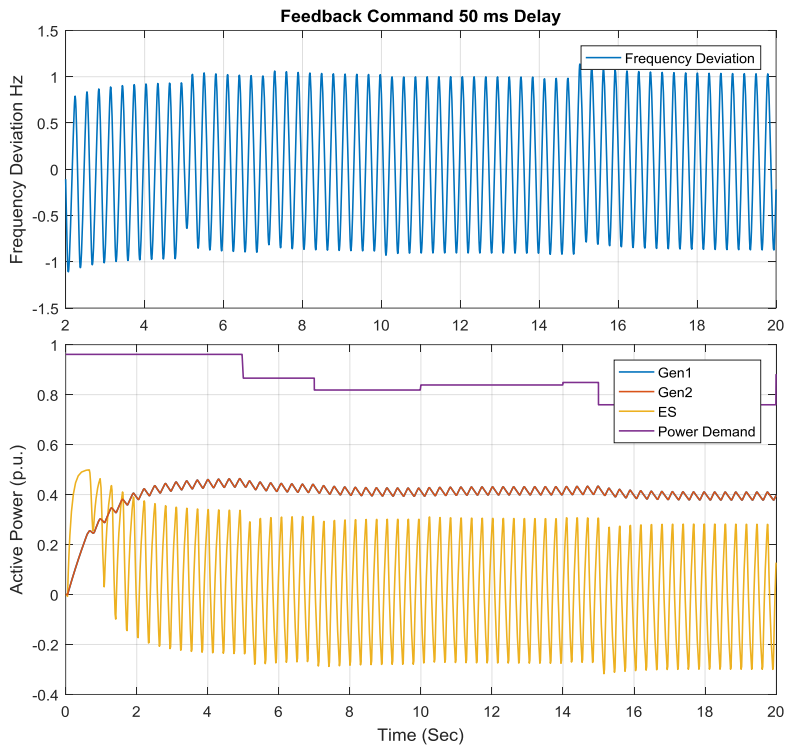
**Figure 3-14 Active power curves for all components with 50 ms delay injection at the Feedback loop.**
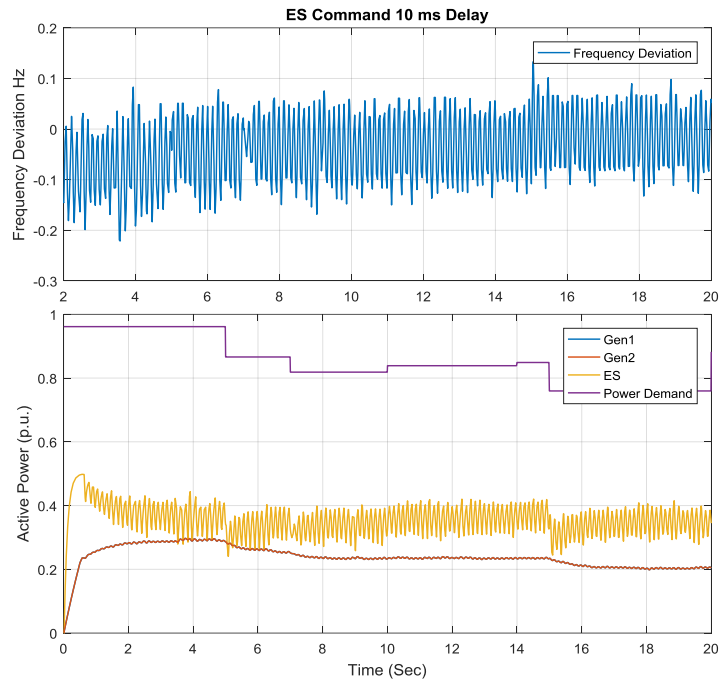


**Figure 3-15 Active power curves for all components with 10 ms delay injection at the Energy storage controller output.**
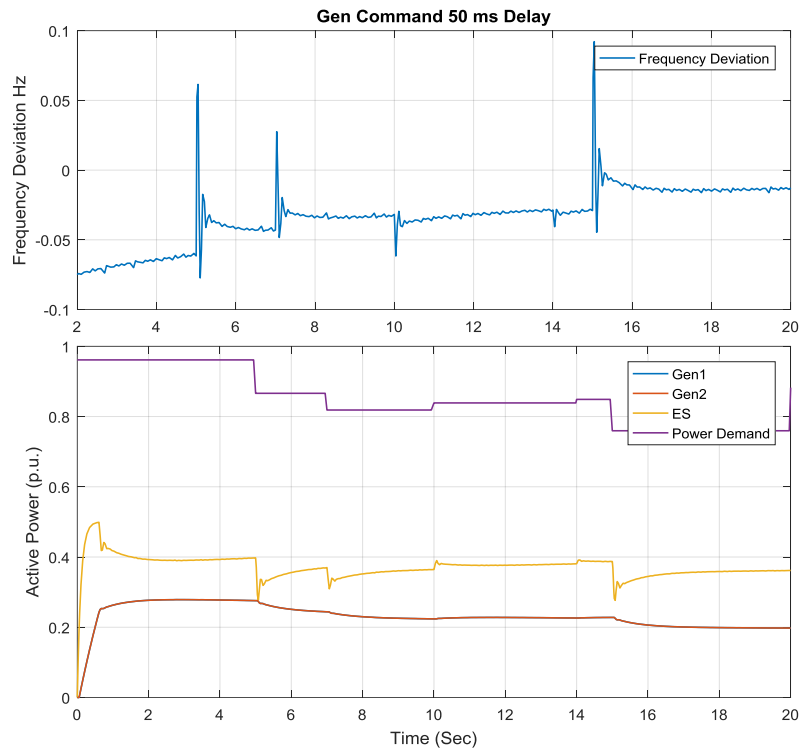
**Figure 3-16 Active power curves for all components with 50 ms delay injection at the Generators controller output.**

# Chapter 4 Concept of True Decentralized Microgrid Control

## 4.1 Distributed Systems

As the distributed energy sources are dispersed over a relatively wide area, interconnection between to each other becomes a challenge in terms of cost and optimality. A true decentralized microgrid control architecture has the following properties:

*Decentralized:* given in the concept, a decentralized architecture suggests having multiple local controllers in order to achieve seamless transients during the operation and acts as if the system has one central controller.

*Resource sharing:* every controller shares the status of its own DER with other controllers in real-time. This requires naming scheme that guarantees unique identification of each controller and its local DER.

*Concurrency:* Each controller must have an up-to-date status of the whole system, especially for the inputs to the microgrid control algorithm running in each controller. This is a key requirement to protect the integrity of the system from being violated, otherwise, inconsistent algorithm outputs and control commands may arise, which can lead to disturbance in the microgrid operation.

*Scalability:* The architecture allows the microgrid to be scaled up or down in terms of the number of power components without affecting the operation or re-engineering the control algorithm.

*Fault-tolerance*: The system must maintain available and operating at the minimum level of reliability. This also include the recovery process in case of faults and possible redundancy that may boost the reliability of the microgrid.
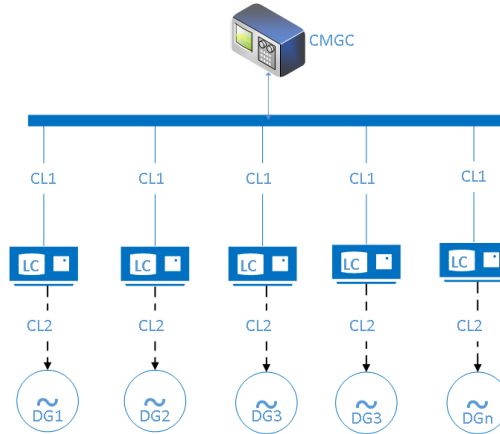


**Figure 4-1 Generic microgrid centralized control architecture model.**
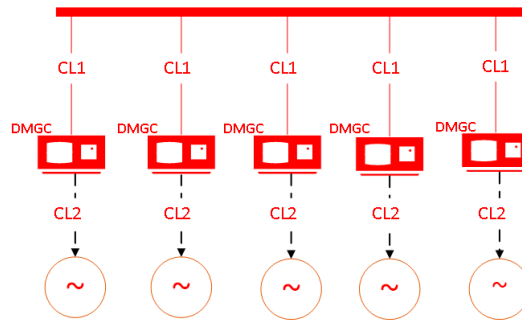


**Figure 4-2 Generic microgrid decentralized control architecture model.**

Figure 4-2 represents the proposed decentralized architecture. As illustrated, the decentralized architecture differs from the architecture in Figure 1-1 by the elimination of the centralized controller, and replacement of local controller with a higher capability decentralized microgrid controller (DMGC), these capabilities are discussed in the controller model.

## 4.2 Proposed Microgrid Control Architecture.

Microgrid control hierarchy [18] identifies three levels of controls; where each level satisfies certain requirements and roles in maintaining power reliability, quality, and economical constraints. Details of each layer are as follows:

### 4.2.1 Primary Control (Device Level)

Device level control entails interacting with the local DER itself to perform certain functions including: physical isolation, on/off, fault clearing (device switching), fault sensing, fault controls, re-synchronization (device protection). For inverter: power conversion, power control, voltage and frequency regulation, primary frequency control (inverter droops, governor droops), island detection, re-synchronization). Most device level controls are performed through tightly-coupled communication media, guaranteeing command delivery and signal delay mitigation.

The proposed system uses Virtual Droop Control [23] which is based on natural droop control [11]. In natural droop, voltage and frequency stability are achieved by drooping the voltage and frequency according to active and reactive power requirement for this control level. For resistive microgrid P/V droop is generally preferred [9], [20]. The various types of droop controllers depending upon the nature of microgrid system, the following are droop equations:

$$f = f^* - m(P - P_{max}) \tag{4-1}$$

$$V = V^* - n(Q - Q_{max}) \tag{4-2}$$
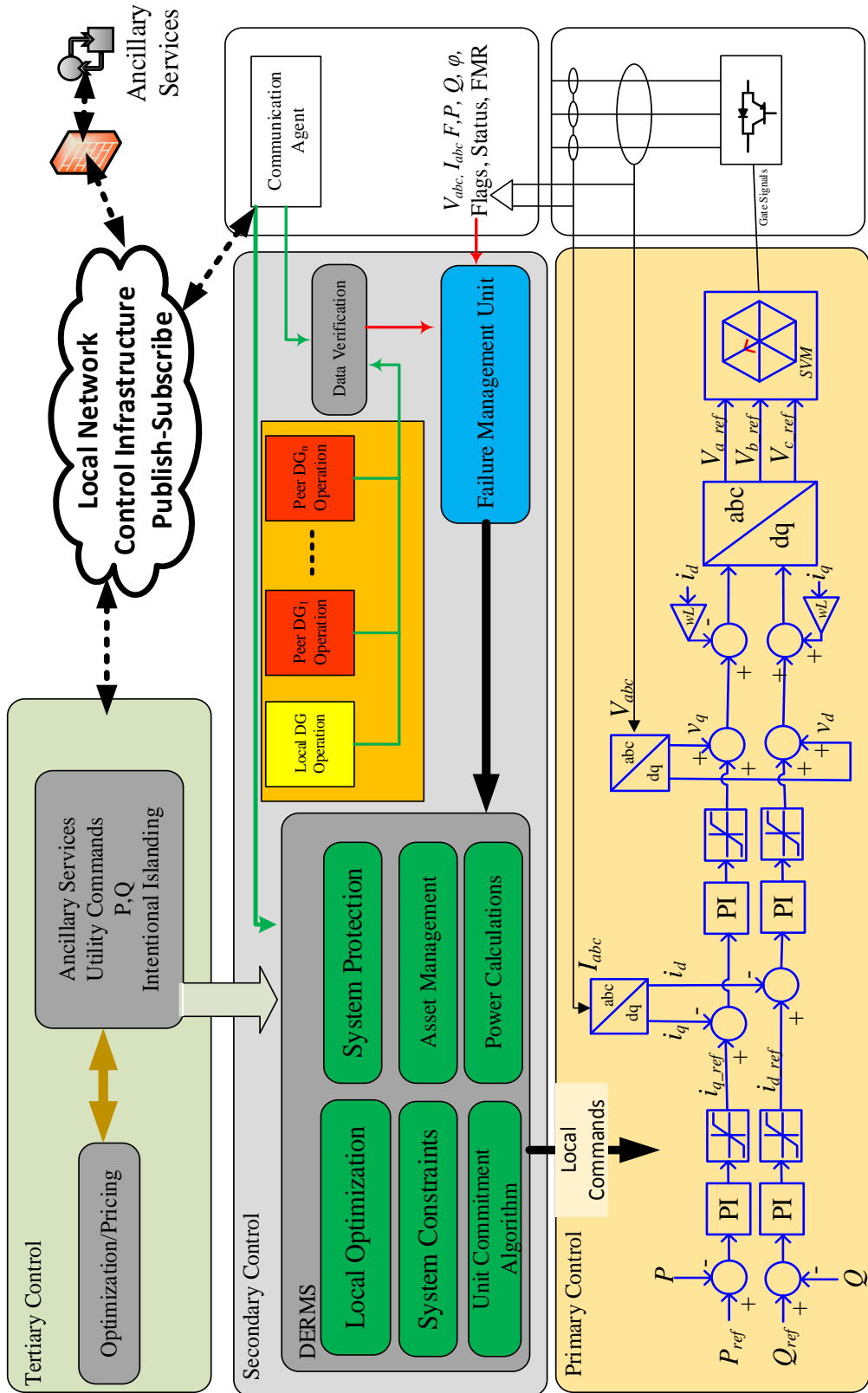
**Figure 4-3 The proposed Decentralized Microgrid Control Architecture (Microgrid Control Hierarchy Implementation).**

where $m$ is the frequency droop coefficient; $n$ is the voltage droop coefficient; $f^*$ is the nominal frequency; $V^*$ is the nominal phase voltage amplitude. Natural droop method is not suitable when the microgrid has nonlinear loads due to the harmonic current. Moreover, all the resources in the microgrid contribute power to the load and operate autonomously

In virtual Droop Control (VDC), a virtual frequency and voltage are created to regulate the active and reactive power output of the sources. The active power output of the energy storage inverter determines the virtual frequency from virtual droop curve. The droop curve is defined between energy storage active power output and virtual frequency. The virtual frequency will determine the active power commands for natural gas generators from a droop relationship, defined between the virtual frequency and active power command of each source. The same concept applies to system voltage. A virtual voltage is determined according to reactive power output of the energy storage inverter. The virtual voltage will determine the reactive power command for natural gas generators from a droop relationship, defined between the virtual voltage of the system and reactive power command of each source. It should be noted that since energy storage inverter is placed in a voltage mode, it supplies the difference between load active and reactive power and other sources in the microgrid. It behaves as a slack bus in a power system concept. Power commands of backup generators are updated only when load variation is greater than defined value. Load variation less than defined value is taken care of by the energy storage inverter [23].

For the Energy Storage, the virtual frequency and virtual voltage are calculated based on the defined curves using the following equations.

$P_{ESmax} < P_{ESmeasured} < P_{ES|f_{rated}}$

$$f_{virtual} = K_{pf}\left(P_{ESmeasured} - P_{ES|f_{rated}}\right) + f_{max}$$

$$K_{pf} = \left(\frac{f_{rated} - f_{max}}{P_{ESmax} - P_{ES|f_{rated}}}\right)$$

(4-3)

$$P_{ES|f_{rated}} < P_{ESmeasured} < P_{ESmin}$$

$$f_{virtual} = K_{pf}(P_{ESmeasured} - P_{ESmin}) + f_{rated}$$

$$K_{pf} = \left(\frac{f_{min} - f_{rated}}{P_{ES|f_{rated}} - P_{ESmin}}\right)$$

(4-4)

$$Q_{ESmax} < Q_{ESmeasured} < Q_{ES|V_{rated}}$$

$$V_{virtual} = K_{vq}\left(Q_{ESmeasured} - Q_{ES|V_{rated}}\right) + V_{max}$$

$$K_{vq} = \left(\frac{V_{rated} - V_{max}}{Q_{ESmax} - Q_{ES|V_{rated}}}\right)$$

(4-5)

$$Q_{ES|V_{rated}} < Q_{ESmeasured} < Q_{ESmin}$$

$$V_{virtual} = K_{vq}(Q_{ESmeasured} - Q_{min}) + V_{rated}$$

(4-6)

$$K_{vq} = \left(\frac{V_{min} - V_{rated}}{Q_{ES|V_{rated}} - Q_{ESmin}}\right)$$

4.2.2   Secondary Control (System Level)

Primary control level is responsible of frequency regulation. During transient operation, deviation of voltage and frequency may occur due to the load power demand fluctuations or intermittency of renewable DGs. In microgrid systems, an advantage of energy storage is enabling the microgrid to compensate for frequency and voltage deviations in a fast manner. The role of secondary control comes at a slower response to frequency fluctuations in comparison the primary control.

The function of the secondary control that works collaboratively to achieve optimization, protection, power calculations (with predefined system constraints), and failure management. Recently, efforts referred to the secondary control as the Energy Management System (EMS), where it continuously monitors the microgrid parameters, going into through data verification, and interacting with the Failure Management Unit. EMS dispatches microgrid components such as energy storage or backup generators for active and reactive power and commands the primary level.

The secondary layer represents the Distributed Energy Resource Management Systems (DERMS) [1]. From the utility perspective, DERs can be in a form of a microgrid (sharing the same bus), or distributed over multiple different feeders in the Distribution System. The following sections explains the operations of this layer, and how they relate the concept of DERMS as a part of microgrid controllers.

### 4.2.3 Tertiary Control (Grid Level)

Generally, the tertiary control level manages the bidirectional power flow between the microgrid and the grid at the point of common coupling (PCC). This level also ensures optimal economical operation of the Microgrid [14]. This dissertation considers implementing the first two layers of controls. The tertiary layer is assigned as a future work.

### 4.3 System Design

Decentralized microgrid control system eliminated the single point of failure (central controller). Three main models are defined to accommodate the requirements of decentralization. For example, the controller should have certain level of embedded intelligence to maintain the

decentralized controllers operating as one virtual unit. Coordination and additional control logic is essential; therefore, three models have been defined as key requirements to proposed architecture.

## 4.3.1 Controller Model

The proposed design of the decentralized controller is shown in Figure 4-4 For simplicity, the design is virtually divided into three main units: Processing unit, where the main control logic algorithm is running, with the interrupt handling routines in case of any system Failures. The processing unit is comprised of data verification and consistency algorithms. These two units are collaboratively responsible of analyzing the inputs from the peer controllers. Faults diagnostic and detection algorithm is required for his design, triggering the interrupt handling routine.
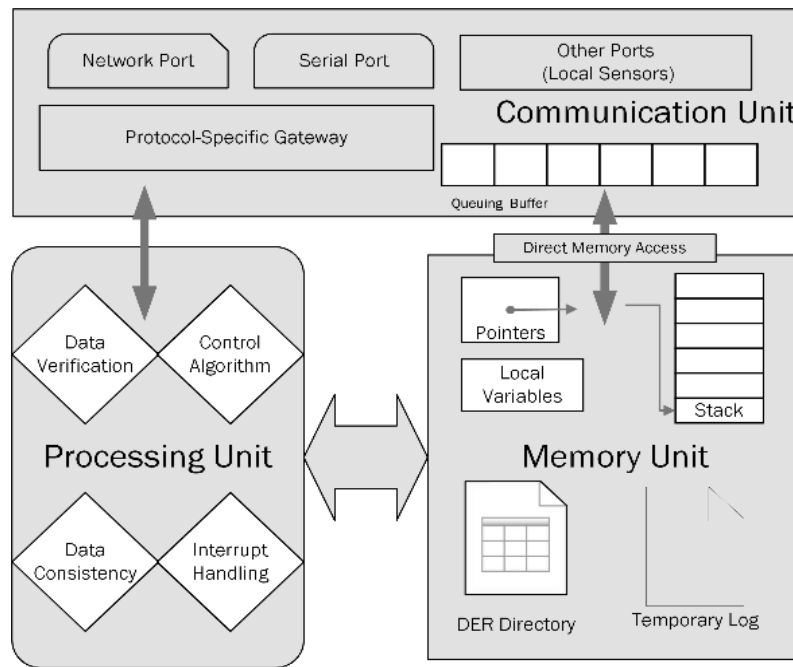


**Figure 4-4. Conceptual Controller design for decentralized controls applications**

The memory unit interacts with the processing unit to manage buffered data and temporary log. It also provides peer controllers information as inputs to the control algorithm. The dynamic DER directory holds the power components object model (Table 4-1).

4.3.2    Data Exchange Model

This model defines three aspects: 1) the necessary data to be exchanged between peer controllers. 2) the way they interact. 3) The frequency of data transmission. Data traffic starts from the electrical component system layer, where the components transmit their status data and measurements through the communication layer. Status data can be breaker status, device warnings or flags, measurements of voltage, active and reactive power, and frequency of each power component. Each controller receives data from its designated DER, validates the received information and synchronizes clocks. Considering possible delays or lost data packets during transmission over the network. Unit commitment and control algorithm utilizes the most recent data inputs and sends back commands through the communication layer, which is responsible of routing the commands to the designated DER.

TABLE 4-1 LOW-BANDWIDTH DEMANDING DATA EXCHANGE MODEL.

| | |
|---|---|
| **DG Type** | Wind, Solar, Energy Storage, Generator…etc. |
| **Identifier** | Unique IP address within the control subnet/Unique ID |
| **Attributes** | Status, active power, reactive power, bus voltage, frequency, breaker status, commands. |

Recently, many efforts have been initiated and led by research institutions, industry partners, and utility to achieve interoperability [1]. For that purpose, many communication frameworks were implemented, adopting certain communication protocols such as DNP3, Modbus, IEC 61850 standard. From a distribution system perspective, DERMS is required to manage a group of DERs.

48

The local controllers are required to communicate to achieve uninterrupted operation. With the evolution of the Industrial IioT, utility suggests using lightweight Publish/Subscribe protocols. The proposed system implements a Publish/Subscribe protocol, which requires low bandwidth communications, and allows more efficient utilization to the bandwidth serving the data exchange frequency. Description of the protocol is provided in Chapter 6.

The control system layer is a combination of the distributed controllers, communication lines, and switching/routing devices in between. Communication agent in Figure 4-3 handles the data exchange between peer controllers, and ensures minimum data loss due to high traffic and network congestion. However, it is tangential to choose the optimal network topology with high connectivity [10]. The proposed system adopts a complete connectivity graph between peer controllers, and applies the concept of consensus cooperative control [16]. Assuming five DERs in a microgrid, the adjacency matrix $A$, this subtopic will be conducted as a future work.

$$A = \begin{bmatrix} 0 & 1 & 1 & 1 & 1 \\ 1 & 0 & 1 & 1 & 1 \\ 1 & 1 & 0 & 1 & 1 \\ 1 & 1 & 1 & 0 & 1 \\ 1 & 1 & 1 & 1 & 0 \end{bmatrix} \tag{4-7}$$

### 4.3.3   Failure model

#### 4.3.3.1   *Failure Model Overview*

One of the challenges that needs to be addressed in any decentralized or distributed system is the resiliency to any component failure that may occur. To consider a system fault-tolerant, each distributed component must have Failure model contains aspects that relate to system reliability and availability (Figure 4-5). Most importantly, designing a self-healing distributed control system relies mainly on the robustness of the recovery algorithm in the interrupt routine.

If power system fault is detected, the controller moves to system fault handling routine. Based on the Status flags reported by peer controllers, faulted DER from the dynamic directory if any failure is detected; the controller goes back to normal operation. Same transitions for detecting communication faults.
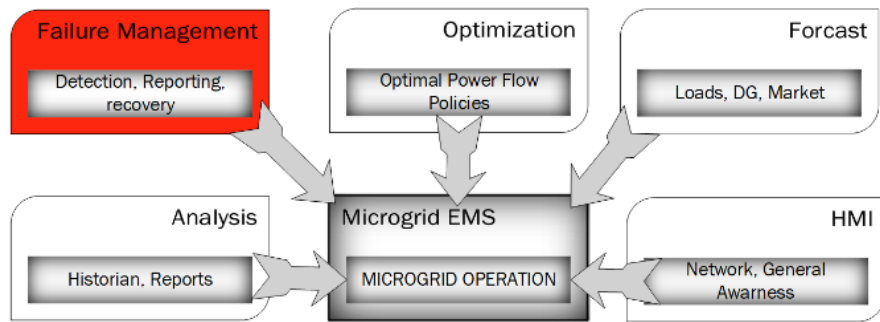


**Figure 4-5. Microgrid Energy Management System sources of optimization data. (Red) is the proposed failure management Unit**

### 4.3.3.2 Fault Detection Methods
#### 4.3.3.2.1 Local Sensing

Sensing local microgrid parameters is essential for microgrid operation control. Leveraging the data collected via local sensing, disturbances can be analyzed to foresee any possible failures in the system. Voltage or frequency changes interpreted as a failure in one power component. Assume a microgrid with $n$ distributed controllers; for a controller $C_i$ at time $t$, local voltage and frequency sensing is governed by equations in Chapter 7.

#### 4.3.3.2.2 Communications

Decentralized architecture dictates the presence of a reliable communication network connecting all peer controllers. Various communication protocols can be applied to such system. Decentralized controllers are designed to have some level of intelligence, where delays and timestamping mismatch can be interpreted as a failure of a controller as in synchronous communications, which triggers the rest of the system to react accordingly. Table 4-2 shows the

difference between the synchronous versus the asynchronous transmissions. The lower bound and upper bound of execution (response) are predefined, and the behavior of communication process can be predicted and used to mitigate any delay effect. For example, in TCP/IP [4], the lack of acknowledgment for the 3-way handshake with any peer controller can be interpreted as a failure, and must be reported.

TABLE 4-2 SYNCHRONOUS VS ASYNCHRONOUS TRANSMISSIONS

| Synchronous | Asynchronous |
| --- | --- |
| Lower and Upper bound for execution time are set | No execution time bounds are set |
| Predictable Behavior (time) | Unpredictable (delays have no bounds) |
| Synchronized time between all components | No synchronization |
| Timeouts can be used to determine communication faults | Timeouts can't be used |

4.3.3.2.3  Peer Reports

We propose a technique for failure detection based on reporting from peer controllers. Since all controllers update their own status and local measurements, a peer report segment (as shown in Figure 4-6)  are allocated to broadcast any detected failures. This overcomes delay of the aforementioned techniques and help propagate the failure incident among all controllers. This technique speeds up the system fault handling as all controllers are informed about any occurring failures.

51
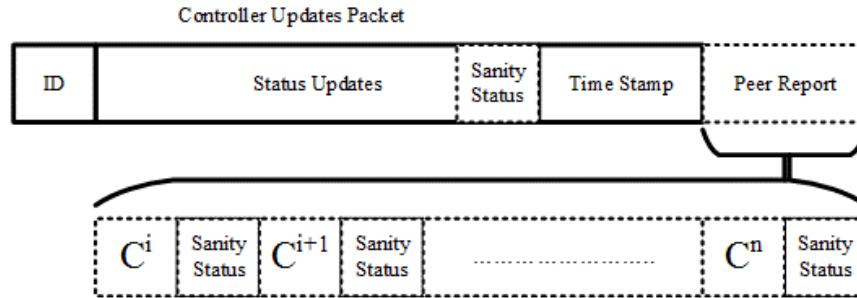
**Figure 4-6 Status update packet with proposed peer report technique.**

4.3.4   Coordinated Failure Management

The system is considered in normal operation when the following conditions are met:

1) Constraint rules are not violated, where the bus voltage and frequency are within limits.

2) Sanity check performed locally results a valid condition.

3) Peer reports are all valid stating that all controllers are working properly and the system is stable.

 Failure analysis are performed continuously after the updates are received from all peers.  In the case of no violations are detected, nor any failure have been reported, the control algorithm maintains at normal operation. If the output from failure analysis and detection is a failure code, the fault handling and recovery takes over and the normal operation algorithm halts.

Unlike other EMS operations, failure management is an essential component of the unit commitment algorithm or the economic dispatch function when decentralized control architecture is deployed. At any time $t$, active and reactive power output of sources and the consumption of

52

loads follows mentioned in Chapter 7. Failure management unit follows algorithms for failure response and recovery, as illustrated in  Figure 4-7 and Figure 4-8.
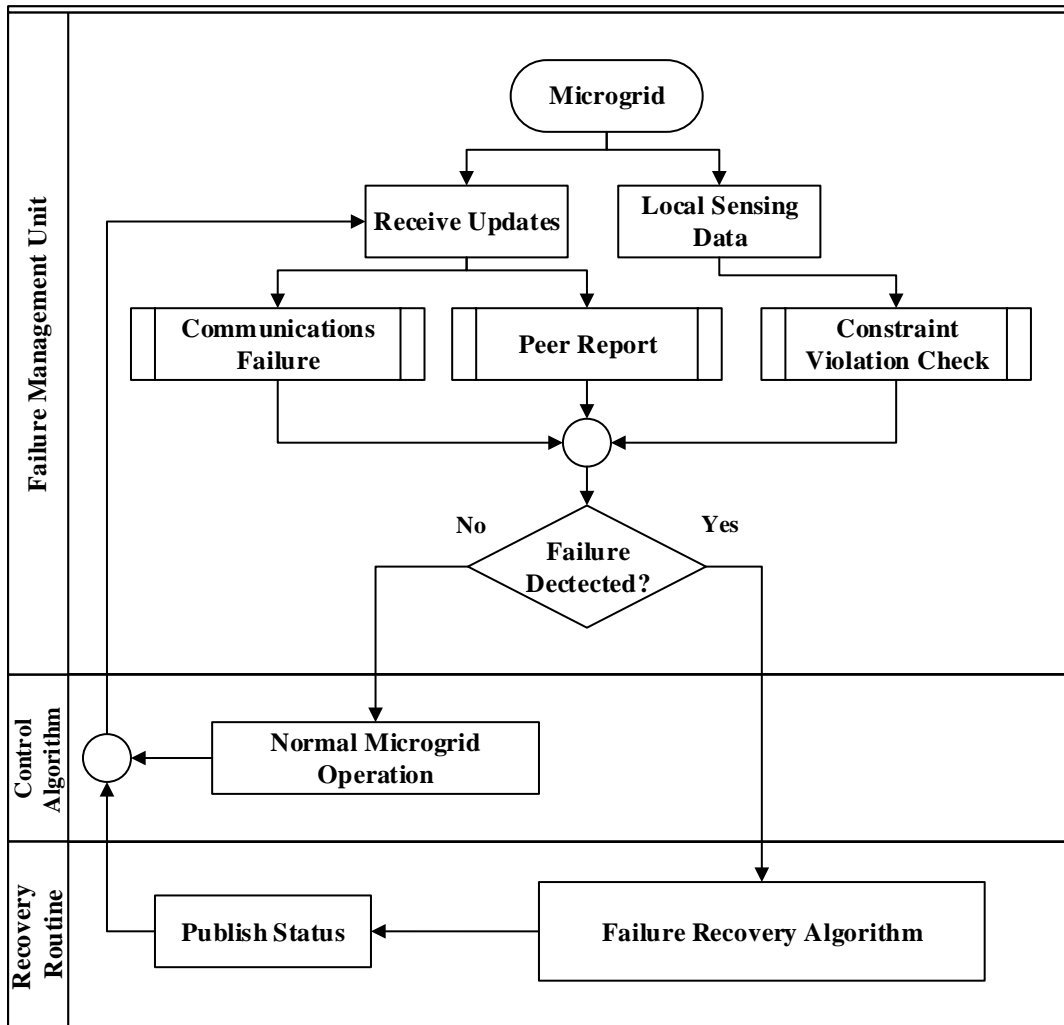


**Figure 4-7 Failure detection and response flowchart**

The flowchart in Figure 4-8 shows the chain of processes that each controller runs to achieve a synchronized outcome for the recovery plan. First, the current power demand is compared to the available DERs' maximum power and dispatches the DERs on a prioritized manner. Depending on the failed controller, the decision of a controller is governed by the impact of the failing branch (controller or DER) on the three main objectives of microgrid operations. Normally, Energy

storage has the fastest response. Worst case scenario is a failure of a component forming the grid

(voltage and frequency), an unintentional reconnection to the grid will be performed.
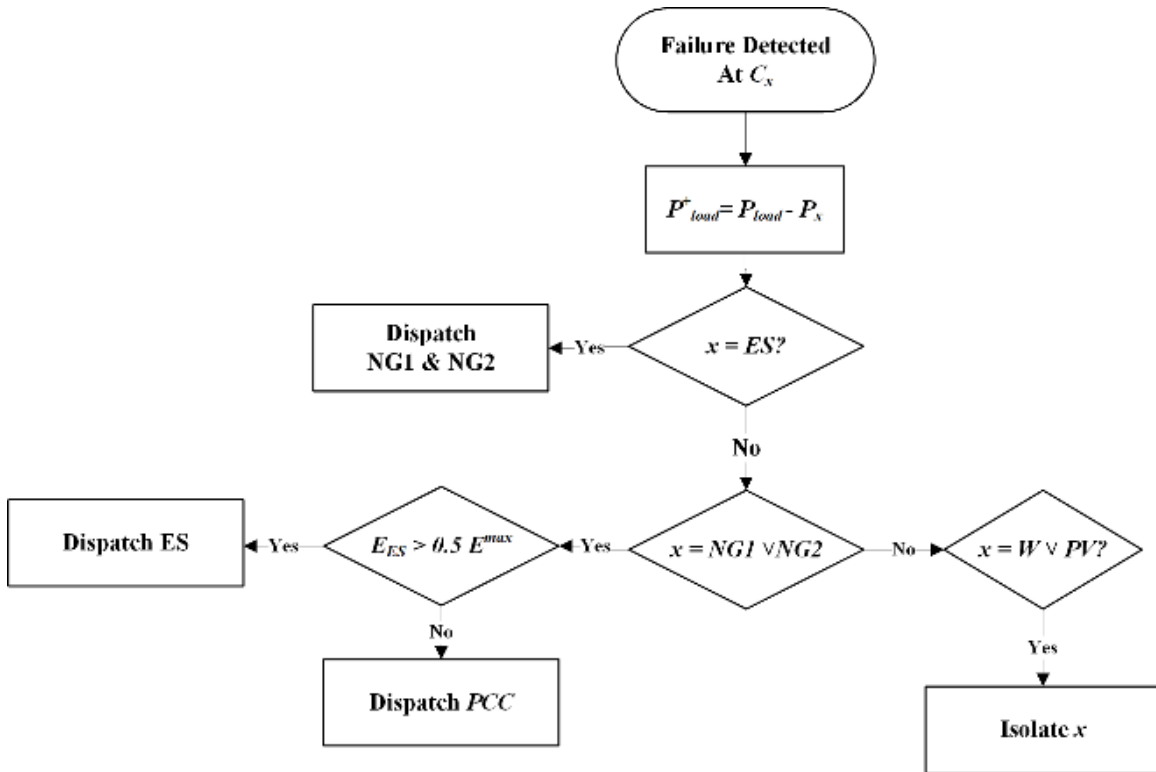


**Figure 4-8 Proposed Failure Recovery Algorithm Flowchart.**

# Chapter 5 Reliability Analysis

## 5.1   Microgrid Reliability

Studying microgrid reliability is a challenge due to the variety of power sources that can be included. Generally, the evaluation of microgrid reliability must consider the load demand, which influences the microgrid architecture at the design stage [50]. Other aspects such as protection schemes are considered as a microgrid reliability enhancement mechanism [51] [52]. The advancement of power electronics research efforts and control strategies for microgrid inverters, and hybrid AC-DC microgrids had invigorated power systems researchers in general to adopt state of the art technologies in designing reliable microgrid systems [53]. Communication-assisted control techniques drove the improvement of microgrid reliability arising cyber-security concerns [63].

The outcome of this chapter is to study the microgrid reliability enhancement and analysis by decentralizing the control architecture, regardless the control method applied. Microgrid reliability analyses are discussed and conducted providing a quantitative evidence of the reliability improvement in decentralized microgrids as opposed to the centrally controlled microgrids.

Microgrids can be deployed for various purposes in an island or grid-connected structure. For example, a microgrid intended to operate in two modes (grid-connected and islanded) can be dispatchable, serving the purpose of supporting the distribution system. Distant microgrids away from the grid usually serve the purpose of continuously and independently supporting local loads. Loads can be categorized into critical and non-critical, and their characteristics can vary from static to dynamic behaviors. Regardless of the type, microgrids under any disturbance or fault condition

have different behavior and performance, while supporting critical loads. The reliability analysis of microgrids is performed here based on three objectives:

1) Supporting critical loads, with the assumption of partially shedable loads.

2) Microgrid bus voltage regulation.

3) Microgrid bus frequency regulation.
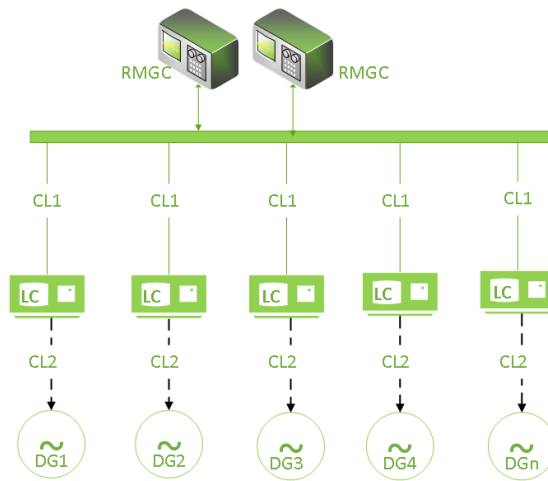


**Figure 5-1 Redundant Control Architecture.**
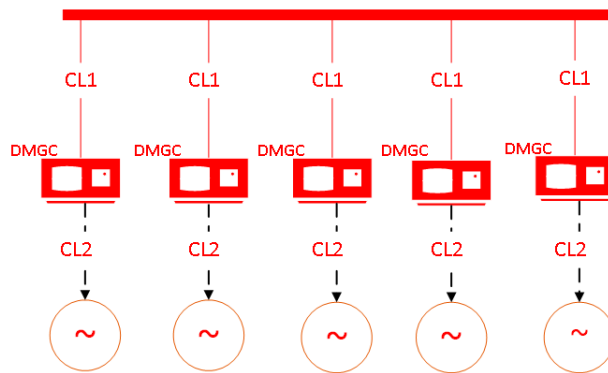


**Figure 5-2 Decentralized Control Architecture.**

## 5.2 Reliability Metrics and Methods

Reliability metrics provide a quantitative representation of how much reliance should we have in a system or a device. In other words, reliability is the probability that a device will perform its intended function under known conditions for a specified time.

### 5.2.1 Metrics and Quantitative Measures

*Definition 1*: Reliability $R(t)$ probability that the component or system experiences does not fail during the during a defined time interval. For repairable systems, if a repair is performed at time $t_1$, reliability curve starts from the initial value of 1.

*Definition 2*: Conditional Failure Rate or Failure Intensity: $\lambda$ is the anticipated number of times an item will fail in a specific time interval. It also can be identified as a reliability measure of a component. This value is normally expressed as failures per million hours (fpmh or $10^6$ hours). Failure rate calculations are based on complex models which include factors using specific component data such as temperature, environment, and stress. In the prediction model, assembled components are structured serially. Thus, calculated failure rates for assemblies are a sum of the individual failure rates for components within the assembly. This is clarified in the following subsections.

Using the failure rate of a component, MTBF, MTTR, MTTF and FIT are reliability terms based on methods and procedures for lifecycle predictions for a product. MTBF (Mean Time Between Failure) in repairable systems, MTTR (Mean Time To Repair), MTTF (Mean Time To Failure) are ways of providing a numeric value based on a compilation of data to quantify a failure rate and the resulting time of expected performance. The numeric value can be expressed using any measure of time, but hours is the most common unit in practice. Figure 5-3 illustrated the

definitions of these metrics. MTBF can be calculated as the inverse of the failure rate $\lambda$ for constant

failure rate systems

$$MTTF = \frac{1}{\lambda}$$ (5-1)

In Repairable systems:

$$MTBF = \frac{1}{\lambda}$$ (5-2)
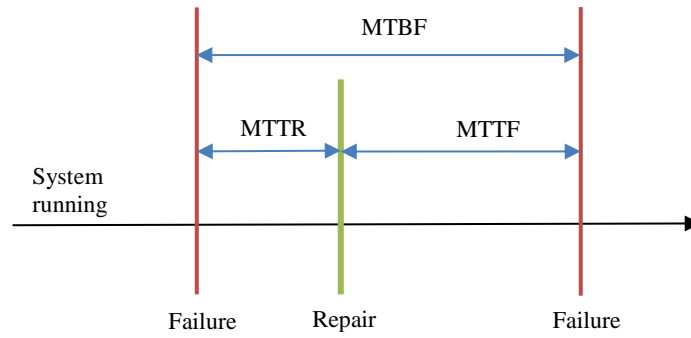


**Figure 5-3 Reliability Metrics Definitions.**

## 5.2.2   Reliability Block Diagrams

The reliability of a system cannot be evaluated or improved unless a detailed understanding of how the elements of the system function and contribute to the overall system operation. A Reliability Block Diagram is a method of modeling how components and sub-system failures combine to cause system failure. Reliability block diagrams may be analyzed to predict the availability of a system and determined the critical components from a reliability viewpoint. A system is considered functioning when there is at least one continuous path from the left side to the right side of the reliability block diagram. The elements in the block diagram may represent only the original components, or redundant components. The following sections provides the

application of RBD on the system being analyzed. The following equations provide some terminology definitions used within this chapter.

Assuming a system of N components, $R_i$ is the reliability of component $X_i$. The reliability of the system assuming the elements are in series (i.e. if a component fails, the whole system fails)

$$R_{series} = \prod_1^N R(X_i)$$

(5-3)

Assuming the system components are all in parallel (i.e. the system fails if all components fail), the reliability is determined by

$$R_{parallel} = \prod_1^N (1 - R(X_i))$$

(5-4)

Figure 6 shows the reliability bock diagram of possible microgrid configurations. Each block represents one possible component or a subsystem with a pre-defined failure rate. A working system remains while a continuous line from left to right is maintained.

Higher reliability of a system is proportional to the degree of parallelization of the reliability model. In microgrids, the controller is a vital component to maintaining operation. As shown in Figure 5-5, The red portion of the diagram represents a controller as in series block to the system. Failure of the controller breaks the line and the system is declared in failure state.

Decentralization of the control architecture eliminates the red portion in  Figure 5-4 making the whole system a bunch of parallel branches. The degree of importance of a controller is calculated using (3) for three cases: 1) Centralized controller architecture. 2) Redundant control

architecture with two controllers. 3) True decentralized control architecture.
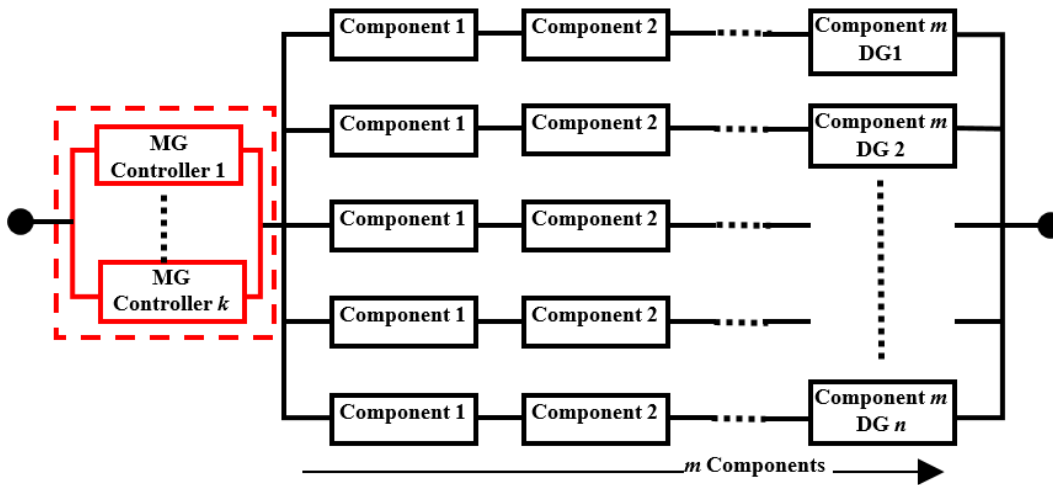


**Figure 5-4 Reliability block diagram of microgrid architecture.**
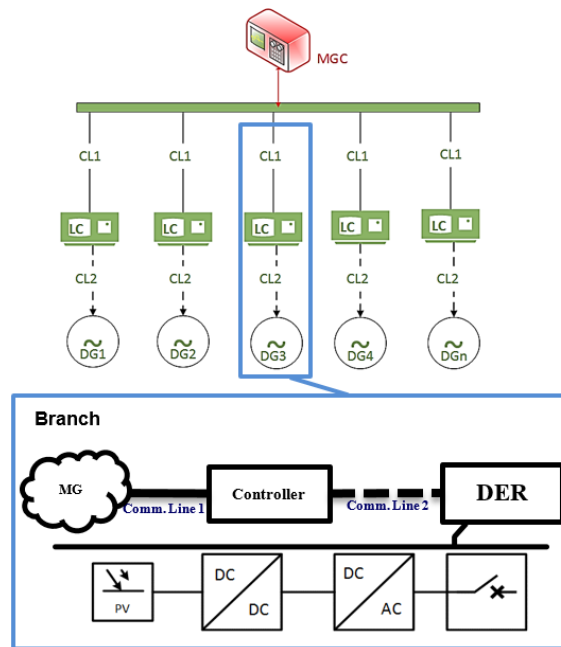


**Figure 5-5 Microgrid Decentralized Control Architecture (Green). Eliminated centralized controller (Red). Example branch components (Subsystem)**

### 5.2.3 Importance of a component (Barlow-Porschan)

The importance of a component indicates the impact of once component's failure on the system

failure [69]. In the early stages of system development, the components life distribution or

60

reliabilities are assumed to be equal. A system with $n$ components, considering a state $x_i$ of component i is defined by

$$x_i = \begin{cases} 1 & if\ i\ is\ functioning \\ 0 & if\ i\ is\ \textbf{not}\ functioning \end{cases} \quad i \in (1, n) \tag{5-5}$$

A deterministic binary function $\varphi$ of the system state, with x as the function vector input $x = (x_1, x_2, \dots, x_n)$.

$$\varphi(x) = \begin{cases} 1 & if\ the\ system\ is\ functioning \\ 0 & if\ the\ system\ is\ \textbf{not}\ functioning \end{cases} \tag{5-6}$$

The structure importance (Barlow-Porschan)

$$I_\varphi(j) = \int_0^1 (h(1_j, P) - (h(0_j, P)\, dp \tag{5-7}$$

In our case, it is possible to calculate the structural importance of component $j$ in structure $\varphi$ using (12).

$$(1_j, P) = (x_1, \dots x_{j-1}, 1, \dots, x_n) \tag{5-8}$$

$$(0_j, P) = (x_1, \dots x_{j-1}, 0, \dots, x_n) \tag{5-9}$$

Where $h(1_j, P)$ the probability that the system operates, as a function of component reliabilities. Equations that govern the importance of three cases from equations (7-9) are shown in the following cases. Where $R_{Cen}(t), R_{Rcon}(t), R_{Dcon}(t)$ are the total system reliability for the three cases, respectively. $R_{CMGC}(t), R_{RMGC}(t), R_{DMGC}(t)$ are the controller reliability for each

case. $R_{PS}(t)$ is the reliability of the system not including the controller (parallel section). $P_{con}, P_{com}$ are the failure probabilities of a controller and any other component, respectively.

Case 1) Centralized:

Figure 5-6 shows the RBD for this case assuming $N = 5$ DGs, the centralized controller in series with the rest of the system. In order to show how much does this configuration affects the system reliability, equations (4-4 to 4-8) are applied. For this case the importance of a centralized controller is very dominant, which can be seen as a single point of failure to the overall system. While the rest of the components contribute to around 3% of the total system reliability.

$$R_i(t) = P$$
(5-10)

$$R_{PS}(t) = 1 - \left(\prod_{i=1}^{n}\left(1 - \prod_{j=1}^{m} R_i(t)\right)\right) = 1 - (1 - P^m)^n$$
(5-11)

$$R_{Cen}(t) = R_{MGC}(t) * R_{sys}(t)$$
(5-12)

$$R_{Cen}(t) = P_{con}(1 - (1 - P_{com}^m)^n)$$
(5-13)

Assuming 5 DGs in the system

$$h(1_{Ccon}, P) = 1 - (1 - P^4)^5$$
(5-14)

$$h(0_{con}, P) = 0$$
(5-15)

$$h(1_{CL1}, P) = P\left(1 - (1 - P^4)^4 * (1 - P^3)\right)$$

$$h(0_{CL1}, P) = P(1 - (1 - P^4)^4)$$

$$I_\varphi(MGC) = \int_0^1 1 - (1 - P^4)^5 - 0 \, dp = 0.4116 = 41.16\%$$

$$I_\varphi(CL1) = I_\varphi(LC) = I_\varphi(CL2) = I_\varphi(DG)$$

$$= \int_0^1 P\left(1 - (1 - P^4)^4 * (1 - P^3)\right) - P(1 - (1 - P^4)^4) \, dp = 0.0294 = 2.94\%$$
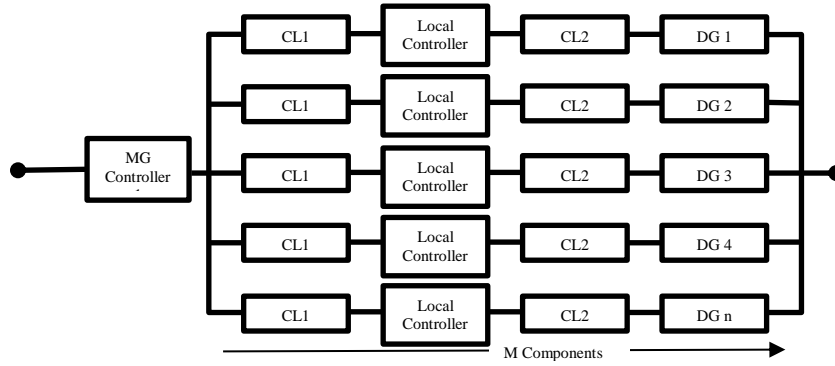


**Figure 5-6 Reliability block diagram for the centralized case.**

Case 2) Redundant:

Similarly, in case of a redundant controller added to the system, the RBD becomes as in Figure 5-7. Applying degree of importance equations results with:

$$R_i(t) = P \tag{5-16}$$

$$R_{RMGC}(t) = 1 - (1 - P)^2 \tag{5-17}$$

$$R_{Cen}(t) = R_{MGC}(t) * R_{sys}(t) \tag{5-18}$$

$$R_{RED}(t) = R_{RMGC}(t) * R_{PS}(t) = 1 - (1 - P)^2 * (1 - (1 - P^m)^n) \tag{5-19}$$

$$h(1_{RMGC}, P) = 1 - (1 - P^4)^5 \tag{5-20}$$

$$h(0_{con}, P) = 0 \tag{5-21}$$

$$h(1_{RMGC}, P) = 1 - (1 - P^4)^5$$

$$h(0_{RMGC}, P) = (1 - (1 - P)) * 1 - (1 - P^4)^5$$

$$h(1_{CL1}, P) = (1 - (1 - P)^2) * \left(1 - (1 - P^4)^4 * (1 - P^3)\right)$$

$$h(0_{CL1}, P) = 1 - (1 - P)^2 * (1 - (1 - P^4)^4)$$

$$I_\varphi(RMGC) = 0.0963 = 9.63\%$$

$$I_\varphi(CL1) = I_\varphi(LC) = I_\varphi(CL2) = I_\varphi(DG)$$

$$= \int_0^1 P\left(1 - (1 - P^4)^4 * (1 - P^3)\right) - P(1 - (1 - P^4)^4) \, dp$$

$$= 0.0404 = 4.04\%$$

For this case, adding redundancy to the controllers decreases the significance of a single controller, which leads to a better reliability of the microgrid system.
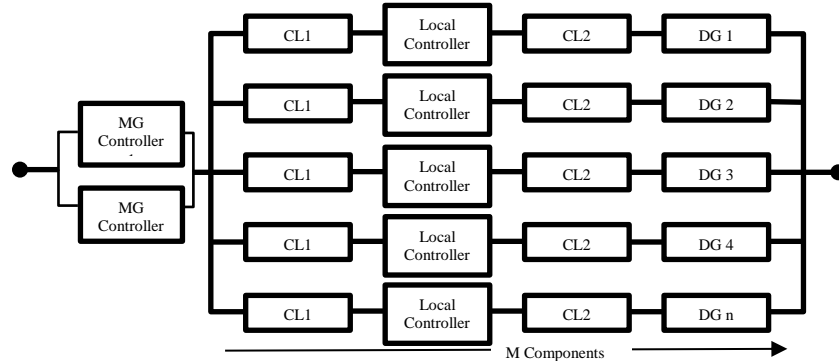


**Figure 5-7 Reliability block diagram for the redundancy case.**

Case 3) Decentralized:

For the decentralized case, the in-series controller block is eliminated and the overall system becomes a bunch of parallel branches. This is expected to improve the microgrid reliability.

Applying the degree of importance equations to determine the degree of importance of the controller results with:

$$R_i(t) = P \tag{5-22}$$

$$R_{DEC}(t) == (1 - (1 - P_{com}^m)^n) \tag{5-23}$$

$$h(1_{DMGC}, P) = 1 - ((1 - P^4)^4 * (1 - P^3)) \tag{5-24}$$

$$h(0_{DMGC}, P) = 1 - (1 - P^4)^4$$

$$h(1_{CL1}, P) = 1 - ((1 - P^4)^4 * (1 - P^3))$$

$$h(0_{CL1}, P) = 1 - (1 - P^4)^4$$

$$I_\varphi(DMGC) = \int_0^1 (1 - (1 - P)^2) * (1 - (1 - P^4)^4 * (1 - P^3)) - (1 - P^4)^5$$

$$- (1 - (1 - P)^2 * (1 - (1 - P^4)^4)) \, dp = 0.05 = 5.0\%$$

$$I_\varphi(CL1) = I_\varphi(LC) = I_\varphi(CL2) = I_\varphi(DG)$$

$$= \int_0^1 P\big(1 - (1 - P^4)^4 * (1 - P^3)\big) - P(1 - (1 - P^4)^4) \, dp$$

$$= 0.05 = 5.0\%$$
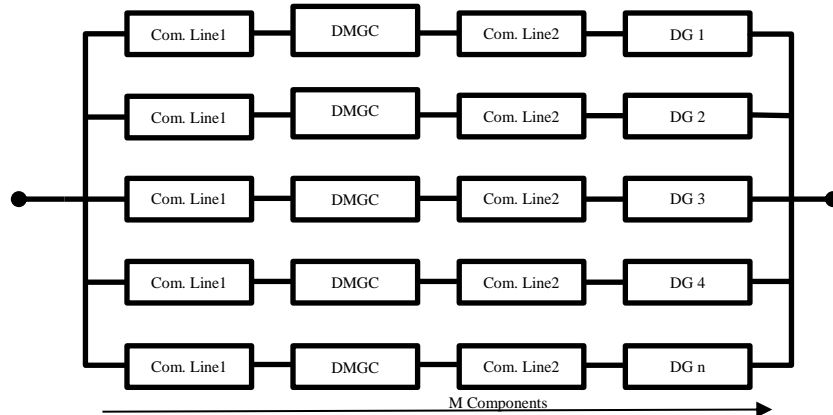


**Figure 5-8 Reliability block diagram for the decentralized case.**

Figure 5-9 shows the calculation results of importance analysis in a microgrid control architecture for the aforementioned cases. Assuming *M = 4* in-series components in a parallel branch, and varying the number of possible DGs in a microgrid. Scaling up the microgrid, the importance of a controller increases in the centralized architecture even with a redundant controller. However, due to parallelization in decentralized architecture, the importance of each controller decreases as the microgrid scales up in in terms of the number of DGs.
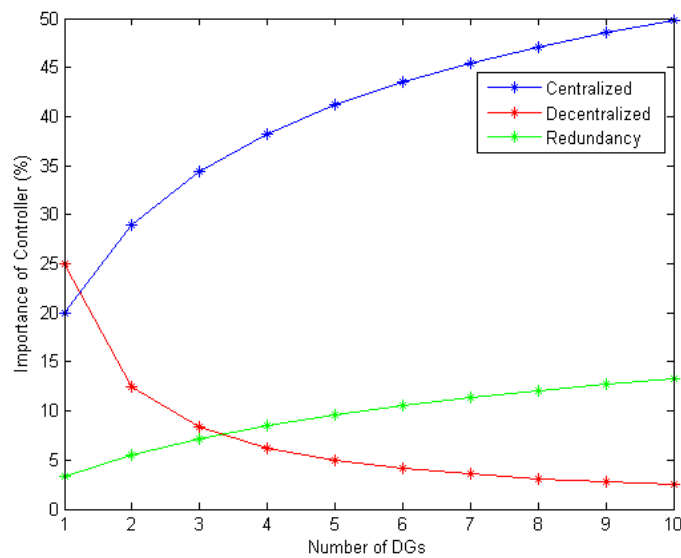


**Figure 5-9 Degree of importance variation of a single controller in a microgrid system.**
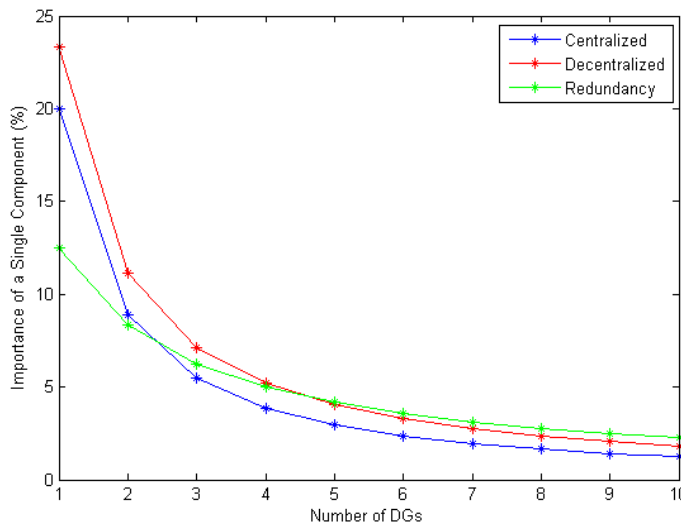


**Figure 5-10 Degree of importance of other components in a microgrid system.**

66

## 5.3　Applying Markov Chain Reliability Method

MRM uses a stochastic process to model the system with several states and transitions between states. A Markov reliability model contains a series of the possible states in the system and uses possible failure rates and repair rates between those states. If *X(t)* is denoted as a random variable in Markov process, then $P_{ij}$ of transitioning probability from state $i$ at *t=0* to state j at *t* is

$$P_{ij} = P[X(t) = j \,|X(t) = i] \qquad\qquad 5\text{-}25)$$

The probability of transitioning from state $i$ to state $j$ does not depend on the global time and only depends on the transition time interval. A simple Markov process for Figure 5-4 is shown in Figure 5-11. The states in Figure 5-11 show transition from state 0 which is the healthy state to state 1, when component A fails but the system survives. State 2 when component 2 fails but the system survives, and state 5 when component 3 fails and the system fails since component 5 ties the rest of the system to the output. Staying at a state means that no new fault even happened. State 5 is an absorbing state of system failure since every physical system is expected to fail at some point in time.

The transition from state $i$ to $j$ depends on the transition time interval $\Delta t$, and does not have a memory characteristic. For a system of $n$ states, a probability transition matrix is defined as

$$\boldsymbol{P}(\Delta t) = \begin{bmatrix} P_{11}(\Delta t) & P_{12}(\Delta t) & \cdots & P_{1n}(\Delta t) \\ P_{21}(\Delta t) & P_{22}(\Delta t) & \cdots & P_{2n}(\Delta t) \\ \vdots & \vdots & \ddots & \vdots \\ P_{n1}(\Delta t) & P_{n2}(\Delta t) & \cdots & P_{nn}(\Delta t) \end{bmatrix} \qquad\qquad 5\text{-}26)$$

Where

$$P_{ij}(\Delta t) \geq 0 \quad i,j \in [1,n] \qquad\qquad 5\text{-}27)$$

$$\sum_{j=1}^{n} P_{ij}(\Delta t) = 1, \quad i \in [1, n] \tag{5-28}$$

Equation (5-26) can be written as (5-29) due to homogeneous property.

$$P = \begin{bmatrix} P_{11} & P_{12} & \cdots & P_{1n} \\ P_{21} & P_{22} & \cdots & P_{2n} \\ \vdots & \vdots & \ddots & \vdots \\ P_{n1} & P_{n2} & \cdots & P_{nn} \end{bmatrix} \tag{5-29}$$

Markov reliability models can be simulated based on failure rates $\lambda$ of system components instead of probability of failure $P$, forming a transition matrix $M$. If the system is repairable, repair rates $\mu$ are included to the transition matrix [70]. Simulation of the reliability model results with a predicted reliability of the system. An example of such technique is proposed in the next section.

## 5.4 Reliably of Decentralized Control Architectures

Figure 5-5 shows the proposed microgrid decentralized control architecture. By eliminating the centralized controller of a conventional architectures, the system transforms into certain number of parallel branches (subsystems). For this study purposes, each branch is assumed to have four components: the local decentralized controller, and two communication lines and the distributed generation (DG) unit. As an example, the DG in the expanded branch illustrates a PV system.

Creating a Markov reliability model for the system in Figure 5-5 results with transition matrix representing 241 states, assuming a microgrid has 5 DGs with centralized architecture, and $2^{40}$ in decentralized architecture. Due to large number of states. Lumping technique is used to simplify the transition matrix for the Microgrid System [20]. Reliability of each branch is evaluated using Markov modeling. Two cases are considered, repairable and non-repairable. In a non-repairable

68

system, failure of any component is considered permanent. A repairable system is a practical case in power systems, where a failed component is repaired or replaced after failure is discovered. Markov chain simulation predicts the steady state reliability of the system. A repairable system converges to certain reliability with time, on the contrary of a non-repairable system where the reliability curves converges to 0, depending on the simulation time.
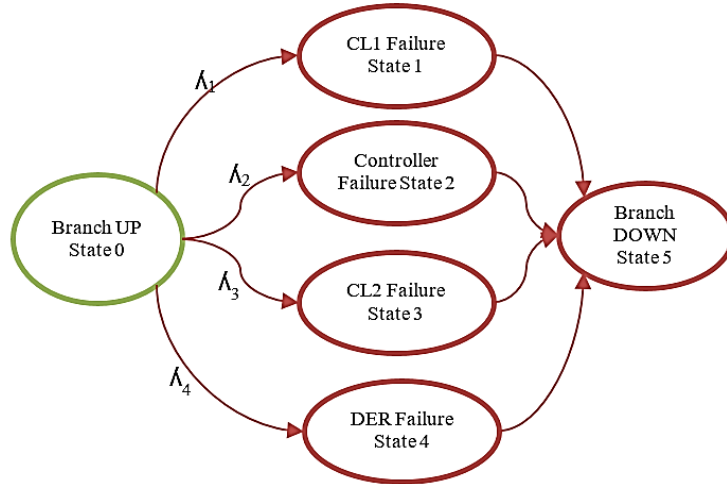


**Figure 5-11 Markov model and state transition diagram for a parallel branch.**

For each branch, the transition matrices as non-repairable and repairable cases are depicted in equations (5-32) (5-33) respectively, following Table of branch states and reliability.

$$P(t) = [P_{00}(t) \quad P_{01}(t) \quad P_{02}(t) \quad P_{03}(t) \quad P_{04}(t)]$$

(5-30)

$$\dot{P}(t) = P(t).M$$

(5-31)

$$M_{No\_Repair} = \begin{bmatrix} * & \lambda_1 & \lambda_2 & \lambda_3 & \lambda_4 \\ 0 & 0 & 0 & 0 & 0 \\ 0 & 0 & 0 & 0 & 0 \\ 0 & 0 & 0 & 0 & 0 \\ 0 & 0 & 0 & 0 & 0 \end{bmatrix}$$

(5-32)

69

$$M_{Repair} = \begin{bmatrix} * & \lambda_1 & \lambda_2 & \lambda_3 & \lambda_4 \\ \mu_1 & -\mu_1 & 0 & 0 & 0 \\ \mu_2 & 0 & -\mu_2 & 0 & 0 \\ \mu_3 & 0 & 0 & -\mu_3 & 0 \\ \mu_4 & 0 & 0 & 0 & -\mu_4 \end{bmatrix} \qquad (5\text{-}33)$$

The asterisk value is the negative summation of the rest of the row. **Figure 5-12** and Figure 5-13 show the reliability curves based on Markov Chain simulation for each branch based on the branch states listed in Table 5-1.

TABLE 5-1 BRANCH STATES AND RELIABILITY.

| State | DER $R_1(t)$ | CL2 $R_2(t)$ | Controller $R_3(t)$ | CL1 $R_4(t)$ | System State C | $P(t)$ |
|---|---|---|---|---|---|---|
| 0 | Up | Up | Up | Up | Up | $R_1(t)* R_2(t)* R_3(t)* R_4(t)$ |
| 1 | Down | Up | Up | Up | Down | $(1\text{-}R_1(t))* R_2(t)* R_3(t)* R_4(t)$ |
| 2 | Up | Down | Up | Up | Down | $R_1(t)* (1\text{-}R_2(t))* R_3(t)* R_4(t)$ |
| 3 | Up | Up | Down | Up | Down | $R_1(t)* R_2(t)* (1\text{-}R_3(t))* R_4(t)$ |
| 4 | Up | Up | Up | Down | Down | $R_1(t)* R_2(t)* R_3(t). (1\text{-}R_4(t))$ |
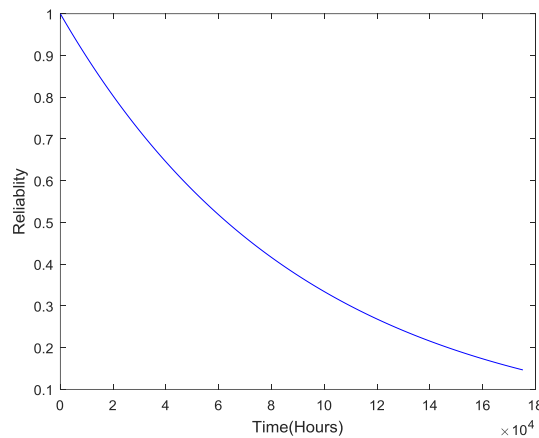


**Figure 5-12 Markov Chain Reliability results for each branch (No Repairs)**
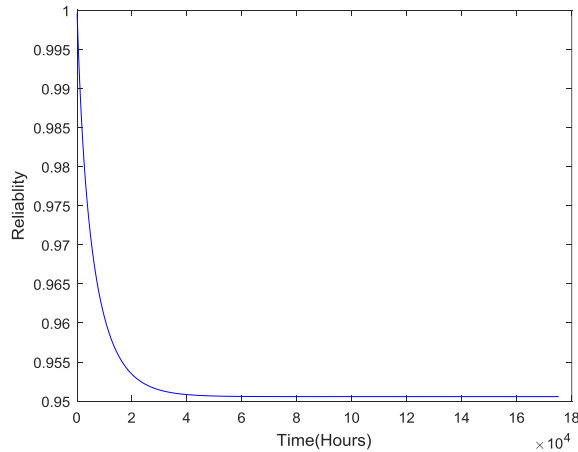
**Figure 5-13 Markov Chain Reliability Simulating Results for Each MG Branch (With Repair)**

Similarly, given a microgrid with 5 DGs, transition matrices are implemented. Using lumping technique, the number of states are reduced, since the microgrid are now consisting of 5 subsystems in addition to the controller (in case of centralized). Equations (5-34) (5-35) shows the transition matrices for both cases.

$$M_{Centralized} = \begin{bmatrix} A \\ B \\ C \\ D \end{bmatrix} \tag{5-34}$$

Where *A* and *B* are 20X64 matrices. *A* and *B* represent the acceptable states and critically acceptable states respectively (total of 20 states). At these states, the centralized controller is in working state, while in *C* and *D* (44X64 matrices)*,* the controller is down and the microgrid system is considered down or unstable and requires shutting down (total 44 states). In case of decentralization of controls, the transition matrix is reduced to 50% in terms of number of states since a single point of failure has been eliminated which is depicted as the red portion of the block diagram in Fig.4. The transition matrix for this case is defined as

71

$$M_{Decentralized} = \begin{bmatrix} A \\ B \end{bmatrix} \qquad\qquad (5\text{-}35)$$

Where *A* and B are 20x32 and 12x32 matrices, respectively. The failure states follow the same description of the centralized transition matrix.

Markov Chain simulation is performed using MATLAB©. Equivalent failure rates for each branch is calculated for the equivalent fault tree [70]. The Matlab code for the simulations can be found in the Appendices B to D. The main purpose of such analysis is to identify the improvement of the overall microgrid system reliability moving from centralized to decentralized architecture. Another purpose is to study the impact of a single controller on the overall system in both architectures. The probability distribution vector (5-36) is obtained using the transition matrix. Figure 5-14 shows the flow chart of the conducted MCM simulations.

$$P(t) = [P_0(t) \dots P_n(t)] \qquad\qquad (5\text{-}36)$$

$$\dot{P}(t) = P(t) \cdot M \qquad\qquad (5\text{-}37)$$

## 5.5  Simulation Results

The results of the Markov reliability simulations are illustrated in Figure 5-15, and Figure 5-16. Figure 5-15 shows the reliability curves of the overall microgrid system for the two architectures: centralized and decentralized. The reliability function R(t) is the probability that an item does not fail in the time interval (0, t].

In centralized case, the oval microgrid reliability decreases with time and goes below 50% at 2.5 years, in comparison to approximately 90% with decentralized architecture. However, for a

practical case where the system is repairable; the reliability of the microgrid converges to 56% in 12 years with a centralized architecture compared to a 94% for the same time period in decentralized architecture.
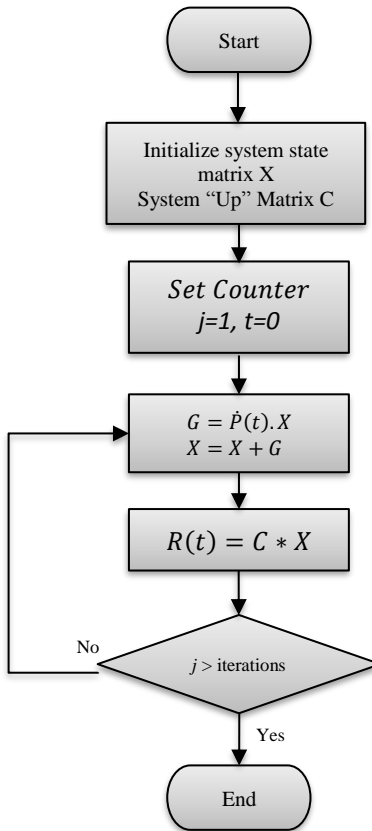


**Figure 5-14 Markov Chain Modeling & Simulation Flow Chart**

Four improvements of controller failure rates are included in simulations results , which reflect 20% decrease in failure rate of single controller. validating the results in Figure 5-9, the degree of importance of a single controller on the overall system reliability is larger in the case of centralized architecture. Generally, scaling up the microgrid (increasing the number of DGs), the overall reliability of the microgrid is improved when the architecture is decentralized, unlike the centralized choice where the reliability decreases.
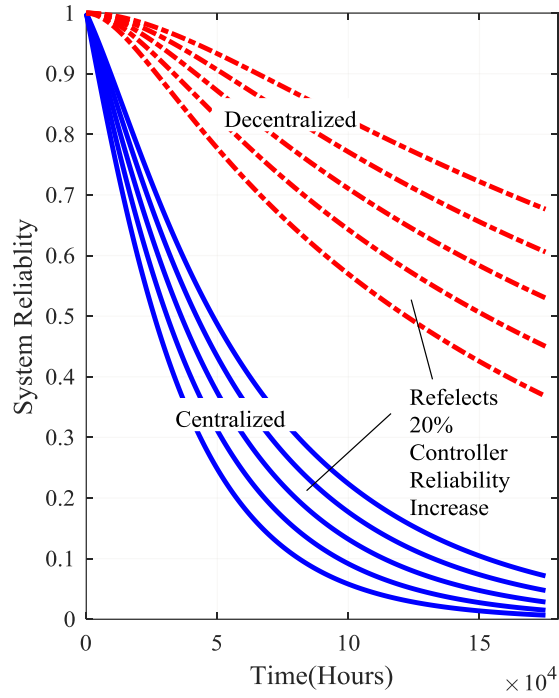
**Figure 5-15 Microgrid system reliability curve assuming no repairs.**
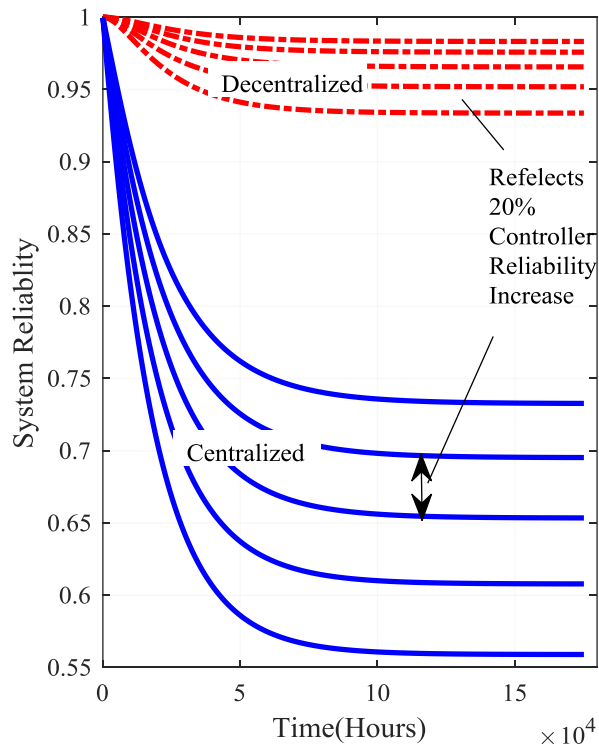


**Figure 5-16 Microgrid system reliability curves (repairable system).**

74

# Chapter 6 Hardware in the loop (HIL) Emulation for Microgrids

## 6.1    Hardware In-the Loop Systems

Hardware-in-the-loop (HIL) simulation is a technique for testing and validating a target controller running a control algorithm. This technique creates a virtual real-time environment that represents a physical plant or a simulated complex system. From the perspective of the controller under testing, the simulated plant is seen as an actual plant as a high accuracy of the plant model is achieved. HIL helps to test the behavior of the control algorithms without physical prototypes. Figure 6-1 Concept of Hardware-In-the-Loop Simulation System.Figure 6-1 shows the concept of a Hardware-In-the-Loop system.
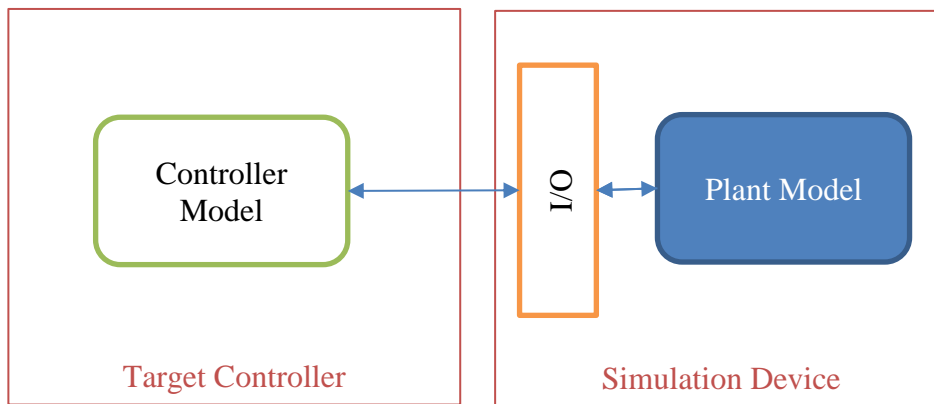


**Figure 6-1 Concept of Hardware-In-the-Loop Simulation System.**

## 6.2    Microgrid HIL Types and Examples

Real-time HILS systems is a powerful and a convenient tool for power system studies due to the possibility allow for hardware device to be tested in a real test conditions before deployment in the actual system and commissioned. It can also minimize the risk and cost to examine extreme conditions to identify hidden flaws before their impact manifests in actual operation. Using HIL,

we can create and simulate a cost effective virtual real-time implementation of physical components such as a plant, sensors, and actuators on a real-time target computer. As seen in Figure 6-2, simulation is an essential part of HIL platforms. For validation purposes, the control algorithm on an embedded controller and run the plant or environment simulation model in real time on a target computer connected to the controller. The embedded controller interacts with the plant model simulation through various I/O channels.

In power system, two major types of HIL platforms is implemented: i) Controller-I.-the-Loop (CIL), and ii) Power Hardware-In-the-Loop (PHIL). The main difference between the two types is the component under testing. In CIL (Figure 6-2 (b)), the controller of a power system (i.e. microgrid controller) communicates with the microgrid simulation model. In PHIL (Figure 6-2 (c)), one or more power components are involved in the emulation. For example, a real inverter is represented as a power source and the measurements are included as analog inputs. For this type, it is recommended to start building the platform with software representations of the components and gradually replace parts of the system environment with the actual hardware components.

Controller HIL testbeds place all the expensive, potentially dangerous, high-voltage, high-power equipment into a real-time simulation. Unlike a pure simulation, the actual device controllers are placed on the benchtop and interfaced to this simulation. The controllers, running the actual, proprietary control code that will be used to control the real microgrid assets, are configured as if they were operating real DERs, protection devices, and distribution equipment. This provides highly representative system behavior and allows the testing of a full range of edge conditions without risking damage to any equipment. The primary challenge with this approach: development of validated models of the power equipment.

Unlike a pure simulation, the actual device controllers are placed on the benchtop and interfaced to this simulation. The controllers, running the actual, proprietary control code that will be used to control the real microgrid assets, are configured as if they were operating real DERs, protection devices, and distribution equipment. This provides highly representative system behavior and allows the testing of a full range of edge conditions without risking damage to any equipment. The primary challenge with this approach: development of validated models of the power equipment.



(a)           (b)           (c)
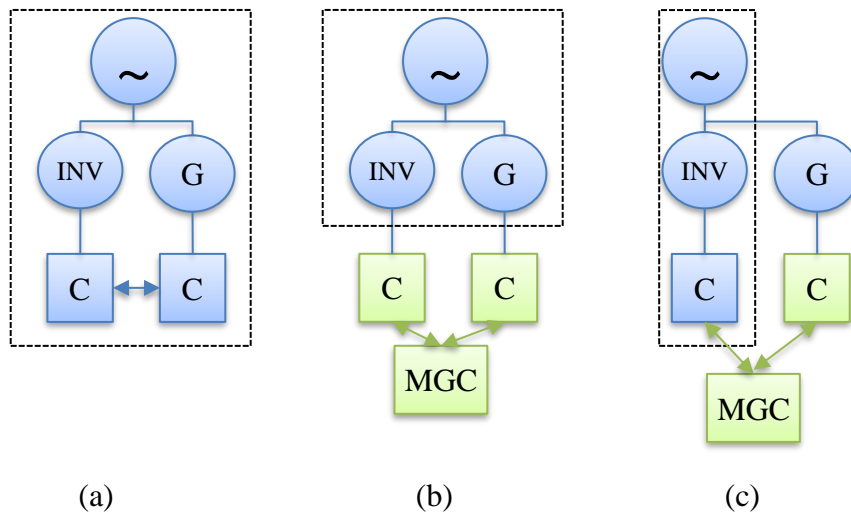
**Figure 6-2 (a) Simulation. (b) Controller-In-the-Loop (CIL). (c) Power Hardware-In-the-Loop (PHIL).**

There are three main benefits for HIL in microgrid design and studies:

1) Microgrid conceptual design.

At early stages of microgrid design, sizing DERs including energy storage is needed to ensure an optimal sitting of the overall system. Additionally, the design of the control platform is necessary to at early stages in order to define control strategies, modes of operation, switching sequences, unit commitment and Energy Management. as well as data-driven insights to modify the design to optimize performance.

2) Short and long-term microgrid configurations

Creating a Digital Twin of a large system comes in handy when testing is required to provide more confidence that the system will perform as expected, Often, the specific use cases and application requirements for a microgrid are somewhat fluid and depend on a multitude of factors, including grid conditions, user energy demand, renewable generation, etc. HIL simulation enables specific use cases to be demonstrated and gather the data from the results. Demonstration may involve critical load uptime and black-start capabilities. Extended outage capabilities. Other demonstration that involve assuring power quality and system resilience.

3) Microgrid protection

Safety analysis is important in Microgrid protection and their fault analysis. Proper safety model provides appropriate level of confidence in protection system. In Microgrid design, safety design of microgrids should meet engineering requirements and standard. HIL allows certain level of necessary studies to perform safety analysis, such as short-circuit and coordination studies, interconnection and islanding requirements and protection analysis.

## 6.3 Implementation of the True Decentralized MG Control system using HIL

### 6.3.1 Overview

The implemented HIL platform is intended to study microgrid operations with actual physical communication layer. Figure 6-3 Laboratory HIL setup component illustration.shows the schematic of the platform showing a dedicated workstation running microgrid simulation model. The workstation is equipped with multi-Ethernet ports, binding the model with a dedicated Ethernet port serves the purpose of avoiding congestion with other network related traffic, i.e. Internet. PSCAD is an ideal candidate for our platform. The simulator is widely used for multi-

phase power systems and control networks in time domain, and mainly dedicated to the study of transients of power system, which is one of the future aspects to study using the proposed platform. Accurate model interaction between power system components and loads with various control topologies is also a preferred feature in simulation that is available in PSCAD.
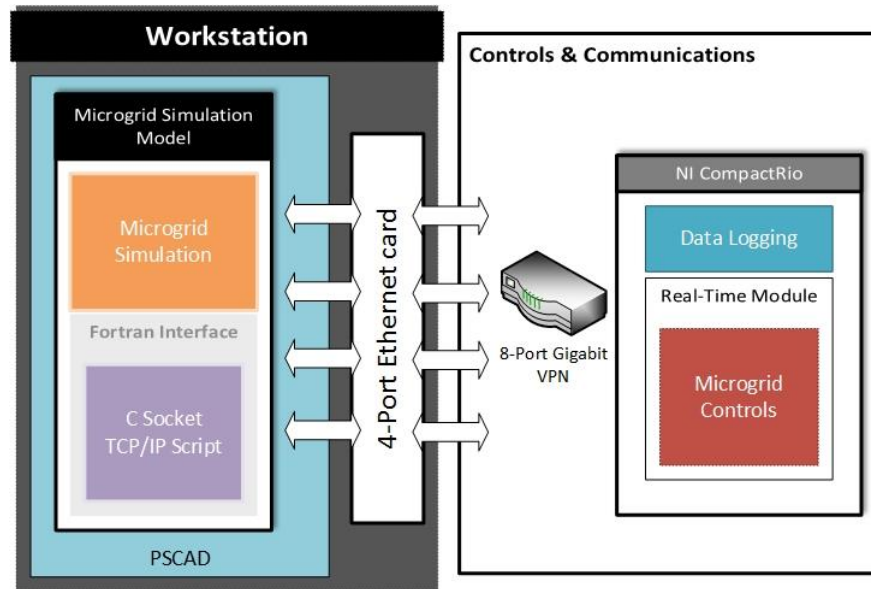


**Figure 6-3 Laboratory HIL setup component illustration.**

6.3.2   Microgrid Component Modeling.

The configuration of the Fort Sill microgrid studied is shown in Figure 6-4. The Fort Sill microgrid is rated at 480V, 60 Hz, and 630-kW. It is connected to the utility grid through a 480V/13.20kV transformer and a static switch. The generations in this microgrid include two natural gas generators each rated at 190 kW, one 90 kW solar PV system, a 2.5 kW wind turbine and a 250-kW energy storage system. The solar PV and wind turbine generators are connected to the system through inverters operating in current mode and the energy storage inverter is operated in voltage mode. The system also includes various motor loads and variable loads. Motor loads

mainly include chillers, water pumps and air compressors. This microgrid can operate in a grid-tie mode or island mode. An energy storage inverter is always connected to the system. During grid-tie operation, natural gas generators are turned off. In an island mode of operation, natural gas generators are responsible of voltage and frequency regulation.

Fort Sill microgrid is used as a case study across this dissertation. The model is implemented in PSCAD. More details on the implementation and integration within the HIL setup will be discussed in this chapter.
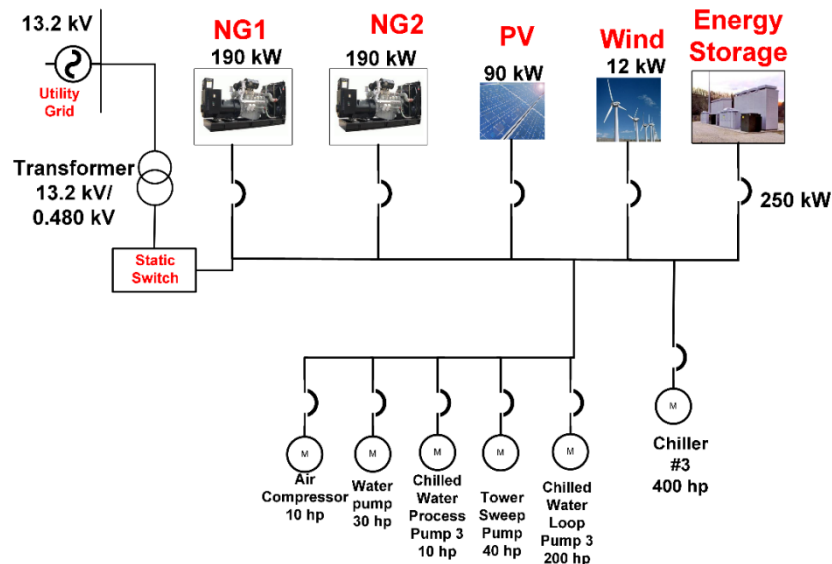


**Figure 6-4 Fort Sill Microgrid.**

*6.3.2.1   Natural Gas generator model.*

Figure 2-3 shows the basic block diagram of a natural generator connected to a grid or microgrid. To accurately study the behavior of a natural gas generator, it is required to model a synchronous generator, excitation, an Automatic Voltage Regulator (AVR) system, a gas engine, and a governor system with sufficient details. The exciter of a natural gas generator oversees reactive power and a governor adjusts the active power. By supplying active and reactive power to the system, it helps to maintain the voltage and frequency of a microgrid to a constant value. The rating details of the synchronous generator is shown in Table 6-1 Main parameters of the

modeled synchronous generator.Table 6-1. A detailed description of the modeled system is found

in [23].
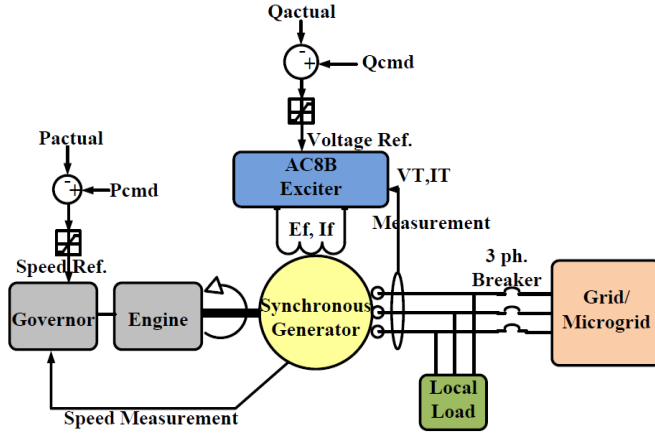


**Figure 6-5 Block diagram of a grid connected Natural Gas Generator.**

TABLE 6-1 MAIN PARAMETERS OF THE MODELED SYNCHRONOUS GENERATOR.

| Parameter | Value [Unit] |
|---|---|
| Rated RMS line to neutral voltage | 0.277 [KV] |
| Rated RMS line current | 0.360.8 [KA] |
| Frequency | 60 Hz |
| Inertia constant | 0.1619 [s] |
| Armature time constant [Ta] | 0.0212 [p.u] |
| Unsaturated reactance[Xd] | 2.7730 [p.u] |
| Unsaturated transient reactance[Xd'] | 0.2611 [p.u] |
| Unsaturated transient reactance time(open)[Td0'] | 1.7410 [s] |
| Unsaturated sub transient reactance[Xd''] | 0.1478 [p.u] |
| Unsaturated sub transient reactance time(open)[Td0''] | 0.0044 [s] |
| Unsaturated reactance[Xq] | 1.6440 [p.u] |
| Unsaturated sub transient reactance[Xq''] | 0.1710 [p.u] |
| Unsaturated sub transient reactance time(open)[Tq0''] | 0.0046 [s] |

### 6.3.2.2   Energy Storage Model

The energy storage system is modeled using a simple controlled source in series with an

internal resistance which is shown in Figure 6-6. The voltage of the controlled voltage source

determined by SOC versus open circuit voltage (OCV) is given by the manufacturer for a specific

battery or it can be derived from testing. The relationship between OCV and SOC can be

represented by an nth order polynomial function in equation or can be represented into lookup table into simulation model [93-95]. In PSCAD software, a piece-wise linear look-up table can be defined, where the XY coordinate points can be specified. The input to this component will be the SOC of the energy storage system and the output will be the OCV, which is the voltage of controlled voltage source. Based on the output current from the energy storage system SOC is calculated as follows:

$$SOC = \frac{Q - i_t}{Q} * 100 \tag{6-1}$$

$$i_t = \frac{1}{3600} \int_0^{Q.3600} i_{out} \tag{6-2}$$

Where Q is the battery capacity (Ah), io is the battery output current (A), and iout is the actual battery charge (Ah).
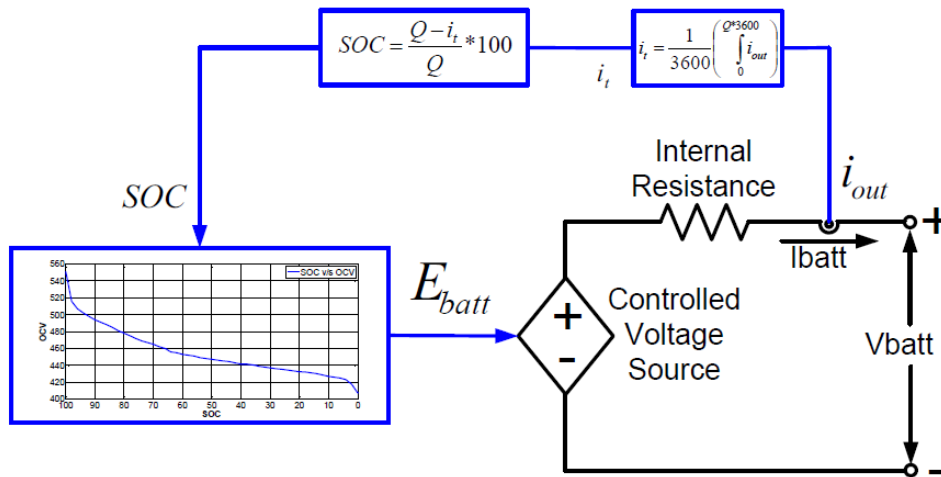


**Figure 6-6 Energy storage system equivalent circuit.**

### 6.3.2.3 Wind turbine generator

The wind energy system with full conversion configuration is modeled in PSCAD [70] [71]. The topology of the turbine is shown in Figure 5-7. The converter is operated in current mode and is configured to provide flexible active and reactive power [74]. A wind turbine extracts kinetic energy from the swept area of the blades. The power in the wind is derived in the following equation

$$P_w = \frac{1}{2}\ \rho\ A\ C_p v^3 \tag{6-3}$$

$$C_p \approx 0.4\ (Power\ coeficient) \tag{6-4}$$

Where $P_w$ is the wind power (Watts), $v$ is wind speed (m/s), and $\rho$ is the air density (kg/m³). $A$ is the turbine swept area.

The above equations have been implemented in PSCAD software to model a wind turbine. Measured wind speed data has been used to calculate the wind power . A Maximum Power Point Tracking (MPPT) algorithm has been implemented. Sample wind turbine power for a period of 24 hours for a 12 kW wind turbine generator is shown in Figure 6-8.
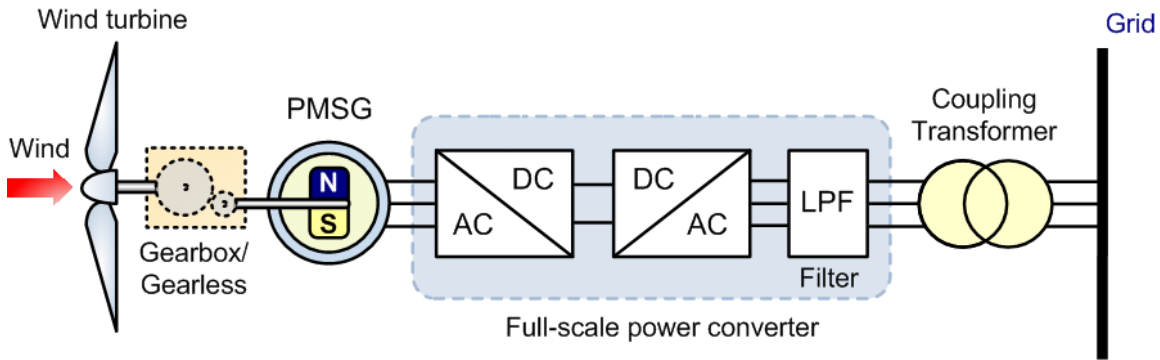


**Figure 6-7 Wind Turbine with full scale converter with grid connection.**
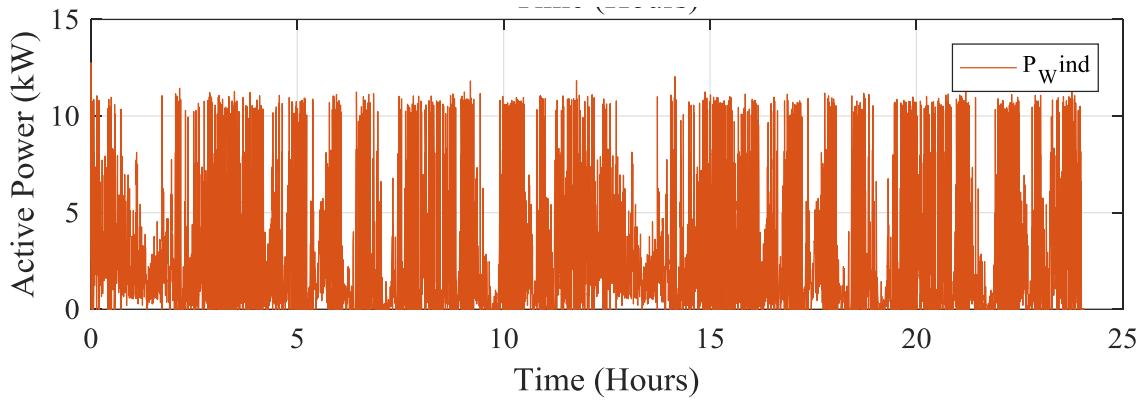
**Figure 6-8 Sample output power of 12 kW wind turbine.**

### 6.3.2.4 Photovoltaic System

Solar arrays are fast growing in installation in efficiency improvements. Microgrid is a convenient environment for photovoltaic (PV) integration into the grid. The integration process takes into consideration all aspect that relate to system voltage, power quality, response to faults and shot circuit contributions. A schematic diagram of a solar PV generator is shown in Figure 6-9. The inverter is modeled as a current source connected to the microgrid/grid. Maximum Power Point Tracking (MPPT) for the panels was developed and simulated [73].
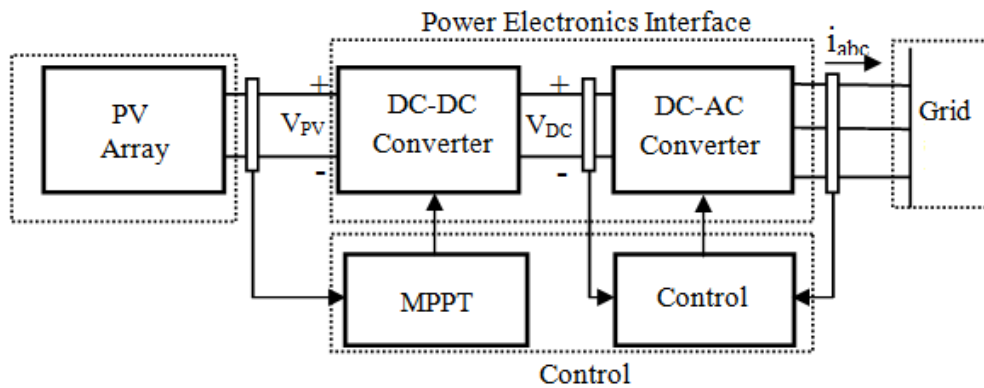


**Figure 6-9 Schematic of grid-connected PV array**

The solar PV array is modeled using an electrical equivalent circuit as shown in Figure 6-10. When solar radiation falls on a solar cell, a DC current ($I_{SC}$) is generated. $I_{SC}$ varies proportionally

84

with changes in solar radiation. Applying Kirchhoff's current law to the equivalent circuit gives [20],

$$I = I_{SC} + I_d + I_{sh} \tag{6-5}$$

$$I_d = I_o \left[ \exp \left( \frac{V + IR_S}{\frac{nkT_c}{q}} \right) - 1 \right] - \frac{V + IR_S}{R_{sh}} \tag{6-6}$$

Where $I_0$ is the reverse saturation current (A), $n$ is the diode ideality factor (1 for an ideal diode), $q$ is the electron charge, $k$ is Boltzmann's constant, and $T_c$ is the absolute temperature.
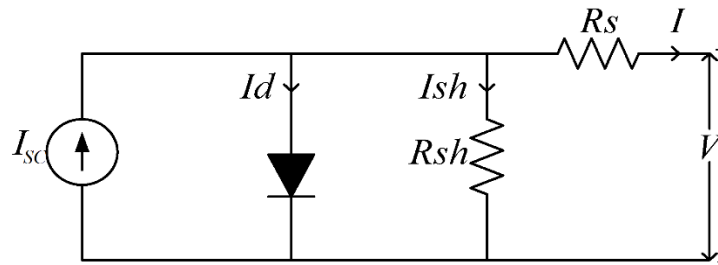


**Figure 6-10 PV array Equivalent Circuit.**

All constants can be determined from the manufacture's specifications of the PV modules and from the I-V curves. A PV array is composed of series and parallel connected modules and the single cell circuit can be scaled up to represent any series/parallel combination. Based on the equations 6-5 and 6-6, PV cell model has been implemented [104].
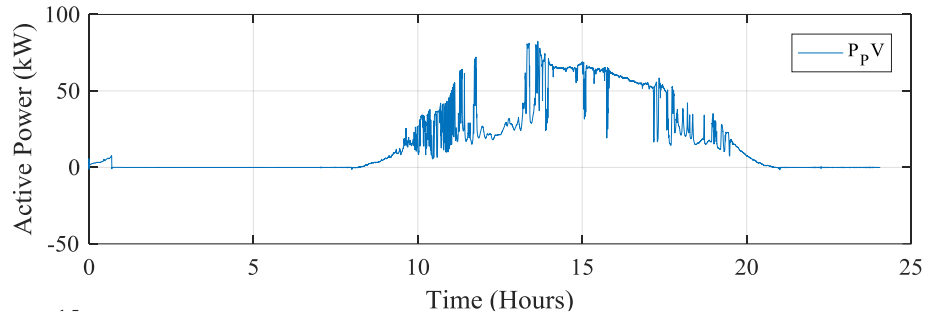
**Figure 6-11 Solar system profile over a 24-hour time period.**
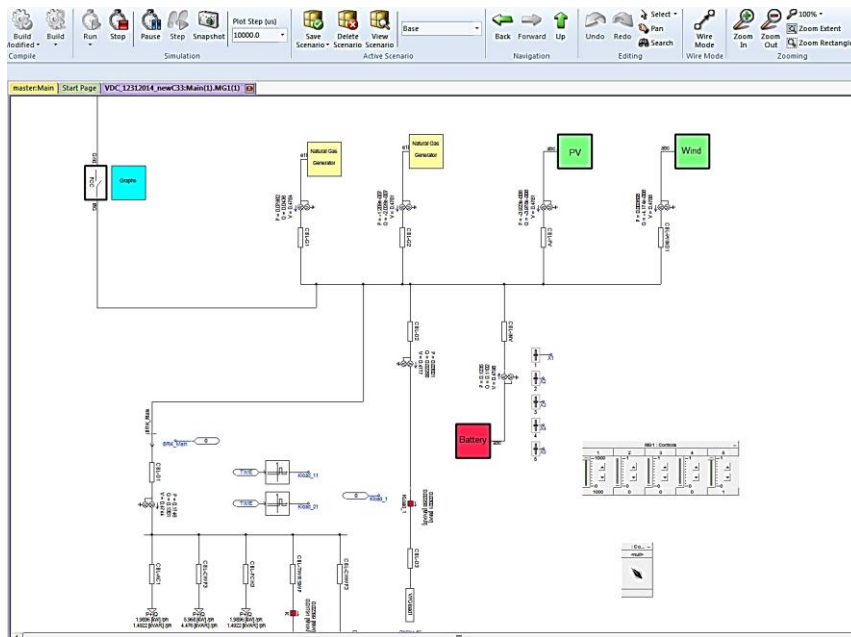


**Figure 6-12 Microgrid model in PSCAD.**

### 6.3.3 Communication Interface from simulation.

The microgrid model is implemented in PSCAD, generally, PSCAD does not support direct data exchange with any software outside the simulation environment. To overcome this issue, a C script is implemented within the simulation environment to move the simulation data to the host workstation and communication with control layer over Ethernet, the communication interface is shown if Figure 6-13.
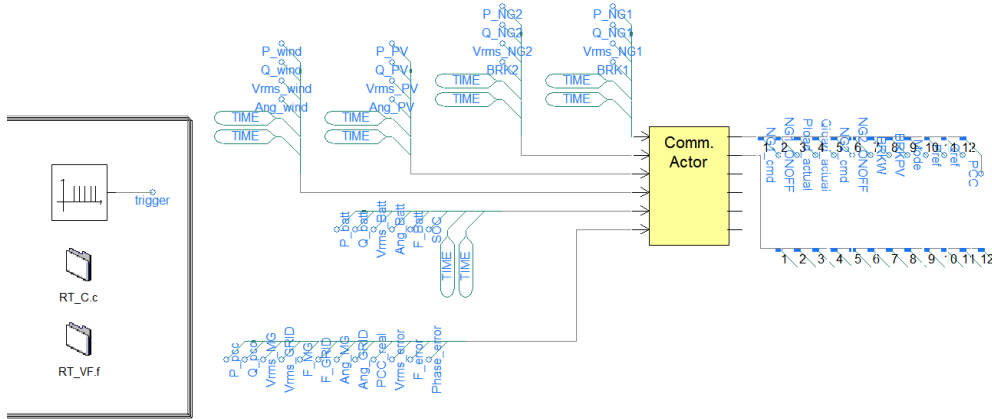
**Figure 6-13 Communication Actor in PSCAD environment.**

The communication actor is responsible of exchanging simulation data between PSCAD and the controller. The communication is performed through a local IP address, where a C# script with 6 isolated software threads is running continuously. Each thread is bound to a dedicated Ethernet port where each controller has direct connection. The data exchange process is shown in Figure 6-14.
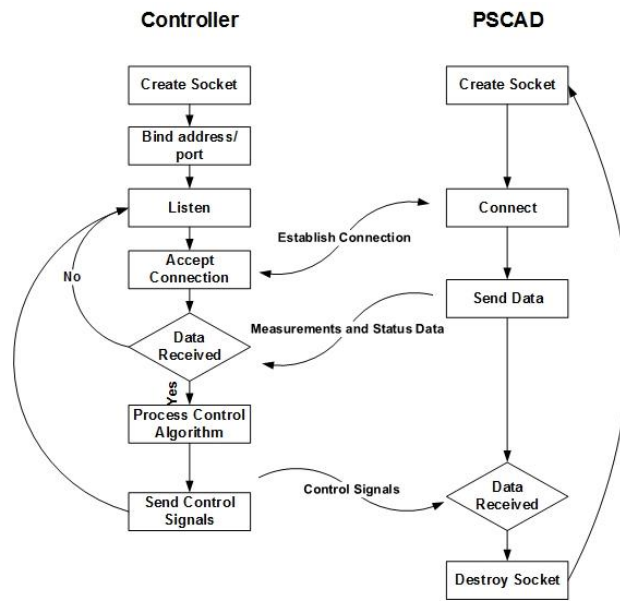


**Figure 6-14  Hardware-Software TCP/IP communication flow diagram.**

### 6.3.4   Control Layer

The microgrid controls in this platform are developed the real-time module of the CompactRio from National Instruments. Its capability to run in real-time interface mode serves the purpose of the platform. Figure 6-15 shows the controller used in the platform, a processor running Linux Real-Time OS, a programmable FPGA, and modular I/O with vision, motion, and display capabilities.

The CompactRIO Controller is a rugged, reliable, high-performance, industrial-grade embedded controller with industry-standard certifications. This controller can be used for applications that need high-speed control or signal processing, hardware algorithm acceleration, hardware reliable tasks, or unique timing and triggering. C Series I/O modules deliver high-accuracy I/O with measurement-specific signal conditioning to connect to any sensor or device on any bus. This controller runs NI Linux Real- Time, which combines the performance of a real-time OS with the openness of Linux. LabVIEW system design software is used to create, debug, and deploy control logic.



**Figure 6-15 System controller (CompactRIO) from national instruments.**

Figure 6-17 Shows the schematic of the actual implementation of the HIL testbed. Each controller runs the control algorithm (as explained in Chapter 5). The communication between the controllers uses a publish/subscribe protocol [76]. The NI Publish and Subscribe Protocol (NI-PSP) is a networking protocol optimized to be the transport for Network Shared Variables.  The

88

lowest level protocol underneath NI-PSP is TCP/IP. Figure 6-16 shows how the Shared Variable

Engine handles the exchanged data, where buffering is help avoiding read/write fluctuations.
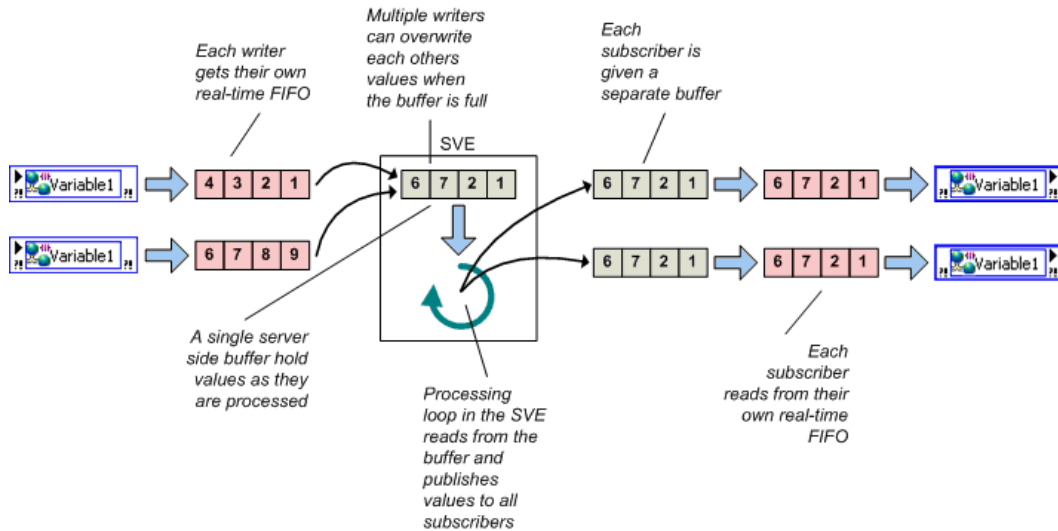


**Figure 6-16 hared Variable Engine and Network Shared Variable buffering.**
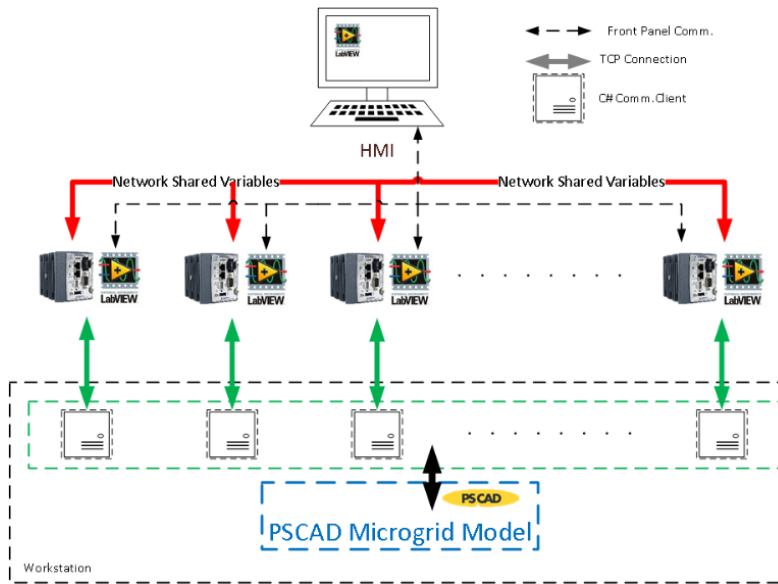


**Figure 6-17 HIL testbed schematic (Lab implementation).**

For monitoring and data logging purposes, a Graphical User Interface (GUI) has been designed

to accommodate the requirement of real-time monitoring of the exchanged data. LabVIEW

management of the controller variable and signal with the GUI is shown in Figure 6-18. The laboratory HIL experimental setup is shown in Figure 6-19.
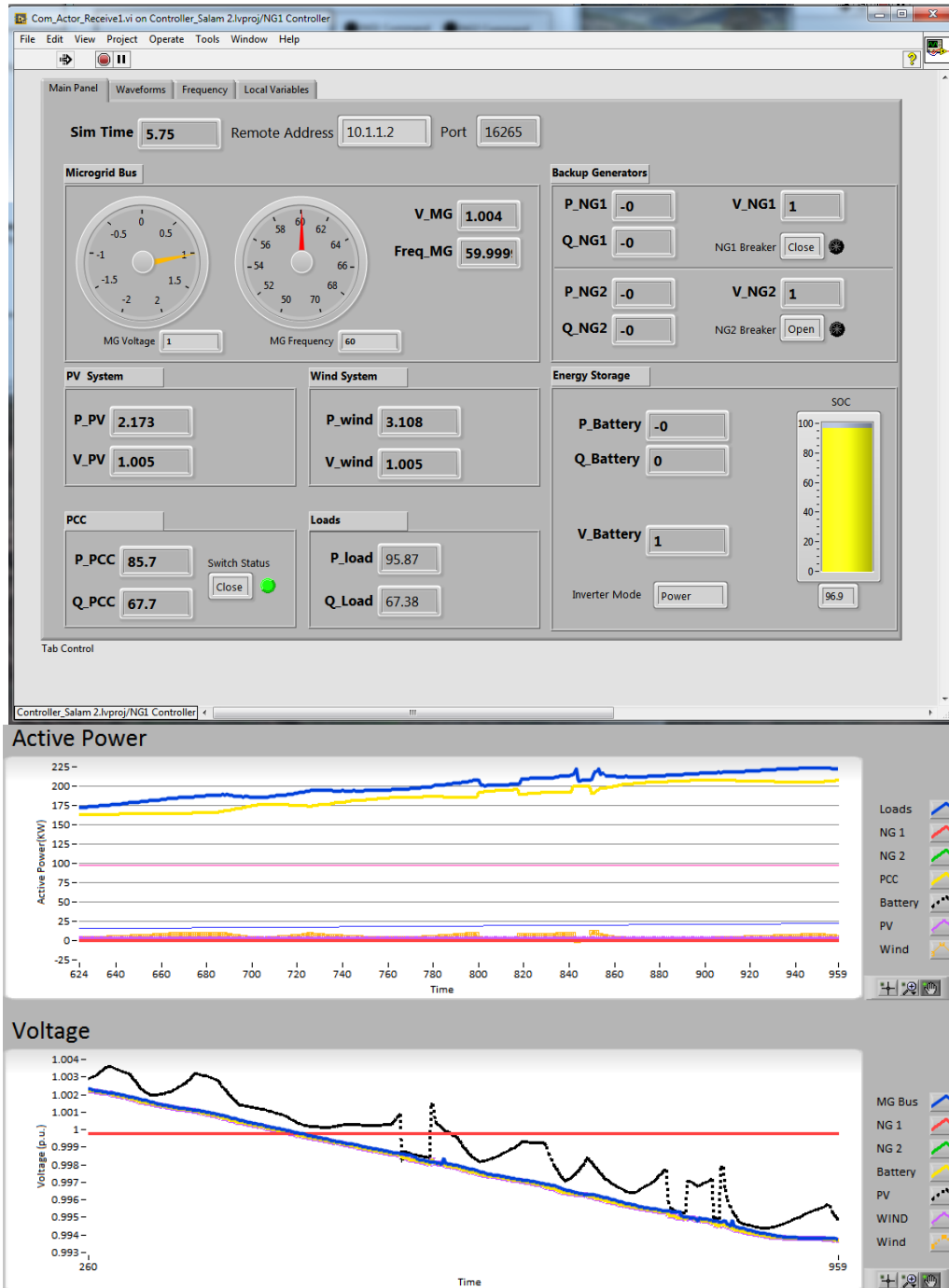


Figure 6-18 Graphical User Interface for real-time monitoring.
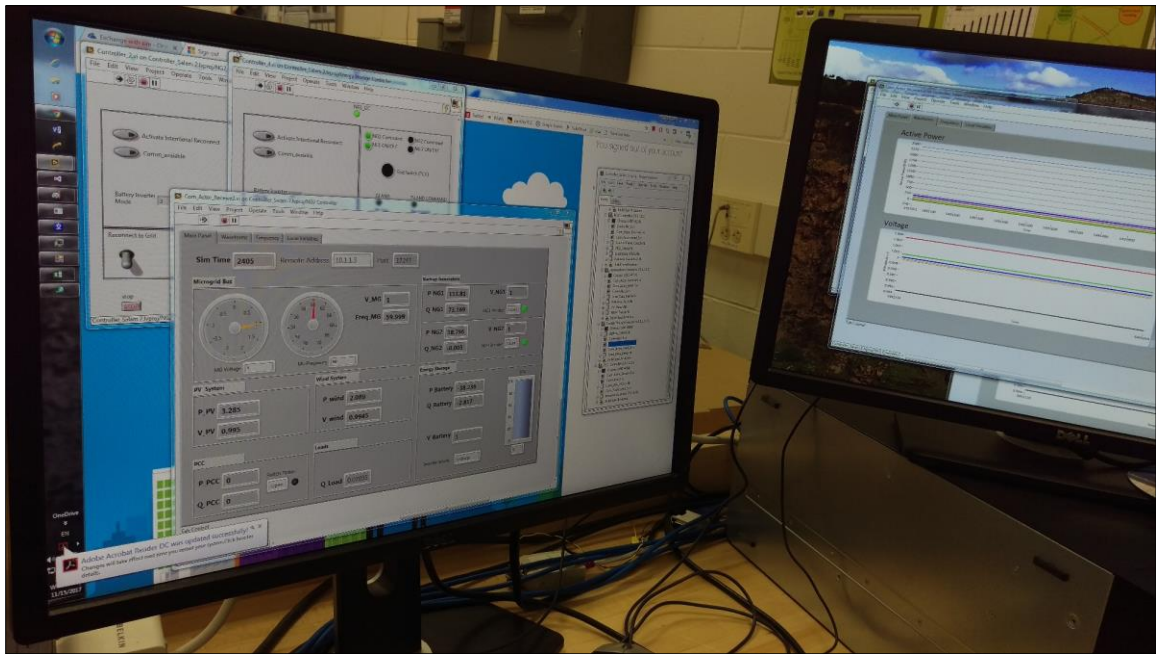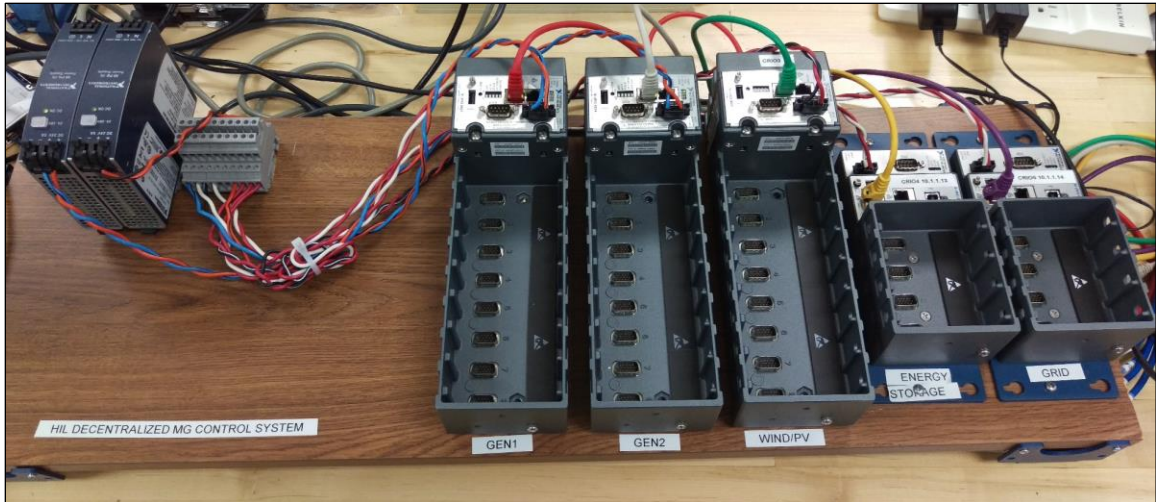
**Figure 6-19 Lab HIL experimental setup.**

# Chapter 7 System Performance and Testing

The case study for the proposed system is a microgrid that consists of various power components. Renewables (PV, wind), Energy Storage (ES), two backup natural gas generators. The schematic of the microgrid is shown in Fig. 9. Figures (10-11) shows the PV, wind, and load profiles of the test system. At $t=T$ The instantaneous load power at each controller is calculated using equation (16) which is derived from equations (12) and (13).

$$P_{LOAD}|_{t=T} = P_{NG1}(T) + P_{NG2}(T) + P_{ES}(T) + P_{Wind}(T) + P_{PV}(T) \tag{7-1}$$

TABLE 7-1 MICROGRID CASE STUDY SPECIFICATIONS.

| DER | Symbol | Rated Power | Dispatchable |
|-----|--------|-------------|--------------|
| Natural Gas Gen | $P_{NG1}^{rated}$ | 190 kW | Y |
| Natural Gas Gen | $P_{NG2}^{rated}$ | 190 kW | Y |
| Energy Storage | $P_{ES}^{rated}$ | 250 kW | Y |
| PV | $P_{PV}^{rated}$ | 90 kW | N |
| Wind | $P_{Wind}^{rated}$ | 12 kW | N |

Each controller is responsible of managing the output power of the DER, considering the constraints in equations (17—20). These constraints can lead to economic and environmental optimization challenges .

$$P_{NG}^{min} < P_{NG}(t) < P_{NG}^{rated} \tag{7-2}$$

$$0 < P_W(t) < P_W^{rated}(t) \tag{7-3}$$

$$0 < P_{PV}(t) < P_{PV}^{rated}(t) \tag{7-4}$$

$$\left. \begin{array}{c} P_{ES}^{min} < P_{ES}(t) < P_{ES}^{rated} \\ E_{ES}^+ = E_{ES}(t) + P_{ES}(t)\,\Delta t \\ E_{ES}^+ > E_{ES}^{min} \end{array} \right\} \tag{7-5}$$

Where $P_x(t)$ is the power output of source x at time t. $P_x^{rated}$ is the rated power of the source. For Energy Storage (ES), $E_{ES}^+$ is the available energy in storage projected after $\Delta t$, $E_{ES}^{min}$ is the minimum energy storage allowed in ES, which reflects the minimum state of charge (SOC).
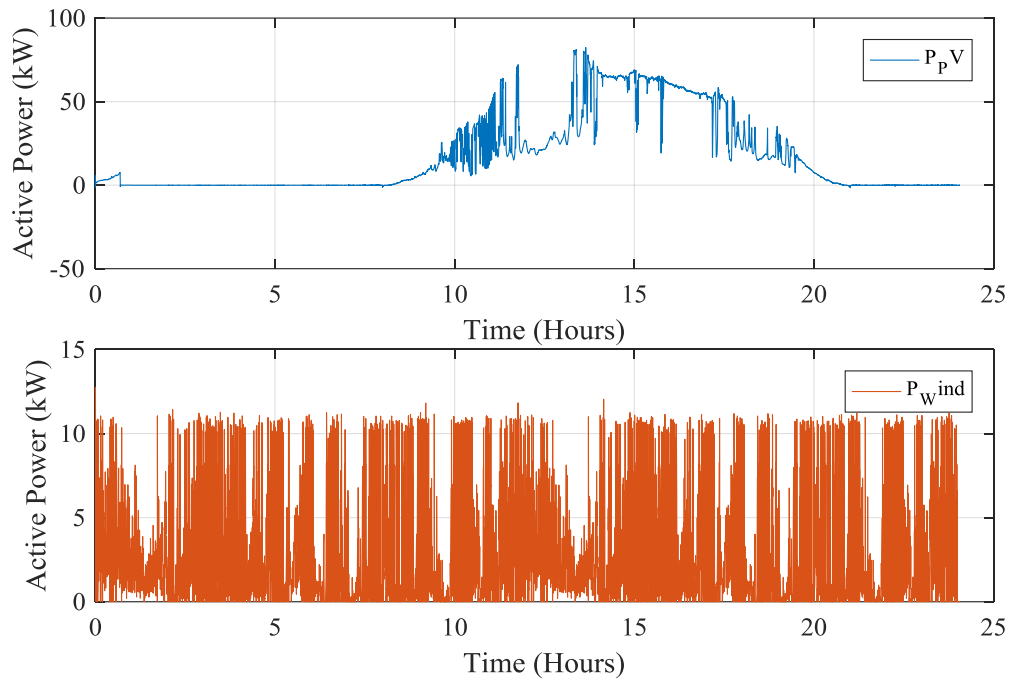


**Figure 7-1. Simulated PV(top) and Wind (bottom) profiles (24-hour profile).**
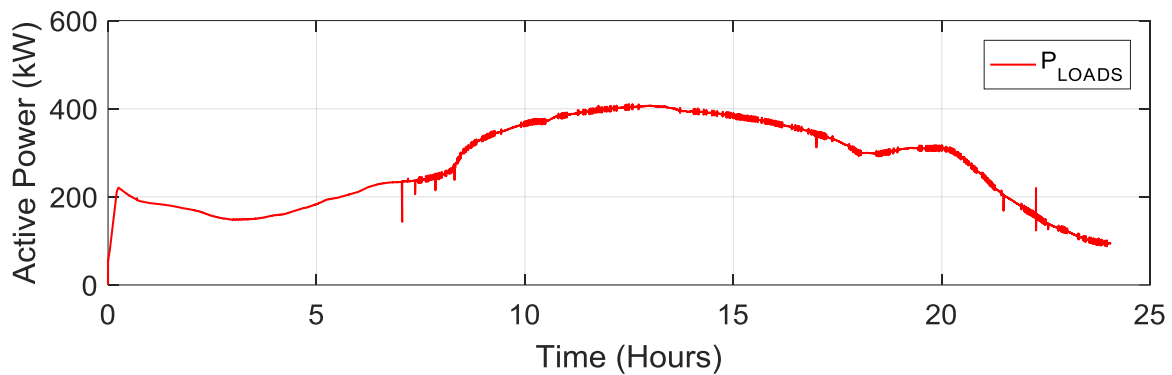
**Figure 7-2. Microgrid Load profile (24 hour).**

For testing purposes, a Hardware-In-the-Loop (HIL) platform were developed to study microgrid operations with real physical communication layer [17]. Chapter 6 describes the schematic of the platform applying the decentralized architecture. Three different experiments were in this Chapter:

1) Proof-of concept of a 24-hour microgrid operation under a decentralized control system.

2) Microgrid transient operations such as intentional islanding.

3) demonstration of the proposed FMU in the recovery algorithm by injecting a controller failure.

## 7.1 System State of Operation

One major issue considered is the communication delays and their impact on the true decentralized microgrid control operations. As shown in Figure 7-3, the control cycle during normal operation of each controller is divided in five main steps. Lengths of time slots in Figure 7-3 does not reflect the actual scale of time during the cycle. It is worth to note that receiving and broadcasting updates with peer controllers include communication delays, these delays can be

94

interpreted as communication faults; which can lead to unnecessary controller state transition (Figure 7-3).
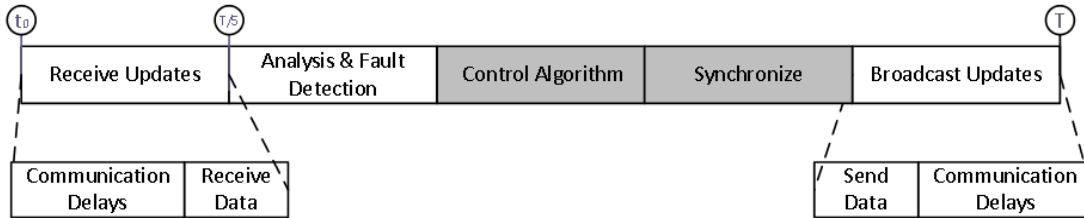


**Figure 7-3  Control Cycle during normal operation.**
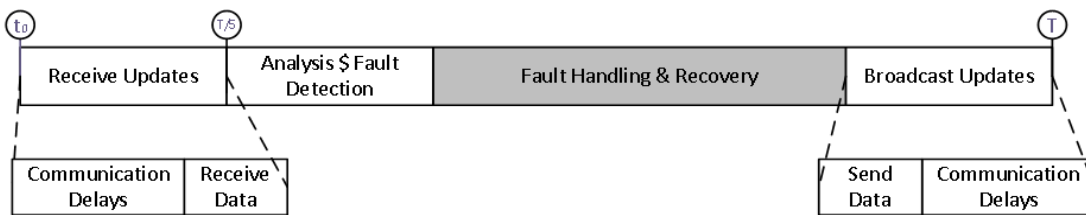


**Figure 7-4 Control Cycle during state transitions (Fault handling).**

Figure 7-5 shows the control cycle of any decentralized controller, the failure analysis is performed right after the updates are received from all peers.  In the case of no violations have been detected, nor any failure have been reported, the control algorithm maintains at normal operation. If the output from failure analysis and detection is a failure code, the fault handling and recovery takes over and the normal operation algorithm halts.

Similarly, the control cycle during state transition (Figure 7-5) requires updates transmission to ensure concurrency. This allows each controller to make an accurate decision. However, the normal operation algorithm halts during self-healing process, but this time should be at minimum to prevent and reflection of this fault onto the microgrid operation. Assume a microgrid where a decentralized control architecture is applied (Table 7-1). The utility grid is assumed to be a power

component when the microgrid is in grid-connected mode. At any time t, the output power is bounded by the following constraints

The system is considered in normal operation when the following conditions are met:

1) Equations (7-6) and (7-7) are not violated, where the bus voltage and frequency are within limits.

2) Sanity check performed locally results a valid condition.

3) Peer reports are all valid stating that all controllers are working properly and the system is stable.

$$V_{Bus}|_t = e_V V_{C_i} = 1 \, p.u \qquad i = 1,2,\dots,n \qquad\qquad (7\text{-}6)$$

$$F_{Bus}|_t = e_F F_{C_i} = 60 \, Hz \qquad i = 1,2,\dots,n \qquad\qquad (7\text{-}7)$$

Where $e_x$ is the allowed mismatch factor to remain in normal operation state.
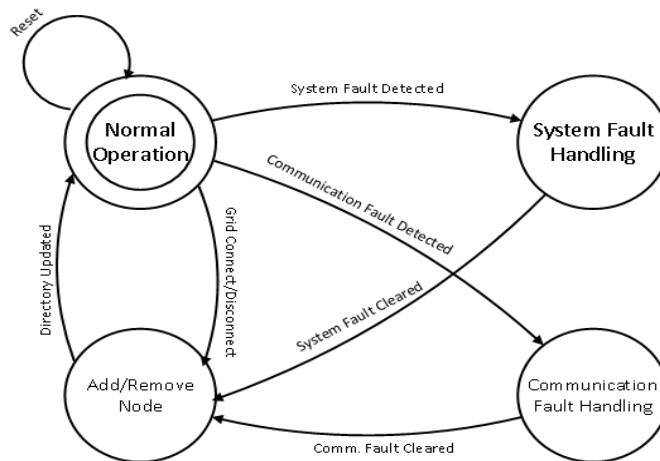


**Figure 7-5  Controller state diagram with fault triggered state transitions.**

## 7.2 Microgrid Normal Operation

Figure 7-7 shows the microgrid normal curves over a 24-hour period of operation. The microgrid operates in a grid tie mode, where the utility supports the load with the power demand in addition the PV and wind. NG1and NG2 are not operating at this point, and ES is in standby mode. island mode. At *t=7.55 hours*, an intentional islanding command is issued by the PCC controller. The grid power support ramps down as the energy storage inverter ramps up the output power, and forms the microgrid bus during the transition period.
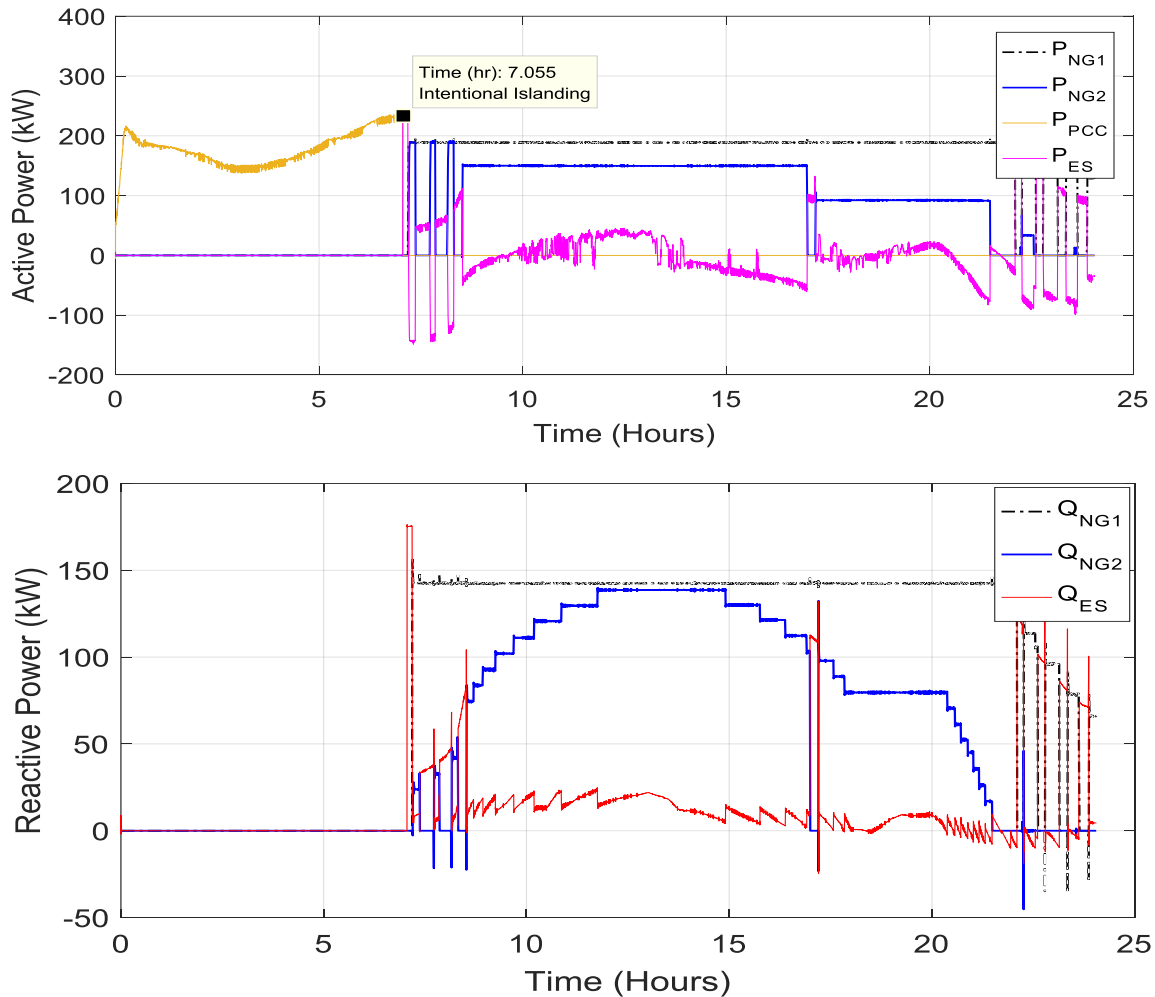


**Figure 7-6. Active and reactive power curves over 24-hour operation period.**

97
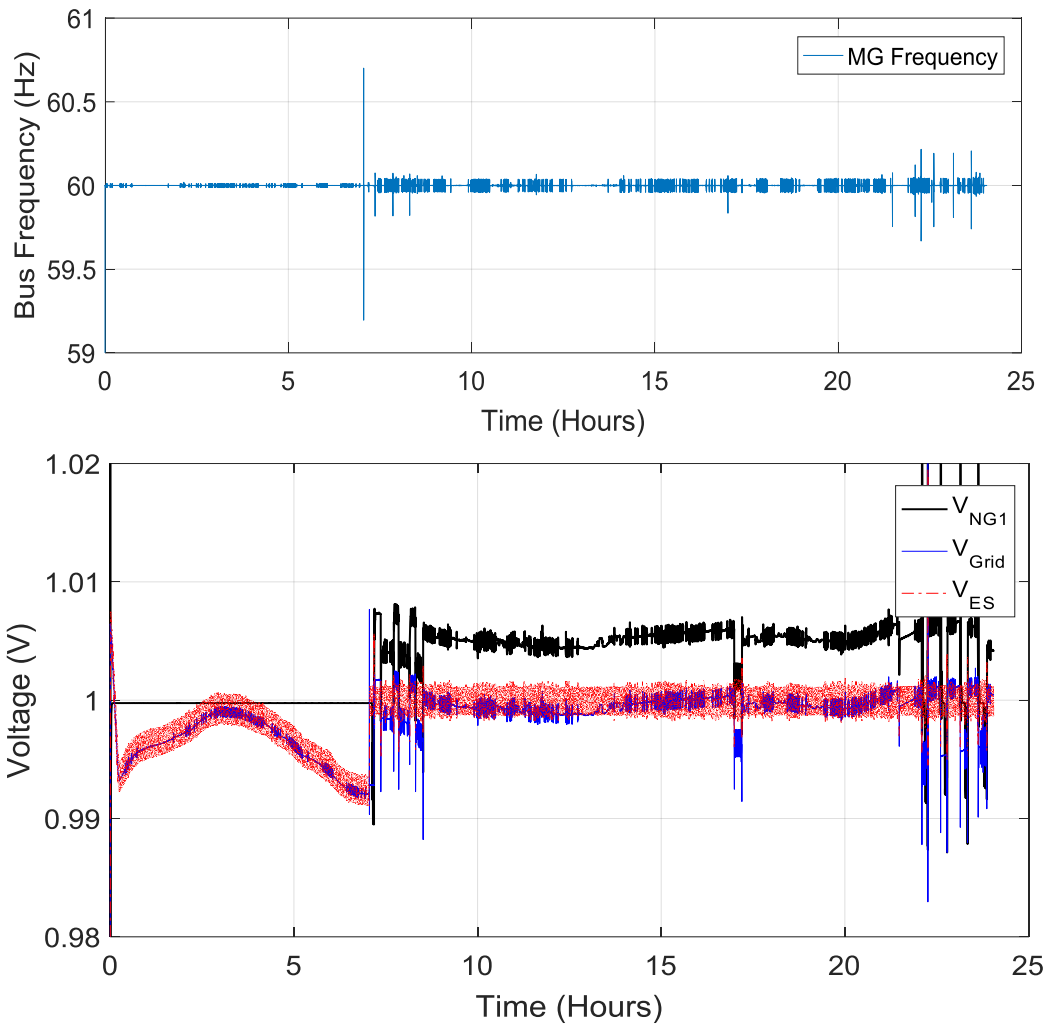
**Figure 7-7. Microgrid voltage and frequency profiles over 24-hour operation period**

## 7.3    System Transients

Figure 4 shows active and reactive curves the microgrid during islanding. System simulation starts with fully charged ES. NG1, NG2 are off and their breakers are open. The nature of the loads varies with time starting with 60 KW and increasing. ES provides the power to the loads for 16 seconds the decentralized controller at the ES unit measures 50% SOC remaining on the battery and publishes the update. The controller at NG1 commands to NG1 to start and synchronize with the bus, and commands the breaker after 6 seconds providing 190KW (NG rated power). Since the load demand is greater than the capacity of NG1, controller of NG2 detects the change of operation

98

and command the generator to connect. The controller of ES detects that NG1 and NG2 are active, and switches to charging mode.
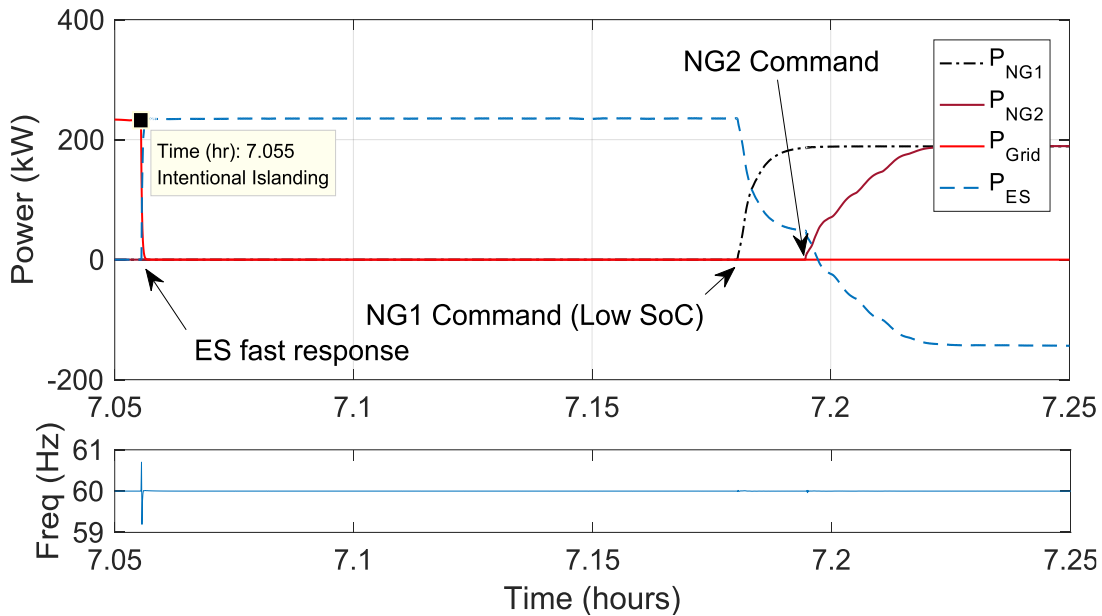


**Figure 7-8. Frequency response and system interaction during islanding operation.**

## 7.4    Failures and recovery

One of the advantages of using HIL platform is the capability of configuring and injecting failures at the hardware and/or software levels. Failing a controller is performed by powering down the controller, or resetting the controller manually. Decentralization of a control system comes with additional algorithm in response, the algorithm is introduced in Chapter 5. The responses of the decentralized controllers insure fast transition to a steady state after the failure occurs.

Figure 7-9 illustrates the case for failure of one decentralized controller, the chosen controller for this test is NG1, which could be one of the extremist cases since the generator could be regulating the bus voltage/frequency. *At t=47.5*s, the controller of NG1 fails while both generators are running and the ES is in charge mode. Two controllers are capable of fast response to this change; ES controller can command ES to take over the load demand, or the PCC controller can

99

command emergency grid connection. For this case, PCC responded since the SOC of the battery is critically low. NG1and NG2 are shut down.
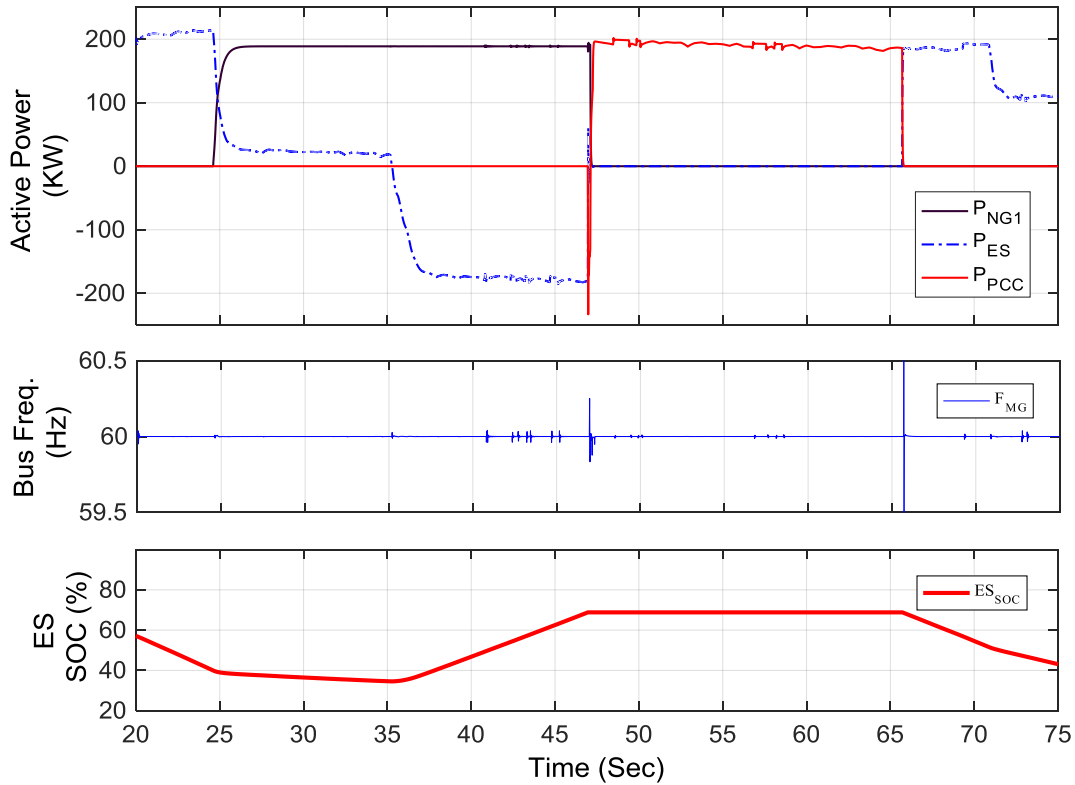


**Figure 7-9. FMU response demonstration, with controller failure.**

Another demonstration of the systems transients due to a failure detection, Figure shows the system response to a failure at NG2 controller. The design of the proposed system calculates the available power generation among all DERs, and determines that ES, PV, Wind and NG1 are capable of handling the demand. Therefore, the controller at ES responds to this failure by compensating the active and reactive power required. During this transition, NG1 remains at full capacity.
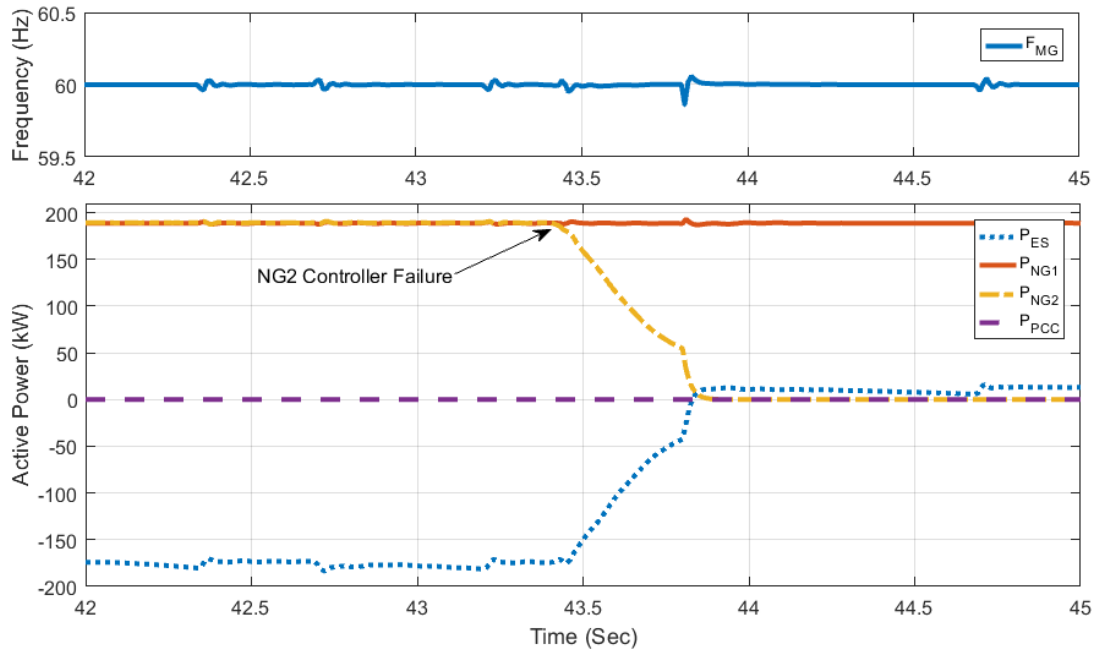
**Figure 7-10 System Response to a failure at NG2 controller.**

During the Failure time of NG2, a repair is performed to the controller, and the status of NG2 is restored. The control architecture guarantees a seamless recovery of NG2, where the controller of NG2 sends a message to the peer controllers. The rest of the system detects the recovery, and waits until NG2 is synchronized with the MG bus and the brokers closes. Figure 7-11 shows the active power curves of the plug-and-play transient due to a controller recovery. The following events describe the scenario:

1.  Due to the failure of NG2, the system was forces into an unintentional connection to the grid due to the high load demand.

2.  The PCC controller detects the recovery of NG2, calculates the available power supply and compares it to the current demand, and generates an automatic islanding command.

3.  The primary control algorithms regulate the bus voltage and frequency during this transition, with a short-term frequency deviation.

4. ES compensates active power shortage until NG2 reconnects.
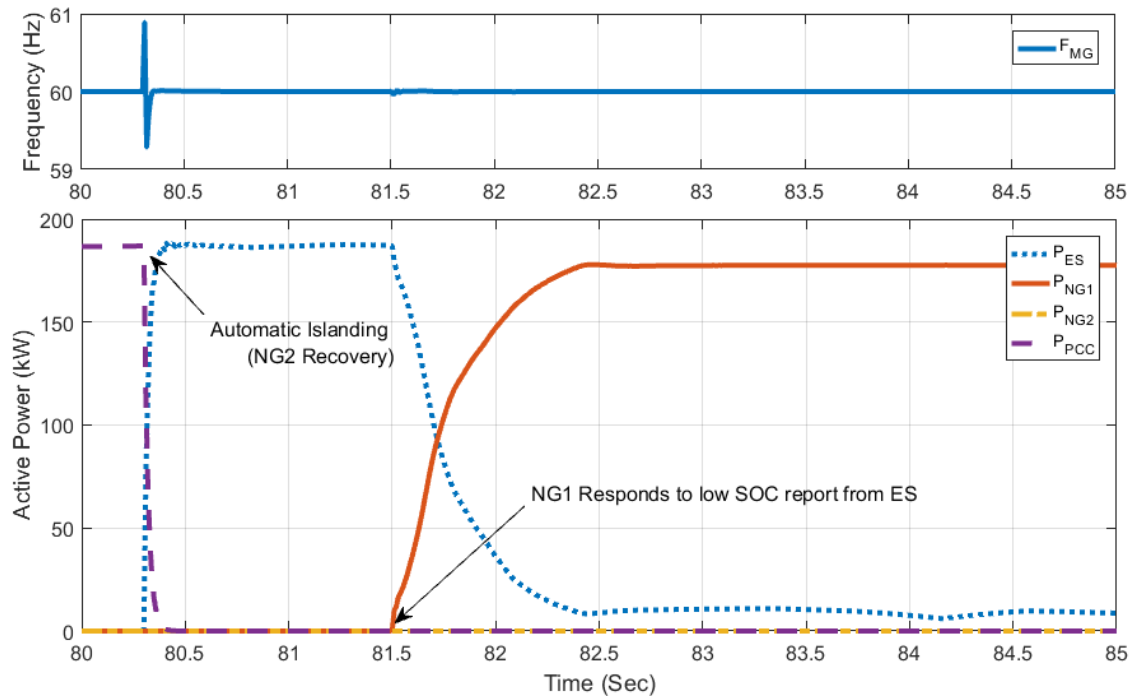


**Figure 7-11 Active power curves during system response to NG2 recovery.**

Figure 7-12 shows the DER voltages during the previous failure demonstration. While the secondary control layer and FMU manages the failure response, the robust primary control mechanism maintains the voltage and frequency within their desired levels.

A less severe case of failure may occur at the renewables controller, leading to isolation of the failing DER branch. In this microgrid case, the size of the renewables is relatively small in comparison to the rest of the DERs. Which leads to a minor frequency disturbance and t=24 sec (as seen in Figure 7-13), the transient at t=25 sec is pre-scheduled, and does not relate to the failure of the renewables controller.
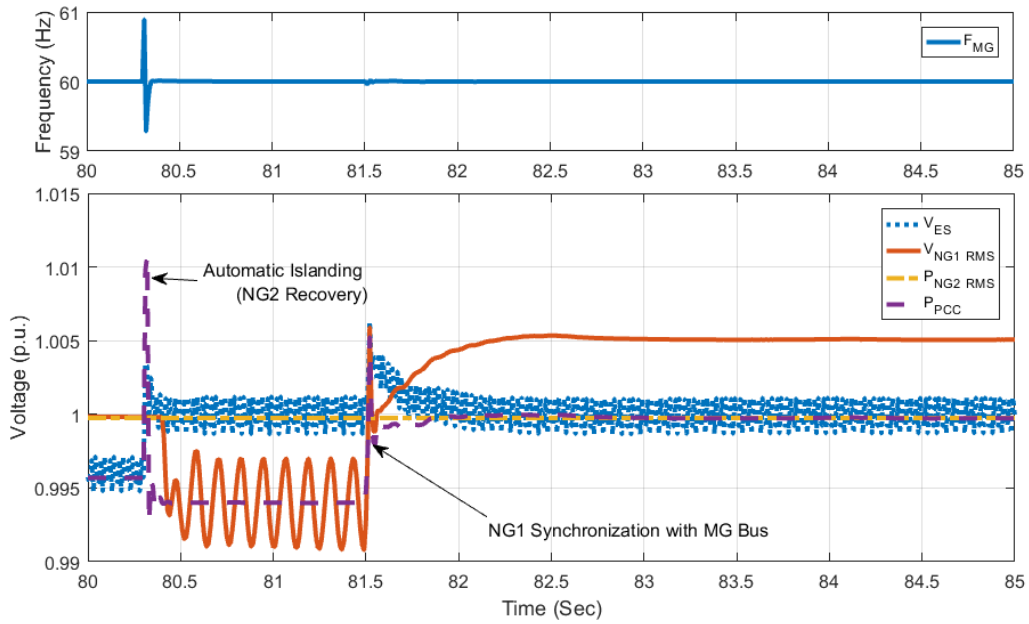
**Figure 7-12 Voltage/Frequency curves during system response to NG2 recovery.**
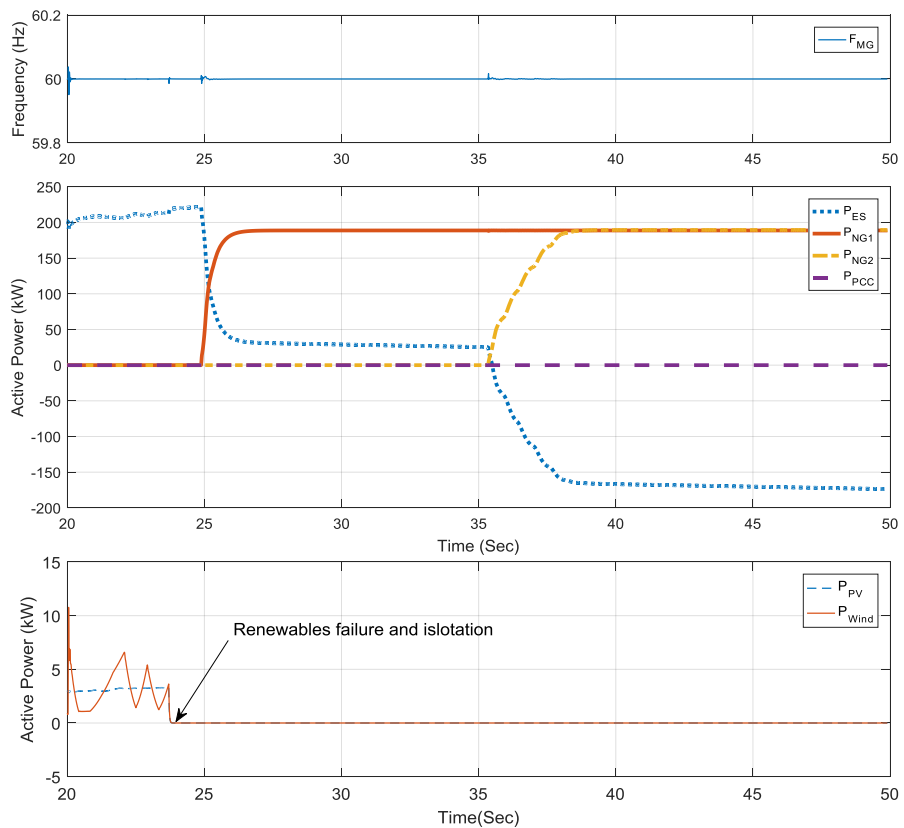


**Figure 7-13 Active power curves during system response to renewables controller failure.**

# Chapter 8 Conclusions

Microgrids serve as an integral part of future power distribution systems. Decentralizing power production aside from the utility providers, local controls are necessary for this type of future solution to power loss due to power transmission to distant areas. Typically, microgrids are managed by centralized controllers. The two main concerns about a single controller are: the single control could become performance and reliability bottleneck for the entire system, where its failure can bring the entire system down and excessive communication delays could degrade the system performance, and the communication delays and packet loss of command signals between the central controller and the microgrid components.

In this dissertation, a true decentralized control architecture for microgrids is proposed. Distributing the controls to local agents decreases the possibility of network congestion to occur. Decentralization will also enhance the reliability of the system since the single point of failure is being replaced with a distributed architecture. Three different model were defined to achieve a complete practical control architecture: The controller model, where the internal firmware and hardware part were identrified. The data exchange model, where the peer-to-peer communications are designed and data models are implemented. The Failure model, where a new unit is proposed as an integral part of the microgrid energy management system.

In the proposed architecture, device level and system level controller and interaction models are designed for a self-coordination. Results shows the robustness of the proposed architecture. Microgrid energy management system and control case scenarios are demonstrated. The proof-of-concept of true decentralization of microgrid control architecture is implemented using Hardware-in-The-Loop platform, developed using real physical communication links and network

components, and applying the concept of decentralization dynamically over a network of real-time controllers. The proposed system ensures reliable data exchange between controllers and microgrid components. The control concept is truly distributed and does not require a master or central controller. Load and generation forecasting can be integrated as well as energy storage operation, improving unit commitment and performance.

A future work of this effort includes: Accurate modeling of DG output power versus bus frequency deviation. Accurate modeling of microgrid frequency versus the change in demand and generation. Include forecast for DG generation in the controls to increase reliability and improving performance. Prediction techniques can be adopted to provide a near future prediction of a failure and speeding up the recovery process. This requires a data buffer carrying a record of data for the overall microgrid.

Other future considerations and analysis involve the cyber-security aspect of decentralized architectures. Conducting a comparative study for cyber-security issue may involve delay considerations due to the time complexity overhead of encryption and intrusion detection techniques.

# References

[1] Office of the National Coordinator for Smart Grid Interoperability, "NIST Framework and Roadmap for Smart Grid Interoperability Standards," National Institute of Standards and Technology, 2010.

[2] "IEEE Smart Grid Domains & Sub-domains," IEEE Smart Grid Society, [Online]. Available: http://smartgrid.ieee.org/domains. [Accessed 01 May 2016].

[3] Grid Interactive Microgrid Controllers and the Management of Aggregated Distributed Energy Resources (DER), EPRI (technical report), 2015.

[4] F. Cleveland, A. Lee, "Cyber Security for DER Systems" (technical report), 2013.

[5] A. Solanki, A. Nasiri, V. Bhavaraju, Y. L. Familiant and Q. Fu, "A New Framework for Microgrid Management: Virtual Droop Control," in *IEEE Transactions on Smart Grid*, vol. 7, no. 2, pp. 554-566, March 2016.

[6] H. Liang, B. J. Choi, W. Zhuang and X. Shen, "Stability Enhancement of Decentralized Inverter Control Through Wireless Communications in Microgrids," in *IEEE Transactions on Smart Grid*, vol. 4, no. 1, pp. 321-331, March 2013.

[7] M. J. Hossain, J. Lu, M. A. Mahmud and T. Aziz, "Advanced decentralized DER control for islanded microgrids," *2014 Australasian Universities Power Engineering Conference (AUPEC), 2014*.

[8] C. M. Colson, M. H. Nehrir and R. W. Gunderson, "Distributed multi-agent microgrids: a decentralized approach to resilient power system self-healing," *2011 4th International Symposium on Resilient Control Systems (ISRCS)*, Boise, ID, 2011, pp. 83-88.

[9] J. M. Guerrero, M. Chandorkar, T. L. Lee and P. C. Loh, "Advanced Control Architectures for Intelligent Microgrids—Part I: Decentralized and Hierarchical Control," in *IEEE Transactions on Industrial Electronics*, vol. 60, no. 4, pp. 1254-1262, April 2013.

[10] Niannian Cai and J. Mitra, "A decentralized control architecture for a microgrid with power electronic interfaces," *North American Power Symposium (NAPS)*, 2010, Arlington, TX, 2010, pp. 1-8.

[11] A. H. Yazdavar; M. A. Azzouz; E. F. El-Saadany, "A Novel Decentralized Control Scheme for Enhanced Nonlinear Load Sharing and Power Quality in Islanded Microgrids," in *IEEE Transactions on Smart Grid*, vol. no.99, pp.1-1

[12] S. Marzal, R. Salas-Puente, R. González-Medina, E. Figueres and G. Garcerá, "Peer-to-peer decentralized control structure for real time monitoring and control of microgrids," *2017 IEEE 26th International Symposium on Industrial Electronics (ISIE)*, Edinburgh, United Kingdom, 2017, pp. 140-145.

[13] W. Liu, W. Gu, W. Sheng, X. Meng, Z. Wu and W. Chen, "Decentralized Multi-Agent System-Based Cooperative Frequency Control for Autonomous Microgrids With Communication Constraints," in *IEEE Transactions on Sustainable Energy*, vol. 5, no. 2, pp. 446-456, April 2014.

[14] F. Shahnia, R. P. S. Chandrasena, S. Rajakaruna and A. Ghosh, "Primary control level of parallel distributed energy resources converters in system of multiple interconnected autonomous microgrids within self-healing networks," in *IET Generation, Transmission & Distribution,* vol. 8, no. 2, pp. 203-222, February 2014.

[15] W. Su, J. Wang, "Energy Management Systems in Microgrid Operations" in *The Electricity Journal*, , vol. 25, no. 8, October 2012.

[16] M. I. Azim, M. J. Hossain, F. H. M. R. Griffith and H. R. Pota, "An improved droop control scheme for islanded microgrids," *2015 5th Australian Control Conference (AUCC)*, Gold Coast, QLD, 2015, pp. 225-229.

[17] J. M. Guerrero, P. C. Loh, T. L. Lee and M. Chandorkar, "Advanced Control Architectures for Intelligent Microgrids—Part II: Power Quality, Energy Storage, and AC/DC Microgrids," in *IEEE Transactions on Industrial Electronics*, vol. 60, no. 4, pp. 1263-1270, April 2013.

[18] M. Zeraati, M. E. H. Golshan and J. M. Guerrero, "A Consensus-Based Cooperative Control of PEV Battery and PV Active Power Curtailment for Voltage Regulation in Distribution Networks," in *IEEE Transactions on Smart Grid*, vol. PP, no. 99, pp. 1-1.

[19] A. Bani-Ahmed and A. Nasiri, "Development of real-time hardware-in-the-loop platform for complex microgrids," *2015 International Conference on Renewable Energy Research and Applications (ICRERA)*, pp. 994-998, Palermo, 2015.

[20] Guerrero J M, Chandorkar M, Lee T, Loh, P C. "Advanced Control Architectures for Intelligent Microgrids—Part I: Decentralized and Hierarchical Control. Industrial Electronics", *IEEE Transactions on Industrial Electronics*, vol.60, no.4, pp.1254-1262.

[21] F. Shahnia, R. P. S. Chandrasena, S. Rajakaruna and A. Ghosh, "Primary control level of parallel distributed energy resources converters in system of multiple interconnected autonomous microgrids within self-healing networks," in IET Generation, Transmission & Distribution, vol. 8, no. 2, pp. 203-222, February 2014.

[22] A. C. Henao-Muñoz, A. J. Saavedra-Montes and C. A. Ramos-Paja, "Energy management system for an isolated microgrid with photovoltaic generation," *2017 14th International Conference on Synthesis, Modeling, Analysis and Simulation Methods and Applications to Circuit Design (SMACD)*, Giardini Naxos, 2017, pp. 1-4.

[23] A. Solanki, "Virtual Droop control framework and stability analyses for microgrids with high Penetration of Renewables", PhD Dissertation, University of Wisconsin-Milwaukee, 2015.

[24] P. Kansal and A. Bose, "Bandwidth and Latency Requirements for Smart Transmission Grid Applications," in *IEEE Transactions on Smart Grid*, vol. 3, no. 3, pp. 1344-1352, Sept. 2012.

[25] A. Roshan, R. Burgos, A.C. Baisden et al., "A D-Q frame controller for a full-bridge single phase inverter used in small distributed power generation systems", *Proc. IEEE Applied Power Electronics Conference and Exposition-APEC. Anaheim*, pp. 641-647, Feb. 2007.

[26] N. DIAZ ALDANA, J. Vasquez and J. Guerrero, "A Communication-less Distributed Control Architecture for Islanded Microgrids with Renewable Generation and Storage," in *IEEE Transactions on Power Electronics*, vol. PP, no. 99, pp. 1-1.

[27] Aris L. Dimeas, Nikos D. Hatziargyriou, "Operation of a Multi-agent System for Microgrid Control", *Power Systems, IEEE Transaction on*, vol. 20, no. 3, pp. 1447-1455, 2005.

[28] M. E. Baran and I. M. Markabi, "A multi-agent-based dispatching scheme for distributed generators for voltage support on distribution feeders,", *IEEE Transactions on Power Systems*, Volume 22, Issue I, pp. 52-59, 2007.

[29] T. V. Vu, S. Paran, F. Diaz-Franco, T. El-Mezyani and C. S. Edrington, "An Alternative Distributed Control Architecture for Improvement in the Transient Response of DC Microgrids," in *IEEE Transactions on Industrial Electronics*, vol. 64, no. 1, pp. 574-584, Jan. 2017.

[30] D. Shi et al., "A Distributed Cooperative Control Framework for Synchronized Reconnection of a Multi-Bus Microgrid," in *IEEE Transactions on Smart Grid*, vol. PP, no. 99, pp. 1-1.

[31] M. Reyasudin Basir Khan, Razali Jidin, Jagadeesh Pasupuleti, "Multi-agent based distributed control architecture for microgrid energy management and optimization", *In Energy Conversion and Management*, Volume 112, 2016, Pages 288-307, 2016.

[32] C.-S. Karavas, G. Kyriakarakos, K.G. Arvanitis, G. Papadakis "A multi-agent decentralized energy management system based on distributed intelligence for the design and control of autonomous polygeneration microgrids", *Energy Conversion Managent*, 103 (2015), pp. 166-179.

[33] C.-X. Dou, W.-Q. Wang, D.-W. Hao, X.-B. L, "MAS-based solution to energy management strategy of distributed generation system", *Int. Journal of Electronic Power Energy Systems*, 69 (2015), pp. 354-366.

[34] Y. Shoham, K. Leyton-Brown," Multiagent systems: algorithmic, game-theoretic, and logical foundations", Cambridge University Press (2008).

[35] J. Lagorse, D. Paire, A. Miraoui, "A multi-agent system for energy management of distributed power sources", *Renewable Energy*, 35 (2010), pp. 174-182.

[36] S. Mocci, N. Natale, F. Pilo, S. Ruggeri, "Demand side integration in LV smart grids with multi-agent control system", *Electric Power Systems Res*, 125 (2015), pp. 23-33.

[37] Z. Jun, L. Junfeng, W. Jie, H. Ngan, "A multi-agent solution to energy management in hybrid renewable energy generation system" *Renewable Energy*, 36 (2011), pp. 1352-1363.

[38] S. Bi; Y. J. A. Zhang, "Graph-based Cyber Security Analysis of State Estimation in Smart Power Grid," in *IEEE Communications Magazine*, vol.99, pp.2-9, February 2017

[39] J. Zhang, L. Guan and X. Wang, "Impacts of island load shedding and restoration strategies on reliability of microgrid in distribution system," *2016 IEEE PES Asia-Pacific Power and Energy Engineering Conference (APPEEC)*, Xi'an, China, 2016, pp. 1594-1598.

[40] J. C. Vasquez, J. M. Guerrero, A. Luna, P. Rodriguez, and R. Teodorescu, ''Adaptive droop control applied to voltage-source inverters operating in grid-connected and islanded modes,'' *IEEE Transactions on Industrial Electronics*, vol. 56, no. 10, pp. 4088–4096, Oct. 2009.

[41] J. C. Vasquez, J. M. Guerrero, J. Miret, M. Castilla and L. Garcia de Vicuna, "Hierarchical Control of Intelligent Microgrids," in *IEEE Industrial Electronics Magazine*, vol. 4, no. 4, pp. 23-29, Dec. 2010.

[42] T. S. Ustun, C. Ozansoy, and A. Zayegh,"Simulation of communication infrastructure of a centralized microgrid protection system based on IEC 61850-7-420". In *2012 IEEE Third International Conference on Smart Grid Communications (SmartGridComm)*, Nov. 2012, pp. 492-497.

[43] E. Kuznetsova, Y. Li, C. Ruiz, and E. Zio, "An integrated framework of agent-based modelling and robust optimization for microgrid energy management". in *Applied Energy*, vol. 129, no. 15, Sep. 2014, pp. 70-88

[44] N. C. Ekneligoda and W. W. Weaver, "Game-Theoretic communication structures in microgrids. in *IEEE Transactions on Power Delivery*, vol. 27, no. 4, Oct. 2012, pp. 2334-2341.

[45] C. P. Nguyen and A. J. Flueck, "Modeling of communication latency in smart grid," *2011 IEEE Power and Energy Society General Meeting*, San Diego, CA, 2011, pp. 1-7.

[46] C. A. Macana, E. Mojica-Nava and N. Quijano, "Time-delay effect on load frequency control for microgrids," *2013 10th IEEE INTERNATIONAL CONFERENCE ON NETWORKING, SENSING AND CONTROL (ICNSC)*, Evry, 2013, pp. 544-549.

[47] K. C. Lee, S. Lee and M. H. Lee, "Worst Case Communication Delay of Real-Time Industrial Switched Ethernet With Multiple Levels," in *IEEE Transactions on Industrial Electronics*, vol. 53, no. 5, pp. 1669-1676, Oct. 2006.

[48] M. D. Ilic, L. Xie, U. A. Khan and J. M. F. Moura, "Modeling of Future Cyber–Physical Energy Systems for Distributed Sensing and Control," in *IEEE Transactions on Systems, Man, and Cybernetics - Part A: Systems and Humans*, vol. 40, no. 4, pp. 825-838, July 2010.

[49] B. Kumar and S. Mishra, "Agc for distributed generation," in *IEEE International Conference on Sustainable Energy Technologies (ICSET 2008)*, pp. 89–94, IEEE, 2008.

[50] X. Xu; T. Wang; L. Mu; J. Mitra, "Predictive Analysis of Microgrid Reliability Using a Probabilistic Model of Protection System Operation," in *IEEE Transactions on Power Systems*. vol, no.99, pp.1-1

[51] X. Xu, J. Mitra, T. Wang and L. Mu, "An Evaluation Strategy for Microgrid Reliability Considering the Effects of Protection System," in *IEEE Transactions on Power Delivery*, vol. 31, no. 5, pp. 1989-1997, Oct. 2016.

[52] P. Baboli, "Flexible and overall reliability analysis of hybrid AC–DC microgrid among various distributed energy resource expansion scenarios," in *IET Generation, Transmission & Distribution*, vol. 10, no. 16, pp. 3978-3984, 12 8 2016.

[53] S. Wang, Z. Li, L. Wu, M. Shahidehpour and Z. Li, "New Metrics for Assessing the Reliability and Economics of Microgrids in Distribution System," in *IEEE Transactions on Power Systems*, vol. 28, no. 3, pp. 2852-2861, Aug. 2013.

[54] D. E. Olivares et al., "Trends in Microgrid Control," in *IEEE Transactions on Smart Grid*, vol. 5, no. 4, pp. 1905-1919, July 2014.

[55] Z. Li, Y. Yuan and F. Li, "Evaluating the reliability of islanded microgrid in an emergency mode," *45th International Universities Power Engineering Conference UPEC2010*, Cardiff, Wales, 2010, pp. 1-5.

[56] A. Solanki, A. Nasiri, V. Bhavaraju, T. Abdullah, D. Yu, "A New Control Method for Microgrid Power Management", *International Conference on Renewable Energy Research and Applications*. Oct. 2013, Madrid.

[57] A. Bani-Ahmed, L. Weber, A. Nasiri and H. Hosseini, "Microgrid communications: State of the art and future trends," *2014 International Conference on Renewable Energy Research and Application (ICRERA)*, Milwaukee, WI, 2014, pp. 780-785.

[58] A. Bani-Ahmed and A. Nasiri, "Development of real-time hardware-in-the-loop platform for complex microgrids," *2015 International Conference on Renewable Energy Research and Applications (ICRERA)*, pp. 994-998, Palermo, 2015.

[59] Guerrero J M, Chandorkar M, Lee T, Loh, P C. "Advanced Control Architectures for Intelligent Microgrids—Part I: Decentralized and Hierarchical Control. Industrial Electronics", *IEEE Transactions on Industrial Electronics*, vol.60, no.4, pp.1254-1262.

[60] W. Liu, W. Gu, W. Sheng, X. Meng, Z. Wu and W. Chen, "Decentralized Multi-Agent System-Based Cooperative Frequency Control for Autonomous Microgrids With Communication Constraints," *in IEEE Transactions on Sustainable Energy*, vol. 5, no. 2, pp. 446-456, April 2014.

[61] F. Shahnia, R. P. S. Chandrasena, S. Rajakaruna and A. Ghosh, "Primary control level of parallel distributed energy resources converters in system of multiple interconnected autonomous microgrids within self-healing networks," in *IET Generation, Transmission & Distribution*, vol. 8, no. 2, pp. 203-222, February 2014.

[62] R. Palma-behnke et al., "A Microgrid Energy Management System Based on the Rolling Horizon Strategy", vol. 4, no. 2, pp. 996-1006, 2013.

[63] T. Wang, D. O'Neill and H. Kamath, "Dynamic Control and Optimization of Distributed Energy Resources in a Microgrid," in *IEEE Transactions on Smart Grid*, vol. 6, no. 6, pp. 2884-2894, Nov. 2015.

[64] M. I. Azim, M. J. Hossain, F. H. M. R. Griffith and H. R. Pota, "An improved droop control scheme for islanded microgrids," *2015 5th Australian Control Conference (AUCC)*, , 2015, pp. 225-229.

[65] C. M. Colson and M. H. Nehrir, "Comprehensive Real-Time Microgrid Power Management and Control With Distributed Agents," in *IEEE Transactions on Smart Grid*, vol. 4, no. 1, pp. 617-627, March 2013.

[66] G. Levitin, L. Xing, H. Ben-Haim and Y. Dai, "Reliability of Series-Parallel Systems With Random Failure Propagation Time," in *IEEE Transactions on Reliability*, vol. 62, no. 3, pp. 637-647, Sept. 2013.

[67] G. Bolch et al., Queueing Networks and Markov Chains, New York, NY: Wiley Interscience. 1998.

[68] A. Bani-Ahmed, A. Nasiri and H. Hosseini, "Design and development of a true decentralized control architecture for microgrid," *2016 IEEE Energy Conversion Congress and Exposition (ECCE)*, Milwaukee, WI, 2016, pp. 1-5.

[69] IEEE Standard for Interconnecting Distributed Resources with Electric Power System, IEEE Std. 1547TM-2003, July 2003.

[70] K. Clark, N.W. Miller and J.J. Sanchez-Gasca, "Modeling of GE wind turbine-generators for grid studies," General Electric International, Technical Report, 2010.

[71] N.W. Miller, W.W. Price and J.J. Sanchez-Gasca, "Dynamic modeling of GE 1.5 and 3.6 wind turbine-generators," GE-Power Systems Energy Consulting, 2003.

[72] S.A. Rahman and R.K. Varma, "PSCAD/EMTDC model of a 3-phase grid connected photovoltaic solar system," in *North American Power Symposium (NAPS)*, 2011, pp. 1-7, 2011.

[73] A. Kalbat, "PSCAD simulation of grid-tied photovoltaic systems and Total Harmonic Distortion analysis," in *Electric Power and Energy Conversion Systems (EPECS)*, 2013 3rd International Conference on, pp. 1-6, 2013.

[74] Zhenhong Guo and Liuchen Chang, "Two-phase converter used for wind turbine PMSG generation system," in *Canadian Conference on Electrical and Computer Engineering*, pp. 001255-001258, 2008.

[75] R. Pena, J. Clare and G. Asher, "Doubly fed induction generator using back-to-back PWM converters and its application to variable-speed wind-energy generation," *IEEE Proceedings-Electric Power Applications*, vol. 143, pp. 231-241, 1996.

[76] National Instruments: www.ni.com

[77] IEEE Draft Standard for the Specification of Microgrid Controllers," in *IEEE P2030.7/D10, July 2017* , vol., no., pp.1-49, Jan. 1 2017

[78] IEEE Draft Standard for the Specification of Microgrid Controllers," in *IEEE P2030.7/D11, August 2017* , vol., no., pp.1-42, Jan. 1 2017

[79] M. Savaghebi, A. Jalilian, J. C. Vasquez, and J. M. Guerrero, "Secondary control scheme for voltage unbalance compensation in an islanded droop-controlled microgrid," *IEEE Transactions on Smart Grid*, vol. 3, no. 2, pp. 797–807, June 2012.

[80] R. Majumder, G. Ledwich, A. Ghosh, S. Chakrabarti, and F. Zare, "Droop control of converter-interfaced microsources in rural distributed generation," *IEEE Trans. Power Delivery*, vol. 25, no. 4, pp. 2768–2778, Oct. 2010.

[81]  C. K. Sao and P. W. Lehn, "Autonomous load sharing of voltage source converters," *IEEE Trans. Power Delivery*, vol. 20, no. 2, pp. 1009– 1016, Apr. 2005.

[82]  T. L. Vandoorn, J. C. Vasquez, J. De Kooning, J. M. Guerrero and L. Vandevelde, "Microgrids: Hierarchical Control and an Overview of the Control and Reserve Management Strategies," in *IEEE Industrial Electronics Magazine*, vol. 7, no. 4, pp. 42-55, Dec. 2013.

## Appendix A: Centralized System states based on the three MG objectives.

| State | Grid | Solar | Wind | NG1 | NG2 | Storage | System |
|---|---|---|---|---|---|---|---|
| 0 | 0 | 0 | 0 | 0 | 0 | 0 | 0 |
| 1 | 0 | 0 | 0 | 0 | 0 | 1 | 1 |
| 2 | 0 | 0 | 0 | 0 | 1 | 0 | 1 |
| 3 | 0 | 0 | 0 | 0 | 1 | 1 | 1 |
| 4 | 0 | 0 | 0 | 1 | 0 | 0 | 1 |
| 5 | 0 | 0 | 0 | 1 | 0 | 1 | 1 |
| 6 | 0 | 0 | 0 | 1 | 1 | 0 | 1 |
| 7 | 0 | 0 | 0 | 1 | 1 | 1 | 1 |
| 8 | 0 | 0 | 1 | 0 | 0 | 0 | 0 |
| 9 | 0 | 0 | 1 | 0 | 0 | 1 | 1 |
| 10 | 0 | 0 | 1 | 0 | 1 | 0 | 1 |
| 11 | 0 | 0 | 1 | 0 | 1 | 1 | 1 |
| 12 | 0 | 0 | 1 | 1 | 0 | 0 | 1 |
| 13 | 0 | 0 | 1 | 1 | 0 | 1 | 1 |
| 14 | 0 | 0 | 1 | 1 | 1 | 0 | 1 |
| 15 | 0 | 0 | 1 | 1 | 1 | 1 | 1 |
| 16 | 0 | 1 | 0 | 0 | 0 | 0 | 0 |
| 17 | 0 | 1 | 0 | 0 | 0 | 1 | 1 |
| 18 | 0 | 1 | 0 | 0 | 1 | 0 | 1 |
| 19 | 0 | 1 | 0 | 0 | 1 | 1 | 1 |
| 20 | 0 | 1 | 0 | 1 | 0 | 0 | 1 |
| 21 | 0 | 1 | 0 | 1 | 0 | 1 | 1 |
| 22 | 0 | 1 | 0 | 1 | 1 | 0 | 1 |
| 23 | 0 | 1 | 0 | 1 | 1 | 1 | 1 |
| 24 | 0 | 1 | 1 | 0 | 0 | 0 | 0 |
| 25 | 0 | 1 | 1 | 0 | 0 | 1 | 1 |
| 26 | 0 | 1 | 1 | 0 | 1 | 0 | 1 |
| 27 | 0 | 1 | 1 | 0 | 1 | 1 | 1 |
| 28 | 0 | 1 | 1 | 1 | 0 | 0 | 1 |
| 29 | 0 | 1 | 1 | 1 | 0 | 1 | 1 |
| 30 | 0 | 1 | 1 | 1 | 1 | 0 | 1 |
| 31 | 0 | 1 | 1 | 1 | 1 | 1 | 1 |
| 32 | 1 | 0 | 0 | 0 | 0 | 0 | 1 |
| 33 | 1 | 0 | 0 | 0 | 0 | 1 | 1 |
| 34 | 1 | 0 | 0 | 0 | 1 | 0 | 1 |

| 35 | 1 | | 0 | 0 | 0 | 1 | 1 | 1 |
|----|---|---|---|---|---|---|---|---|
| 36 | 1 | | 0 | 0 | 1 | 0 | 0 | 1 |
| 37 | 1 | | 0 | 0 | 1 | 0 | 1 | 1 |
| 38 | 1 | | 0 | 0 | 1 | 1 | 0 | 1 |
| 39 | 1 | | 0 | 0 | 1 | 1 | 1 | 1 |
| 40 | 1 | | 0 | 1 | 0 | 0 | 0 | 1 |
| 41 | 1 | | 0 | 1 | 0 | 0 | 1 | 1 |
| 42 | 1 | | 0 | 1 | 0 | 1 | 0 | 1 |
| 43 | 1 | | 0 | 1 | 0 | 1 | 1 | 1 |
| 44 | 1 | | 0 | 1 | 1 | 0 | 0 | 1 |
| 45 | 1 | | 0 | 1 | 1 | 0 | 1 | 1 |
| 46 | 1 | | 0 | 1 | 1 | 1 | 0 | 1 |
| 47 | 1 | | 0 | 1 | 1 | 1 | 1 | 1 |
| 48 | 1 | | 1 | 0 | 0 | 0 | 0 | 1 |
| 49 | 1 | | 1 | 0 | 0 | 0 | 1 | 1 |
| 50 | 1 | | 1 | 0 | 0 | 1 | 0 | 1 |
| 51 | 1 | | 1 | 0 | 0 | 1 | 1 | 1 |
| 52 | 1 | | 1 | 0 | 1 | 0 | 0 | 1 |
| 53 | 1 | | 1 | 0 | 1 | 0 | 1 | 1 |
| 54 | 1 | | 1 | 0 | 1 | 1 | 0 | 1 |
| 55 | 1 | | 1 | 0 | 1 | 1 | 1 | 1 |
| 56 | 1 | | 1 | 1 | 0 | 0 | 0 | 1 |
| 57 | 1 | | 1 | 1 | 0 | 0 | 1 | 1 |
| 58 | 1 | | 1 | 1 | 0 | 1 | 0 | 1 |
| 59 | 1 | | 1 | 1 | 0 | 1 | 1 | 1 |
| 60 | 1 | | 1 | 1 | 1 | 0 | 0 | 1 |
| 61 | 1 | | 1 | 1 | 1 | 0 | 1 | 1 |
| 62 | 1 | | 1 | 1 | 1 | 1 | 0 | 1 |
| 63 | 1 | | 1 | 1 | 1 | 1 | 1 | 1 |

# Appendix B. Degree of Importance Calculations (Matlab)

```matlab
syms P
for i=1:1:10
h1_MGC=P*(1-(1-P)^i)^4;
h0_MGC=0;
intee(i)=double(int(h1_MGC-h0_MGC,0,1));
end
SumMGC=intee(4)
plot(intee)
h1_DG=P*(1-(1-P)^4)*(1-(1-P)^4)*(1-(1-P)^4)*(1-(1-P)^4);
h0_DG=P*(1-(1-P)^3)*(1-(1-P)^3)*(1-(1-P)^3)*(1-(1-P)^3);
intee_DG=double(int(h1_DG-h0_DG,0,1))

hold on

for i=1:1:10
h1=P^i*(1-(1-P)^i)^5;
h0=0;
intee(i)=double(int(h1-h0,0,1));
end
plot(intee);
hold off
SumMGC;
Sum2=sum(intee);
```

## Appendix C: Markov Chain Simulation for Centralized Microgrid Model (Matlab)

```matlab
clear
%Initialize Failure rates
sf;
wf;
ef;
n1;
n22;
cf2;
 %Initialize repair rates (Zeros if no-repair)
cr;
n1r;
n2r;
sr=;
wr=;
er=;



for kk=1:5
    hold on

   A= [Matrix initialization size (64x64)]
%A=A'+A;
jj=1;
for ii=33:64
    A(jj,ii)=cr;
    jj=jj+1;
end

jj=1;
for ii=17:32
    A(jj,ii)=n1r;
    A(jj+33,ii+32)=n1r;
    jj=jj+1;
end

jj=1;
for ii=9:16
    A(jj,ii)=n2r;
    A(jj+17,ii+16)=n2r;
    A(jj+33,ii+32)=n2r;
    A(jj+49,ii+48)=n2r;
    jj=jj+1;
end

jj=1;
for ii=5:8
    A(jj,ii)=er;
    A(jj+9,ii+8)=er;
    A(jj+17,ii+16)=er;
    A(jj+25,ii+24)=er;
```

```matlab
    A(jj+33,ii+32)=er;
    A(jj+41,ii+40)=er;
    A(jj+49,ii+48)=er;
    A(jj+57,ii+56)=er;
%   A(jj+,ii+28)=er;
    jj=jj+1;
end
jj=1;
for ii=3:4:63
    A(jj,ii)=sr;
    A(jj+1,ii+1)=sr;
    jj=jj+4;
end


jj=1;
for ii=2:2:64
    A(jj,ii)=wr;
    jj=jj+2;
end


for j=1:64
    for k=1:64
        if j==k
            A(k,j)=-1* (sum(A(:,j )));
        end
    end
end

Time=20;
DIV=5000;
dt=Time/DIV


X=[1;0;0;0;  0;0;0;0;   0;0;0;0;   0;0;0;0; 0;0;0;0;   0;0;0;0; 0;0;0;0;
0;0;0;0;     0;0;0;0;   0;0;0;0;
    0;0;0;0;  0;0;0;0;    0;0;0;0;    0;0;0;0; 0;0;0;0;   0;0;0;0;]
C=[1,1,1,1,1,1,1,1,1,1,1,1,0,0,0,0,1,1,1,1,0,0,0,0,1,1,1,1,0,0,0,0,0,0,0,0,0,
0,0,0,0,0,0,0,0,0,0,0,0,0,0,0,0,0,0,0,0,0,0,0,0,0,0,0];

for i=1:1:DIV
G=A*X;
X = X + G*dt;
Rel(i,kk)=C*X;
Reliability = C*X;

end
cf2(kk)=cf;
xx=dt:dt:Time;
xx=xx.*8760;

%figure(2);
plot(xx,Rel,'g');
```

```matlab
xlabel('Time(Hours)');
ylabel('Reliablity');
T=sum(dt.*Rel);
display(T)
cf=cf-(cf*0.2);
wf=wf;
sf=sf;
n1f=n1f;
n2f=n2f;
ef=ef;
end
```

## Appendix D: Markov Chain Simulation for Decentralized Microgrid Model (Matlab)

```matlab
Clear
for kk=1:5
    hold on
A=[Matrix initialization (32X32)].

jj=1;
for ii=17:32
    A(jj,ii)=n1r;
    %A(jj+33,ii+32)=n1r;
    jj=jj+1;
end

jj=1;
for ii=9:16
    A(jj,ii)=n2r;
    A(jj+17,ii+16)=n2r;
    %A(jj+33,ii+32)=n2r;
    jj=jj+1;
end

jj=1;
for ii=5:8
    A(jj,ii)=er;
    A(jj+9,ii+8)=er;
    A(jj+17,ii+16)=er;
    A(jj+25,ii+24)=er;
 %   A(jj+33,ii+32)=er;
  %  A(jj+,ii+28)=er;
    jj=jj+1;
end
jj=1;
for ii=3:4:32
    A(jj,ii)=sr;
    A(jj+1,ii+1)=sr;
    jj=jj+4;
end

jj=1;
for ii=2:2:32
    A(jj,ii)=wr;
    jj=jj+2;
end

for j=1:32
    for k=1:32
        if j==k
            A(k,j)=-1*(sum(A(:,j)));
        end
    end
```

```matlab
end


B=A;
Time=20;
DIV=5000;
dt=Time/DIV;

X=[1;0;0;0;   0;0;0;0;    0;0;0;0;    0;0;0;0;
    0;0;0;0;   0;0;0;0;    0;0;0;0;    0;0;0;0 ]
C=[1,1,1,1,1,1,1,1,1,1,1,1,0,0,0,0,1,1,1,1,0,0,0,0,1,1,1,1,0,0,0,0];

for i=1:1:DIV
G=A*X;
X = X + G*dt;
Rel(i,kk)=C*X;
Reliability = C*X;
end

xx=dt:dt:Time;
xx=xx.*8760;
%figure(2);
%plot(Rel);
plot(xx,Rel,'g');

xlabel('Time(Hours)');
ylabel('Reliablity');
T=sum(dt.*Rel);
display(T);
wf=wf-(wf*0.2);
sf=sf-(sf*0.2);
n1f=n1f-(n1f*0.2);
n2f=n2f-(n2f*0.2);
ef=ef-(ef*0.2);
end
hold off
```

# Curriculum Vitae

# Abedalsalam (Salam) Bani-Ahmed

## Interests & Skills

My interests in Smart Grids cover wide area of the concept domains, power distribution systems, smart grids and microgrids, distributed generation and energy storage. System level architecture design including sensors, wired and wireless communications, and real-time connectivity applying the concept of Internet of Things (IoT). Exploiting a can-do mentality in designing & deploying secure connected entities in a micro-scaled system, spanning up the energy networks tree

Unique expertise in power electronics and power conversion and communications. Automation and Control of Microgrid Distributed Resources. Smart Grid Optimization. Industrial Communication and Cyber-Security Protocols and Standards.

Experience with typical embedded control peripherals, coding, and hardware.

C/C++/Python, NI LabVIEW / NI CRIO (Real-Time/FPGA), Matlab/Simulink, HIL Platforms, ANSYS Simplorer, PSCAD, Linux RTOS.

## Experience

Jan 2018-Present      Eaton Corporation      Menomonee Falls, WI

### Lead Power Systems Engineer
- Research and development of Distributed Energy Resources Management Systems, Energy Networks and Cyber systems for microgrids.
- Energy storage inverter controller design using generated hardware-independent IEC 61131-3 structured Text and Ladder Diagrams from Simulink® models (PLC programming).
- Model Predictive Control implementation in Microgrid applications.
- Embedded hardware design for DC microgrid controllers.

Oct 2017-Dec 2017      Eaton Corporation      Menomonee Falls, WI

### Power Systems Engineer
- Research and development of Distributed Energy Resources Management Systems, Energy Networks and Cyber systems for microgrids.
- Energy storage inverter controller design using generated hardware-independent IEC 61131-3 structured Text and Ladder Diagrams from Simulink® models (PLC programming).
- Model Predictive Control implementation in Microgrid applications.
- Embedded hardware design for DC microgrid controllers.

| Jun 2017-Aug 2017 | Eaton Corporation | Menomonee Falls, WI |

**Energy Network Research Engineer Intern**
- Research and development of Distributed Energy Resources Management Systems (DERMS).
- Energy Networks and Industrial Internet-of-Things platforms.
- Reporting to The Global Technology Manager (Eaton Corporate Research and Technology).
- Team projects including DER controls and software/hardware implementation

| Jan 2012-Present | University of Wisconsin-Milwaukee | Milwaukee, WI |

**Graduate Research Assistant**
- Defined, developed, and executed R&D platforms & applications for innovative autonomous system concepts and solutions for distributed controls, energy automation and management.
- Implemented architecture concepts and solutions in HIL prototypes, reliability and feasibility studies, and technical specifications and standardization.
- Involved in writing funding proposals for research grants.
- Real world problem solving and a hands-on, can-do mentality in industry partnered projects.
- Software/Firmware development for digital control of power electronics converters & interfacing for energy storage systems.

| Jan 2015-Aug 2015 | Eaton Corporation | Menomonee Falls, WI |

**Research Engineer/Contract**
- Working on controls and communications for a deployable microgrid system.
- Constructing prototype concepts and model verification for renewable resources and energy storage systems. Developing algorithms and interfacing between controllers and microgrid components.
- Constructing prototype concepts for microgrid controls and communications by integrating various communication protocols and standards

## Education

| Sep 2012 – Dec 2017 | University of Wisconsin-Milwaukee | Milwaukee, WI |

**PhD in Electrical Engineering**

| Sep 2007 - Dec 2010 | Jordan University of Science & Technology | Irbid, Jordan |

**MSc in Computer Engineering**

| Sep 2002 - Jun 2007 | Yarmouk University | Irbid, Jordan |

**BSc in Electrical &Computer Engineering**

## Publications

- ➢ **Peer Reviewed Journals:**
- **A. Bani-Ahmed**, A. Nasiri, M. Rashidi, "Decentralized Resilient Autonomous Control Architecture for Dynamic Microgrids". IEEE Transactions on Smart Grid (Under Review).
- **A. Bani-Ahmed**, A. Nasiri, "Reliability Analysis of Decentralized Microgrid Control Architecture", IEEE Transactions on Smart Grid (Second Review).
- M. Rashidi, **A. Bani-Ahmed**, A. Nasiri, Rob Cuzner" Application of Multi-Port Solid State Transformers for Microgrid Based Distribution Systems" Submitted to IEEE Transactions on Industry Applications.
- M. Rashidi, **A. Bani-Ahmed**, A. Nasiri, M. Sabbah "Design and Implementation and Multiport Solid-State Transformer" Submitted to IEEE Transactions on Industry Applications.
- Q. Fu, A. Nasiri, A. Solanki, **A. Bani-Ahmed**, L. Weber, V. Bhavaraju. "Microgrids: Architectures, Controls, Protection, and Demonstration," Electric Power Components and Systems, Vol. 43, Issue 12, pp. 1453-1465. 2015.

- ➢ **Conference Papers:**
- **A. Bani-Ahmed**, A. Nasiri, "Coordinated Failure Response and Recovery in a Decentralized Microgrid Architecture". In proceedings of 2017 IEEE Energy Conversion Congress and Exposition (ECCE).
- **Mohammad Rashidi**, Mohamad Sabbah, Abedalsalam Bani-Ahmed, Mohammad Hasan Balali, Adel Nasiri "Design and Implementation of a Series Resonant Solid-State Transformer" 2017 IEEE Energy Conversion Congress and Exposition, Cincinnati, Ohio.
- M. Rashidi, **A. Bani-Ahmed**, Robabeh Nasiri, Azadeh Mazaheri, Adel Nasiri, "Design and Implementation of a Multi Winding High-Frequency Transformer for MPSST Application" 6th International Conference on Renewable Energy Research and Applications (ICRERA), Nov 2017, San Diego, California, USA.
- M. Rashidi, **A. Bani-Ahmed**, A. Nasiri, "Application of Multi-Port Solid State Transformer for Volt-VAR Control in Distribution System". In proceedings of IEEE Power & Energy Society General Meeting 2017.
- **A. Bani-Ahmed**, A. Nasiri and H. Hosseini, "Design and development of a true decentralized control architecture for microgrid," 2016 IEEE Energy Conversion Congress and Exposition (ECCE), Milwaukee, WI, USA, 2016, pp. 1-5.
- **Bani-Ahmed**, A. Nasiri, "Development of real-time hardware-in-the-loop platform for complex microgrids," 2015 International Conference on Renewable Energy Research and Applications (ICRERA), Palermo, 2015, pp. 994-998.
- **A. Bani-Ahmed** and A. Nasiri, "Microgrid Communications: State of the Art and Future Trends," in Proc. International Conference on Renewable Energy Research and Applications (ICRERA), Milwaukee, USA, Oct 19-22, 2014.
- **A. Bani-Ahmed**. "The Impact of Modeling the Overshooting Effect in Subthreshold Region for Nanoscale CMOS Inverter," in Proc. 7th International IEEE Conference on Innovations in Information Technology (Innovations '11), pp. 343-346. 2011. Abu-Dhabi, UAE, 2011.

- ➢ **Whitepapers:**
- • "**IEEE Smart Grid R&D Committee: Process and Synopsis of Collation of Topics"** (IEEE Smart Grid R&D committee.
- • "**Big Data Analytics in the Smart Grid"** (IEEE Smart Grid Big Data Analytics, Machine Learning and Artificial Intelligence in the Smart Grid Working Group)

## Courses:

- • Cybersecurity Technology and Applications (Chicago, IL)
- • Security of Wireless Networking (Bologna, Italy)
- • Design with an ARM-Based SoC. (Chicago, IL)
- • Developing Software for an ARM-Based SoC. (Chicago, IL)
- • Introduction to OpenCL for Alterations FPGAs. (Chicago, IL)
- • Introduction to renewable energy. (Chicago, IL)
- • OPAL-RT HIL Simulation. (Milwaukee, WI)

## Professional Memberships:

- ➢ Institute of Electrical & Electronics Engineers (IEEE)
  Societies: Power & Energy Society, Smart Grid Society, Smart Cities Society.
- ➢ Committee Member:
  - • IEEE Smart Grid R&D Committee. (Current).
  - • IEEE Smart Grid Operations Committee. (Current).
  - • IEEE Smart Cities Publications Committee (Current).
  - • IEEE Smart Cities Education Committee. (Current).
  - • IEEE Smart Cities R&D Committee. (Current).